

UNCLASSIFIED

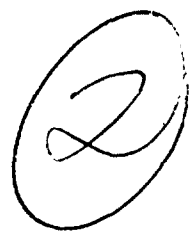
AD NUMBER
ADB012103
NEW LIMITATION CHANGE
TO Approved for public release, distribution unlimited
FROM Distribution authorized to U.S. Gov't. agencies only; Test and Evaluation; Jun 1976. Other requests shall be referred to Director, USA Ballistic Research Laboratories, ATTN: DRXBR-SS, Aberdeen Proving Ground, MD, 21005.
AUTHORITY
USAARDC ltr, 5 Sep 1979

THIS PAGE IS UNCLASSIFIED



BRL MR 2631

# BRL



AD

MEMORANDUM REPORT NO. 2631 ✓

(Supersedes IMR No. 61)

## MILLIMETER WAVE RADAR APPLICATIONS TO WEAPONS SYSTEMS

Victor W. Richard

June 1976

Reproduced From  
Best Available Copy

DDC  
R  
JUL 14 1976  
A

Distribution limited to US Government agencies only; Test and Evaluation; Jun 1976. Other requests for this document must be referred to Director, USA Ballistic Research Laboratories, ATTN: DRXBR-SS, Aberdeen Proving Ground, Maryland 21005.

USA BALLISTIC RESEARCH LABORATORIES  
ABERDEEN PROVING GROUND, MARYLAND

AD NO. ...  
JC FILE COPY ADB 012103

65  
Destroy this report when it is no longer needed.  
Do not return it to the originator.

Secondary distribution of this report by originating  
or sponsoring activity is prohibited.

Additional copies of this report may be obtained  
from the Defense Documentation Center, Cameron  
Station, Alexandria, Virginia 22314.

The findings in this report are not to be construed as  
an official Department of the Army position, unless  
so designated by other authorized documents.

UNCLASSIFIED

SECURITY CLASSIFICATION OF THIS PAGE (When Data Entered)

REPORT DOCUMENTATION PAGE		READ INSTRUCTIONS BEFORE COMPLETING FORM	
1. REPORT NUMBER BRL-MEMORANDUM REPORT NO. 2631	2. GOVT ACCESSION NO.	3. RECIPIENT'S CATALOG NUMBER	
4. TITLE (and Subtitle) MILLIMETER WAVE RADAR APPLICATIONS TO WEAPONS SYSTEMS	5. TYPE OF REPORT & PERIOD COVERED Final $\gamma = \rho \tau$		
7. AUTHOR(s) Victor W. / Richard	8. CONTR/CT OR GRANT NUMBER(s)		
9. PERFORMING ORGANIZATION NAME AND ADDRESS US Army Ballistic Research Laboratories Aberdeen Proving Ground, Maryland 21005	10. PROGRAM ELEMENT PROJECT, TASK AREA & WORK UNIT NUMBERS RD71 1161101A91A (ILIR) 1W562603A005 (Frankford Arsenal - ACT Program) 1M262303A214 (MICOM)		
11. CONTROLLING OFFICE NAME AND ADDRESS US Army Materiel Development & Readiness Command 5001 Eisenhower Avenue Alexandria, Virginia 22333	12. Report Date: JUNE 1976		
14. MONITORING AGENCY NAME & ADDRESS (if different from Controlling Office) 118p.	13. NUMBER OF PAGES 125		
16. DISTRIBUTION STATEMENT (of this Report) Distribution limited to US Government agencies only; Test and Evaluation; June 1976. Other requests for this document must be referred to Director, USA Ballistic Research Laboratories, ATTN: DRXBR-SS, Aberdeen Proving Ground, Maryland 21005.		15. SECURITY CLASS. (of this report) UNCLASSIFIED	
17. DISTRIBUTION STATEMENT (of the abstract entered in Block 20, if different from Report) F.D.T./E-1-W-161101-A-91-A DA-1-W-562603-A-005			
18. SUPPLEMENTARY NOTES Supersedes BRL Interim Memorandum Report No. 61			
19. KEY WORDS (Continue on reverse side if necessary and identify by block number) Millimeter Wave Radar, Ground Clutter, Millimeter Wave Propagation, Multipath, Radar Range in Rain, Foliage Obscuration, Automatic Tracking, Weapons Systems Applications			
20. ABSTRACT (Continue on reverse side if necessary and identify by block number) (Kst) Applications of millimeter wave radars in ground-to-air, ground-to-ground, and air-to-ground weapons systems are presented. The advantages and limitations of operating at millimeter wavelengths are defined.  The characteristics of millimeter wave propagation in adverse weather are described with emphasis on rain backscatter and attenuation theory, experimental data, and rain effects on radar system performance.  (Continued)			



TABLE OF CONTENTS

	Page
I. INTRODUCTION . . . . .	9
II. MILLIMETER WAVE PROPAGATION CHARACTERISTICS . . . . .	9
A. Atmospheric Effects . . . . .	9
B. Radar Range in Rain . . . . .	16
C. Optimum Radar Frequencies . . . . .	26
III. MILLIMETER WAVE RADAR CHARACTERISTICS . . . . .	27
A. General . . . . .	27
B. Ground-to-Air Millimeter Wave Radar Characteristics . . . . .	29
1. General . . . . .	29
2. Radar Return From Helicopter. . . . .	30
3. Automatic Tracking Tests. . . . .	44
4. Ground Multipath. . . . .	46
C. Ground-to-Ground Millimeter Wave Radar Characteristics. . . . .	48
1. General . . . . .	48
2. Multipath . . . . .	49
3. Ground Clutter. . . . .	52
4. Foliage Obscuration . . . . .	56
D. Air-to-Ground Millimeter Wave Radar Characteristics . . . . .	56
E. Target Acquisition Millimeter Wave Radar Characteristics. . . . .	57
IV. MILLIMETER WAVE RADAR AND COMPONENT STATUS. . . . .	59
A. Existing Radars . . . . .	59
B. Radar Components. . . . .	61
V. TECHNOLOGY ADVANCES REQUIRED. . . . .	61
A. Weather Effects . . . . .	62
B. Target and Background Signatures. . . . .	62
C. Basic Propagation Characteristics . . . . .	62
D. Target Acquisition Techniques . . . . .	62
E. Component Improvement and Development . . . . .	62

TABLE OF CONTENTS (CONT.)

	Page
VI. CONCLUSIONS . . . . .	63
A. Ground-to-Air . . . . .	63
B. Ground-to-Ground. . . . .	63
C. Air-to-Ground . . . . .	64
VII. ACKNOWLEDGEMENTS. . . . .	64
REFERENCES. . . . .	65
BIBLIOGRAPHY. . . . .	67
APPENDIX A - Millimeter Wave Propagation. . . . .	77
APPENDIX B - Fluctuating Clutter. . . . .	107
APPENDIX C - Clutter Discriminating Techniques. . . . .	117
DISTRIBUTION LIST . . . . .	121

## LIST OF ILLUSTRATIONS

Figure	Page
1. Atmospheric Attenuation vs Frequency. . . . .	11
2. Rain and Fog Attenuation vs Frequency . . . . .	11
3. A-Scope Photographs of Rain Backscatter at 70 GHz vs Rainfall Rate . . . . .	13
4. Measured Rain Backscatter Coefficient vs Rainfall Rate. . . . .	14
5. Calculated Rain Backscatter Coefficient vs Frequency. . . . .	15
6. Range at which Rain Return Equals Target Return vs Frequency and Rain Rate with Constant Antenna Size. . . . .	17
7. Superiority of 95 GHz over 70 and 35 GHz Radar to Detect Target in Rain. . . . .	19
8. Backscatter Limited Range vs Frequency with Constant Antenna Beamwidth . . . . .	21
9. Calculated 35-GHz Radar Tracking Range in Rain. . . . .	22
10. Calculated 95-GHz Radar Tracking Range in Rain. . . . .	23
11. Reduction of Rain Backscatter and Target Return with Circular Polarization at 70 GHz. . . . .	25
12. BRL 70-GHz Tracking Radar Antenna and Mount . . . . .	31
13. BRL 70-GHz Tracking Radar Interior Showing A-Scope TV Recording . . . . .	33
14. Norden 70-GHz All-Polarization Radar. . . . .	34
15. Helicopter Flying Crossing Course . . . . .	35
16. Helicopter Flying Crossing Course, Going Behind Trees . . . . .	36
17. Helicopter Flying Crossing Course, Only Tail Rotor Exposed. . . . .	37
18. Helicopter Flying Crossing Course, Completely Obscured by Trees . . . . .	38
19. Helicopter Flying Radar Course, Just Above Trees. . . . .	39
20. Helicopter Flying Radar Course, Behind Heavy Tree Cover But Visible Through Gap . . . . .	40

LIST OF ILLUSTRATIONS (CONT.)

Figure	Page
21. Helicopter Hovering 7.5 Meters Above Water. . . . .	41
22. Radar Return from Helicopter Hovering, Direct A-Scope Photograph. . . . .	42
23. Radar Return from Helicopter Flying Crossing Course over Trees, Direct A-Scope Photograph. . . . .	43
24. Automatic Tracking of Helicopter with BRL 70-GHz Radar. . . . .	45
25. Automatic Tracking of Helicopter Behind Trees . . . . .	47
26. Automatic Tracking of Pickup Truck with BRL 70-GHz Radar. . . . .	51
27. Ground Clutter at 70 GHz. . . . .	53
28. 70-GHz Radar Return from Tank in Clear Field. . . . .	54
29. 70-GHz Radar Return from Tank in High Grass . . . . .	55
A-1. One Way Attenuation per Kilometer for Horizontal Propagation in Clear Air (Rosenblum). . . . .	78
A-2. One Way Attenuation per Kilometer for Horizontal Propagation in Clear Air. . . . .	80
A-3. Cross Sections of Water Spheres at 18°C for 4.3 mm Wavelength Energy [1]. . . . .	83
A-4. Rainfall Drop Size Distribution as a Function of Rain Rate for Laws and Parsons Data with 0.25 mm Diameter Interval [16]. . . . .	86
A-5. One-Way Attenuation in Rain at 70 GHz . . . . .	88
A-6. One-Way Attenuation in Rain [20]. . . . .	90
A-7. Backscatter Cross Section Per Unit Volume of Rain at 0°C [20]. . . . .	91
A-8. Backscatter Cross Section Per Unit Volume of Rain at 70 GHz . . . . .	92
A-9. Correlation of Visibility in Fog to Liquid Water Content. . . . .	95
A-10. One-Way Attenuation in Fog as a Function of Liquid Water Content . . . . .	99

LIST OF ILLUSTRATIONS (CONT.)

Figure	Page
A-11. Figure Merit of Radar Performance in Target Cross Section = 1 Square Meter. . . . .	105
B-1. The Rayleigh Probability Density Function . . . . .	109
B-2. Clutter Spectrum of Wooded Ground at Millimeter Wavelengths . . . . .	111
B-3. Characteristics of the Radar-Video Return from a Fluctuating Target. . . . .	112
B-4. Characteristics of the Radar-Video Return from a Fluctuating Target. . . . .	113
C-1. Range-Gated Doppler Signal Processor. . . . .	119

## I. INTRODUCTION

Applications of millimeter wave radars in Army ground-to-ground, ground-to-air, and air-to-ground weapons systems are discussed in this report. The advantages and limitations of operating at millimeter wavelengths in these applications are defined.

The characteristics of millimeter wave propagation in adverse weather are presented; emphasis is placed on rain backscatter and attenuation theory, experimental data, and rain effects on radar system performance.

The theory of fluctuating clutter is described and a terrain clutter model is presented whose output is characterized by its power spectral density and probability density function. Several clutter discrimination techniques are described.

To extend the range of millimeter wave radars in adverse weather, the use of more complex modulation waveforms, such as FM/CW, along with more sophisticated data processing techniques, is proposed. Extended ranges would result from the increased sensitivity of the radar system derived from the use of reduced, optimized bandwidths commensurate with the data rates required. The extra complication of such radars would be justified in applications where the other unique properties of millimeter wave radars are required, such as improved low-angle tracking, high angular resolution of multiple targets, secure operation, and reduced interference between adjacent radars.

Frequencies in the regions of 16, 35, and 95 GHz are suitable for high-accuracy, low-angle tracking. The tracking accuracy improves with increasing frequency. However, at 35 GHz the rain backscatter is relatively large and, therefore, the use of this frequency might be restricted to moving targets where MTI can be used.

## II. MILLIMETER WAVE PROPAGATION CHARACTERISTICS

### A. Atmospheric Effects

The maximum range of a millimeter wave radar is limited not only by component performance but also by the propagation characteristics of the atmosphere. Millimeter waves are attenuated by (1) the molecular absorption of water vapor and oxygen in clear weather, (2) the absorption of condensed water droplets in fog and rain, and (3) the scattering from water droplets in rain. In addition, raindrops scatter energy back into the radar antenna that appears as noise at the receiver and can obscure desired targets.

There are propagation windows at nominal frequencies of 35, 94, 140, 240, 360, 420, and 890 GHz, as shown in Figure 1. The atmospheric attenuation at these window frequencies increases with increasing frequency, except in the region of 240 GHz where the attenuation is less than at 140 GHz by about 1.3 dB/km. Only the coarse structure of the attenuation curve is shown in Figure 1, although the major propagation windows are shown. A comparison of the attenuation at optical and radar wavelengths can be conveniently made from Figure 1.

The clear-weather atmospheric attenuation at 35, 70, and 94 GHz is generally small compared with other radar system losses and propagation effects. At 140 and 240 GHz, atmospheric attenuation is appreciable, and at 360 GHz and above, it is usually prohibitively large for all but very short-range system applications.

Figure 1 also shows the rain plus atmospheric attenuation at the propagation window frequencies for 4, 10, and 25 mm/hr rainfall rates. The increase in attenuation from rain over clear weather attenuation can be seen in this figure.

Figure 2 shows calculated rain attenuation versus frequency curves that have been found to be in good agreement with measured attenuation. A curve of calculated fog attenuation is also included in Figure 2 which shows the relatively low attenuation in the millimeter wave region compared with the high attenuation in the optical region. It is this unique characteristic of millimeter waves to penetrate fog, drizzle, dust, and dry snow with very little attenuation that makes them useful where good performance must be maintained through conditions of poor visibility.

As stated previously, in addition to attenuation by the atmosphere and rain, further degradation of radar performance can be caused by the backscatter from condensed water droplets. The theory of millimeter wave rain propagation through rain is discussed in Appendix A. The uncertainty that existed previously between calculated and observed rain backscatter at millimeter wavelengths has been resolved with a study conducted by BRL in which rain backscatter and attenuation were measured at 9.375, 35, 70, and 95 GHz.<sup>1</sup> The quantitative relationship between rain characteristics and backscatter was determined experimentally over a wide range of rainfall rates.

---

<sup>1</sup>V.W. Richard and J.E. Kammerer, "Rain Backscatter Measurements and Theory at Millimeter Wavelengths," BRL Report No. 1838, October 1975 (AD B008173L).

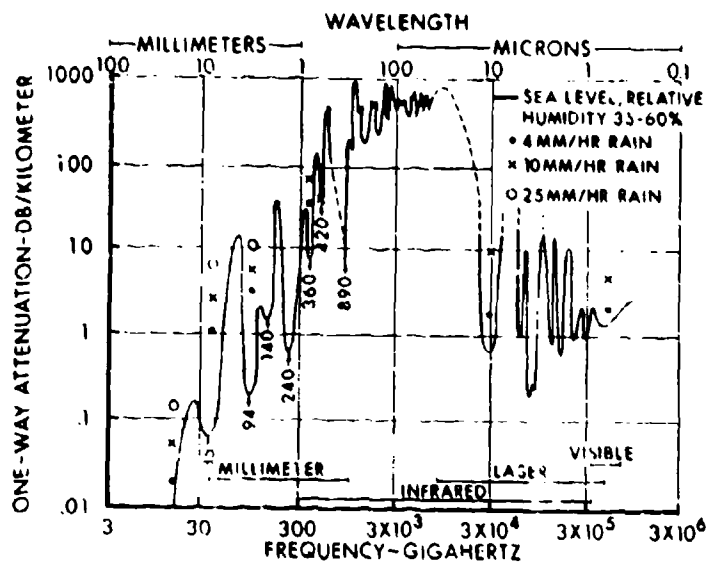


Figure 1. Atmospheric Attenuation vs Frequency

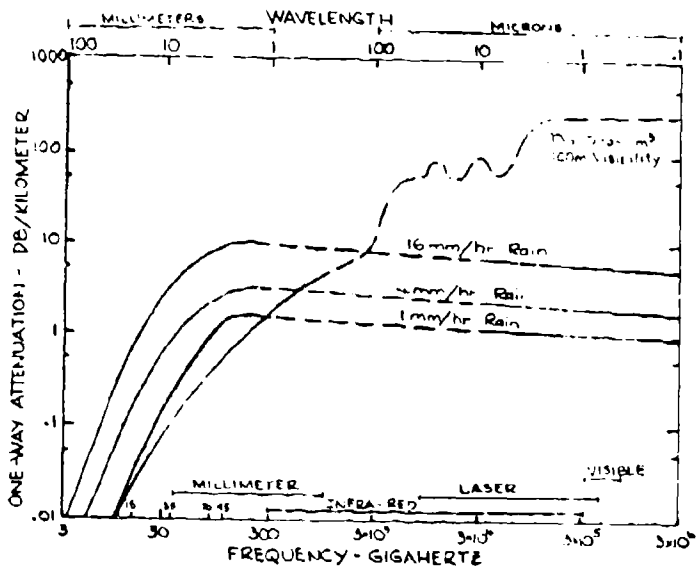


Figure 2. Rain and Fog Attenuation vs Frequency

Figure 3 shows A-scope photographs of rain backscatter measured at 70 GHz for rainfall rates of 1 to 100 mm/hr which are illustrative of the amplitude characteristics of rain clutter. In these photographs, the rain backscatter trace rises to a maximum deflection at a range of about 0.1 km because of the recovery time of the receiver-protector device and then decreases with increasing range because of the normal propagation spreading loss plus rain attenuation. The broad band of noise on the trace is the fluctuation of rain echoes caused by the rapidly changing interference effects between the randomly falling raindrops. The backscatter from light rainfall (Figure 3a, 1 mm/hr) is characterized by a gradually diminishing amplitude versus range. The backscatter from somewhat heavier rainfall (Figures 3b and 3c, 6 and 15 mm/hr) has a greater amplitude at short range and falls off more rapidly with increasing range. For heavy rainfall (Figures 3d, 3e, and 3f, 26-100 mm/hr) the maximum rain return at short ranges is about the same amplitude as medium rainfall, but the backscatter falls off more rapidly with increasing range because of the greater attenuation caused by the heavier rainfall. The reduction in the trihedral target return with increasing rainfall rate is also evident in these photographs.

The maximum range at which the rain backscatter is above the receiver noise is not very large in the photographs in Figure 3, but field radars with higher power and better sensitivity than the experimental radar used for this experiment would show rain backscatter above receiver noise out to much greater ranges.

Figure 3 additionally illustrates the increase in the slope of the rain backscatter trace as the rainfall intensity increases. It has been observed that this slope bears a very definitive relationship to the rainfall rate and, once calibrated, can be used as a very fast response rainfall intensity indicator. This slope technique is particularly useful in evaluating the rainfall rate as a function of range in order to quickly assess the range capability of a millimeter wave radar in rain from moment to moment under rapidly changing rainfall conditions.

The results of the BRL rain backscatter measurement experiment are shown in Figure 4 in the form of rain backscatter coefficient versus rainfall rate for 9.375, 35, 70, and 95 GHz. An extensive review of other experimental and theoretical data on rain backscatter and attenuation is given in Reference 1. For example, Figure 5 shows calculated rain backscatter data by Rozenberg<sup>2</sup> for the frequency range of 10 to 10,000 GHz along with BRL measured data points.

---

<sup>2</sup>V.I. Rozenberg, "Radar Characteristics of Rain in Submillimeter Range," Radio Eng. and Elec. Physics, Vol. 15, No. 12, 2157-2163, 1970.

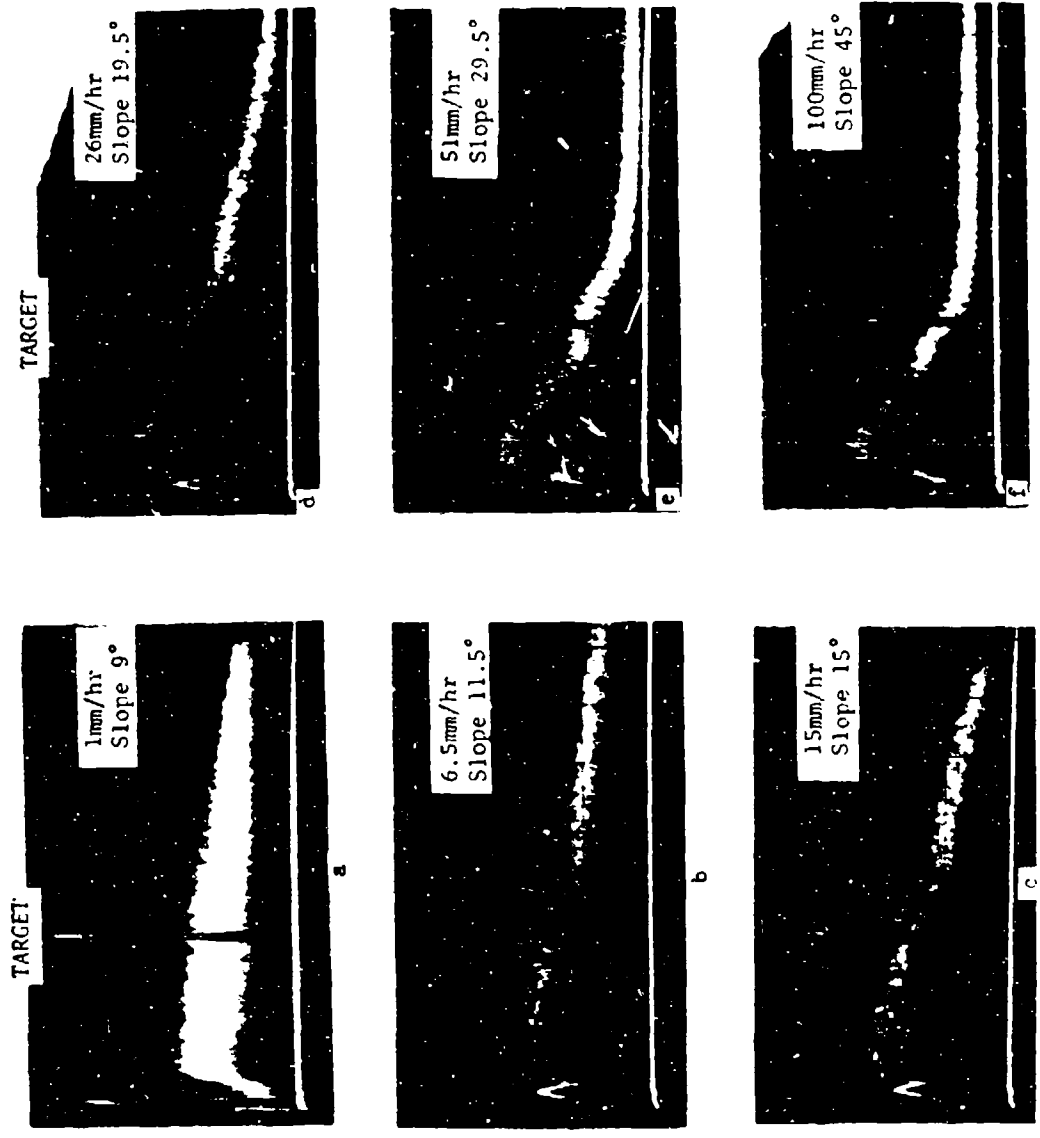


Figure 3. A-Scope Photographs of Rain Backscatter at 70 GHz vs Rainfall Rate

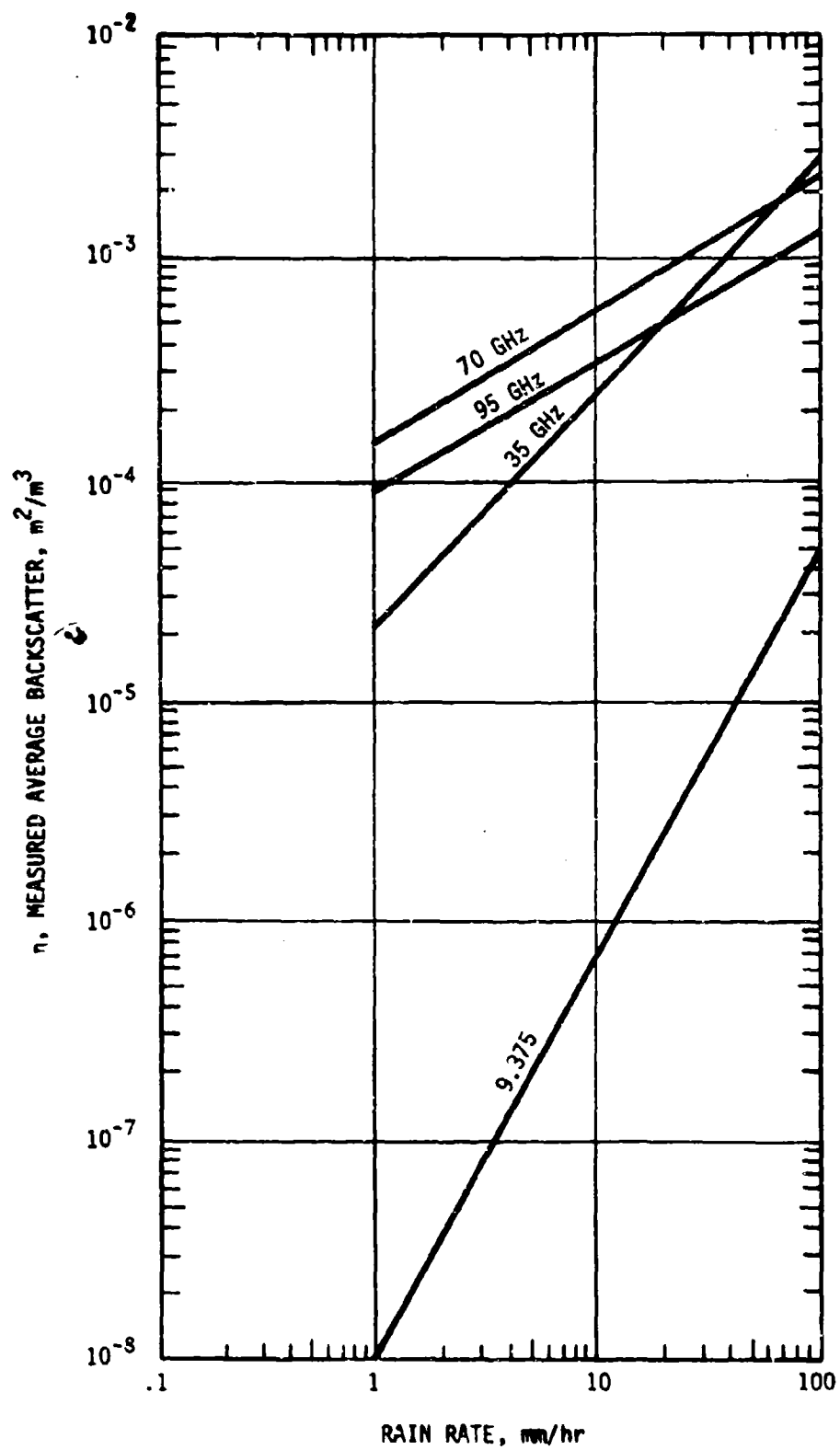


Figure 4. Measured Rain Backscatter Coefficient vs Rainfall Rate

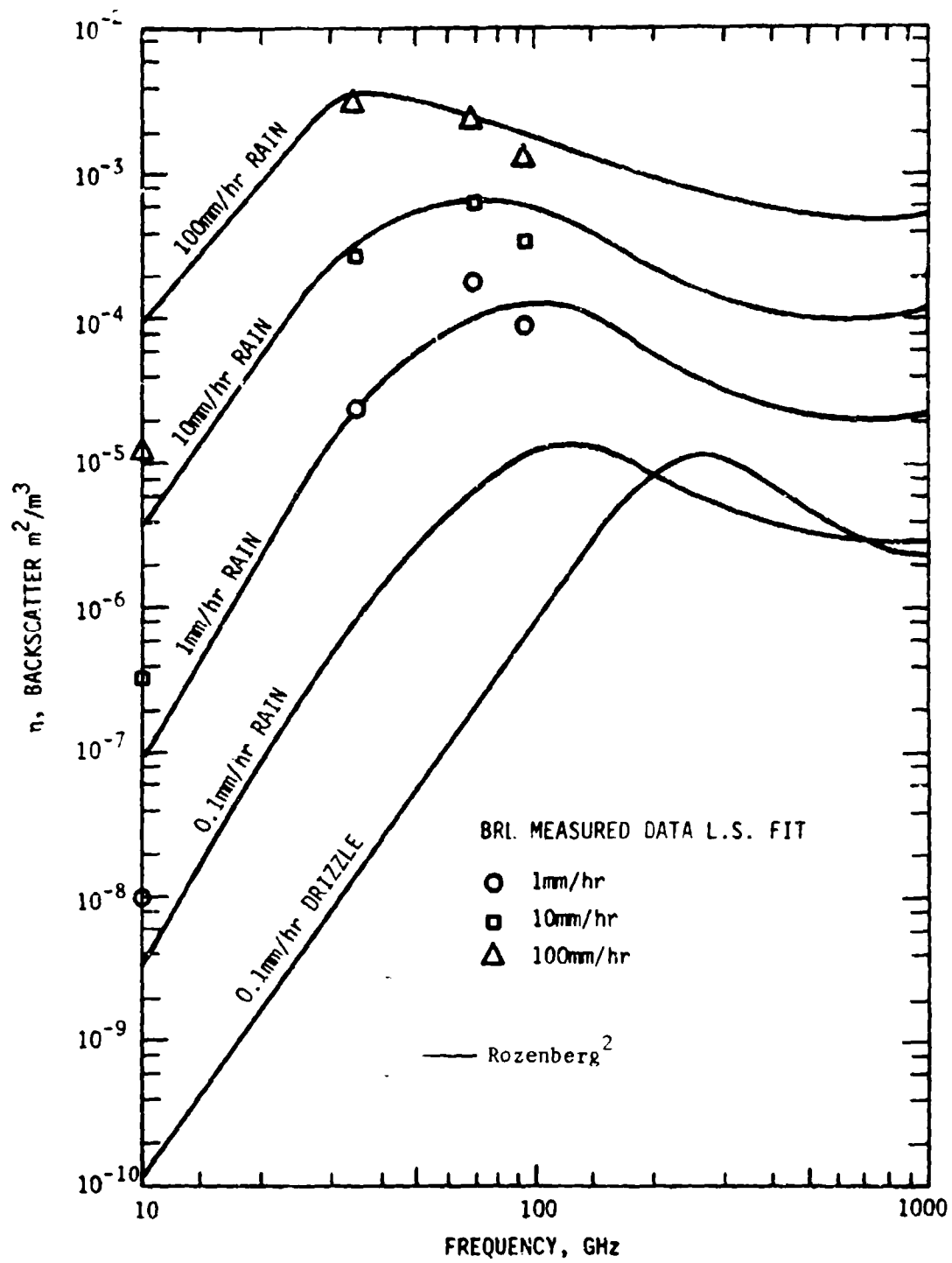


Figure 5. Calculated Rain Backscatter Coefficient vs Frequency

## B. Radar Range in Rain

The equations and data in Appendix A and Reference 1 provide basic propagation data from which calculations can be made of the performance of millimeter wave radar systems in rain over a wide range of frequencies and rainfall rates. The combined effects of rain backscatter and attenuation must be taken into account when calculating the maximum radar range in rain. The magnitude of the effect of rain backscatter in reducing range is shown in Figure 6 for radars with a fixed antenna size of 1 meter diameter operating between 10 and 300 GHz. The range at which the rain return is equal to the target return is shown in Figure 6 for targets of 1 and 5 square meters.

The radar range for the condition where the rain return is equal to the target return is given by the following equation which is derived in Reference 1,

$$D = \left( \frac{d^2 \sigma_t}{1.35 \times 10^8 \tau \lambda^2 n} \right)^{1/2}, \quad (1)$$

where  $D \equiv$  range, m (it is assumed that the radar has sufficient power and sensitivity to achieve this range)

$d \equiv$  antenna diameter, m

$\sigma_t \equiv$  target cross section,  $m^2$

$\tau \equiv$  pulse duration, seconds

$\lambda \equiv$  wavelength, m

$n \equiv$  rain backscatter coefficient,  $m^2/m^3$ .

The rain backscatter coefficient values used are given in Table I (from Reference 1). It should be noted that the backscatter-limited range of Figure 6 goes through a broad minimum, in the region of 20 to 40 GHz, indicating that  $K_a$  band frequencies (35 GHz) are more strongly affected by rain backscatter than frequencies lower or higher for a radar that is antenna-size limited; i.e., the antenna size is held constant as the comparison is made. This phenomenon was consistently observed during the BRL rain experiment, as shown in Figure 7 which illustrates the superiority of a 95-GHz radar over 70- and 35-GHz radars (all with the same antenna size) in detecting a sphere target of 0.05 square meter in a heavy rain. The target return is well above the rain backscatter at 95 GHz but is completely obscured at 70 and 35 GHz.

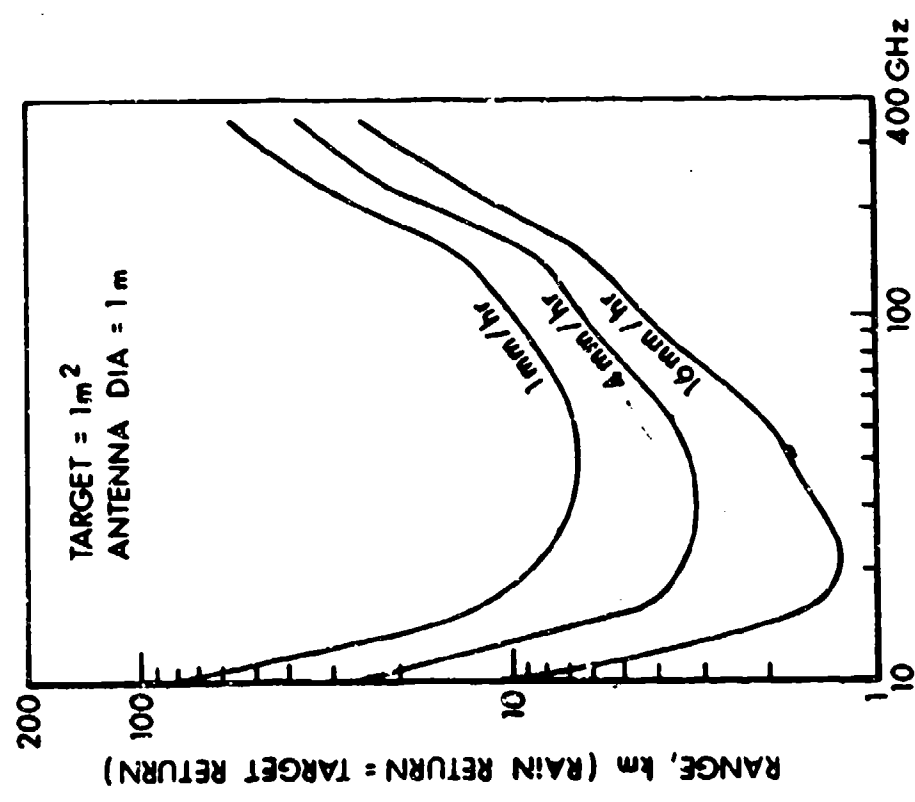
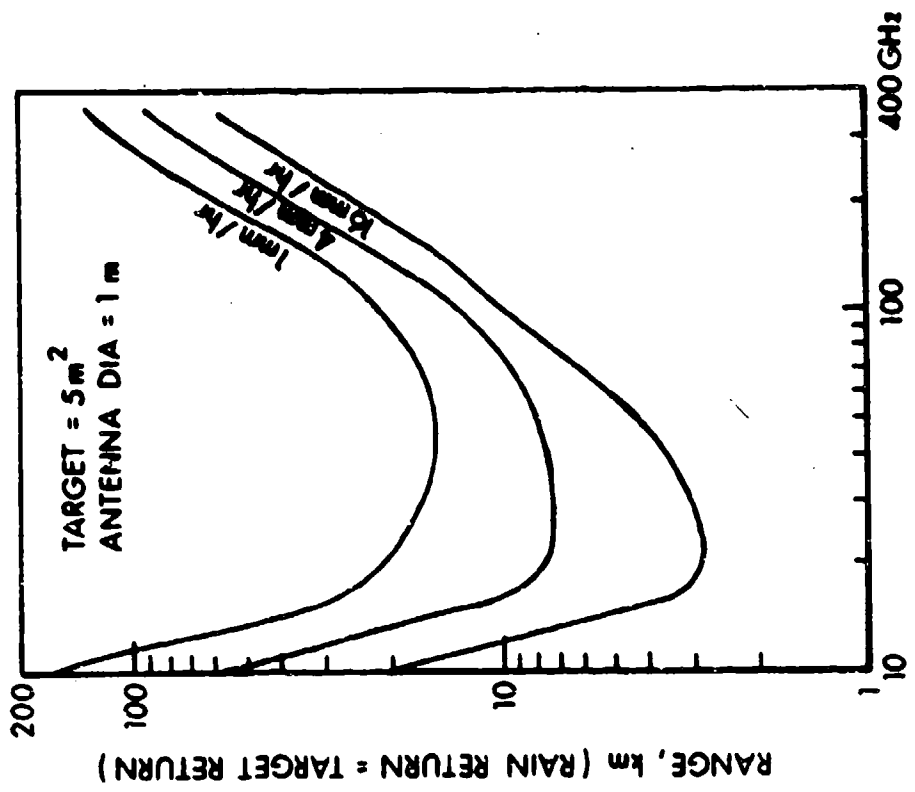


Figure 6. Range at which Rain Return Equals Target Return vs Frequency and Rain Rate with Constant Antenna Size

TABLE 1  
RAIN BACKSCATTER COEFFICIENT

Frequency, GHz	Rainfall Rate, mm/hr		
	1	4	16
	$\eta, \text{m}^2/\text{m}^3$		
9.375	$1.03 \times 10^{-8}$	$8.5 \times 10^{-8}$	$6.9 \times 10^{-7}$
16	$1.4 \times 10^{-6}$	$1.1 \times 10^{-5}$	$9.5 \times 10^{-5}$
25	$8.5 \times 10^{-6}$	$5 \times 10^{-5}$	$3 \times 10^{-4}$
35	$2.2 \times 10^{-5}$	$9.2 \times 10^{-5}$	$4.1 \times 10^{-4}$
55	$5.5 \times 10^{-5}$	$1.9 \times 10^{-4}$	$6.4 \times 10^{-4}$
70	$1.44 \times 10^{-4}$	$3.2 \times 10^{-4}$	$5.52 \times 10^{-4}$
95	$8.7 \times 10^{-5}$	$1.9 \times 10^{-4}$	$4.3 \times 10^{-4}$
140	$9.5 \times 10^{-5}$	$2.2 \times 10^{-4}$	$4.6 \times 10^{-4}$
240	$4.2 \times 10^{-5}$	$9.5 \times 10^{-5}$	$2.2 \times 10^{-4}$
360	$3.2 \times 10^{-5}$	$7.2 \times 10^{-5}$	$1.7 \times 10^{-4}$

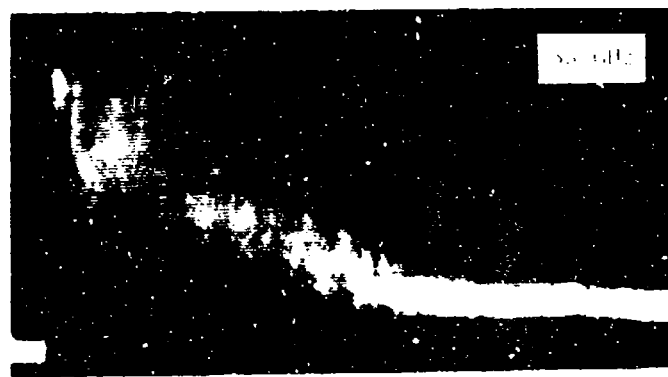
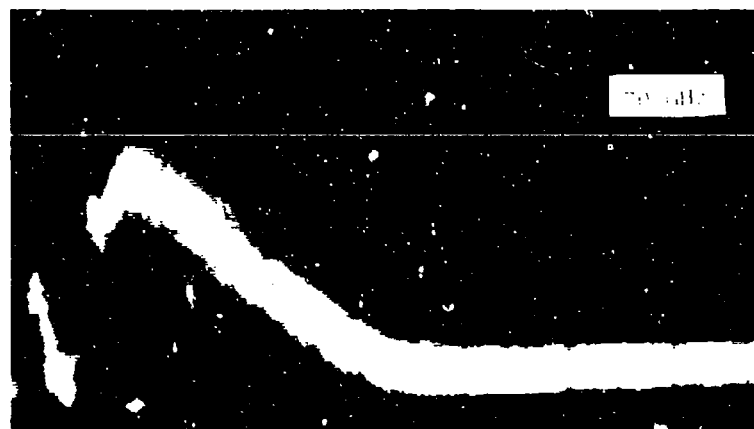


Figure 7. Superiority of 95 GHz over 70 and 35 GHz Radar to Detect Target in Rain

Figure 8 shows the rain backscatter-limited range when the antenna beamwidth is held constant (0.68 degree in this example, the beamwidth for a 1-meter-diameter antenna at 35 GHz) and the antenna size is decreased with increasing frequency. For this case, the rain backscatter-limited range is a minimum in the region of 100 GHz for light rain and 60 GHz for heavy rain.

The magnitude of the range reduction by rain attenuation is illustrated in Figures 9 and 10 for tracking radars operating at 35 and 95 GHz, respectively. Maximum tracking range was calculated using the following equation, radar system parameters, and atmospheric conditions.<sup>1</sup>

$$D = \left( \frac{P_T C^2 \lambda^2 \sigma_t \exp - 0.461 \alpha D}{(4\pi)^3 K T (B_{IF} B_{TR})^{1/2} F (S/N)} \right)^{1/4}, \quad (2)$$

where  $D \equiv$  range, m

$P_T \equiv$  peak transmitted power, w

$G \equiv$  antenna gain, power ratio

$\lambda \equiv$  wavelength, m

$\sigma_t \equiv$  target cross section, m<sup>2</sup>

$\alpha \equiv$  one-way rain attenuation, dB/m

$K T \equiv 4 \times 10^{-21}$  watts/Hz

$B_{IF} \equiv$  IF bandwidth, Hz

$B_{TR} \equiv$  tracking loop bandwidth, Hz

$F \equiv$  receiving system noise figure, power ratio

$S/N \equiv$  signal-to-noise power ratio.

Tracking ranges were calculated using the following radar system parameters and operating conditions:

Frequency, GHz	35	95
Target cross section, m <sup>2</sup>	5	5
Antenna diameter, m	1	1

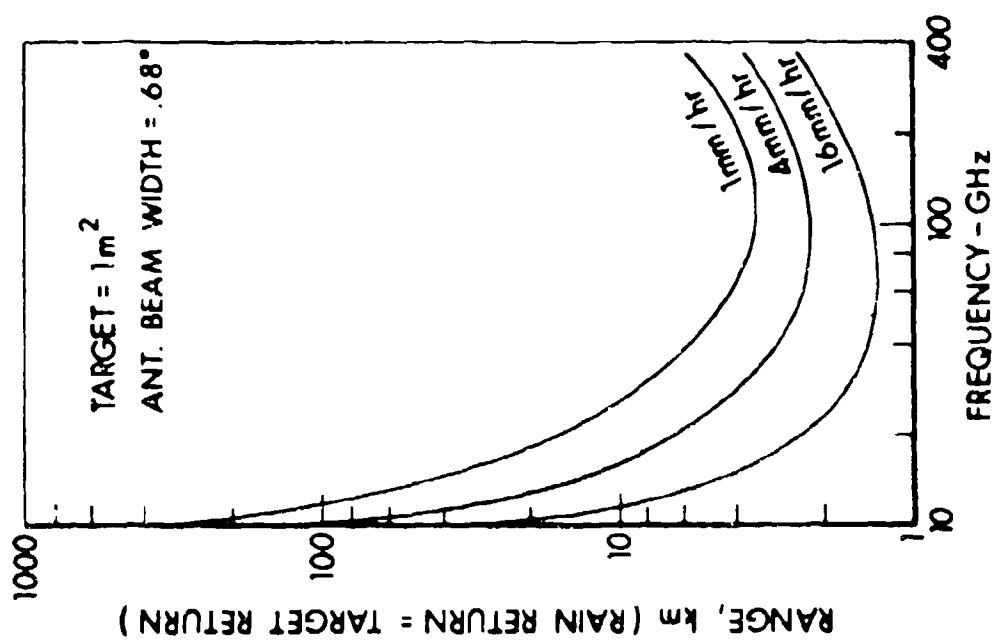
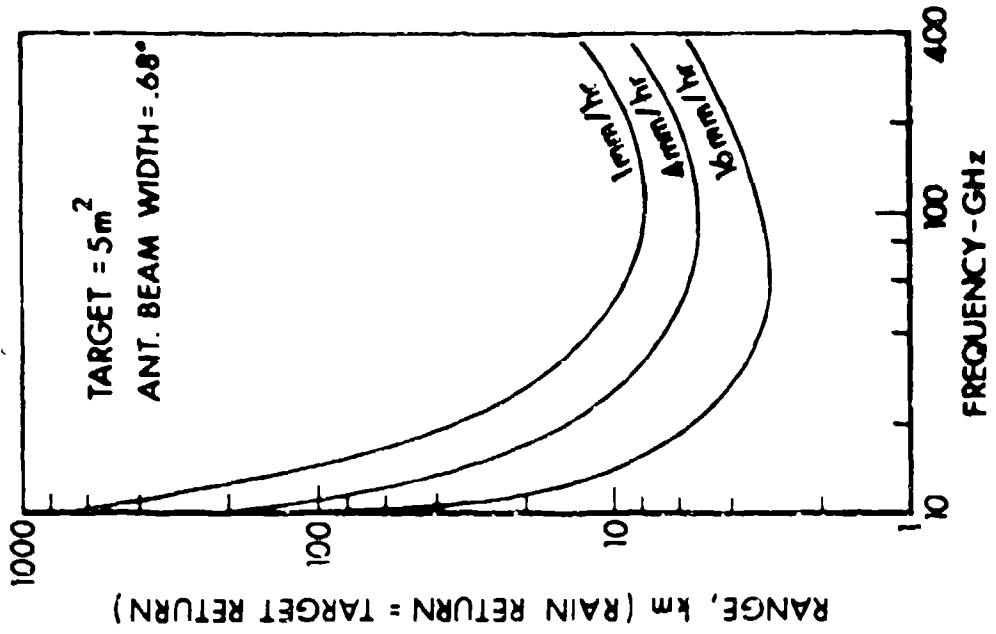


Figure 8. Backscatter Limited Range vs Frequency with Constant Antenna Beamwidth

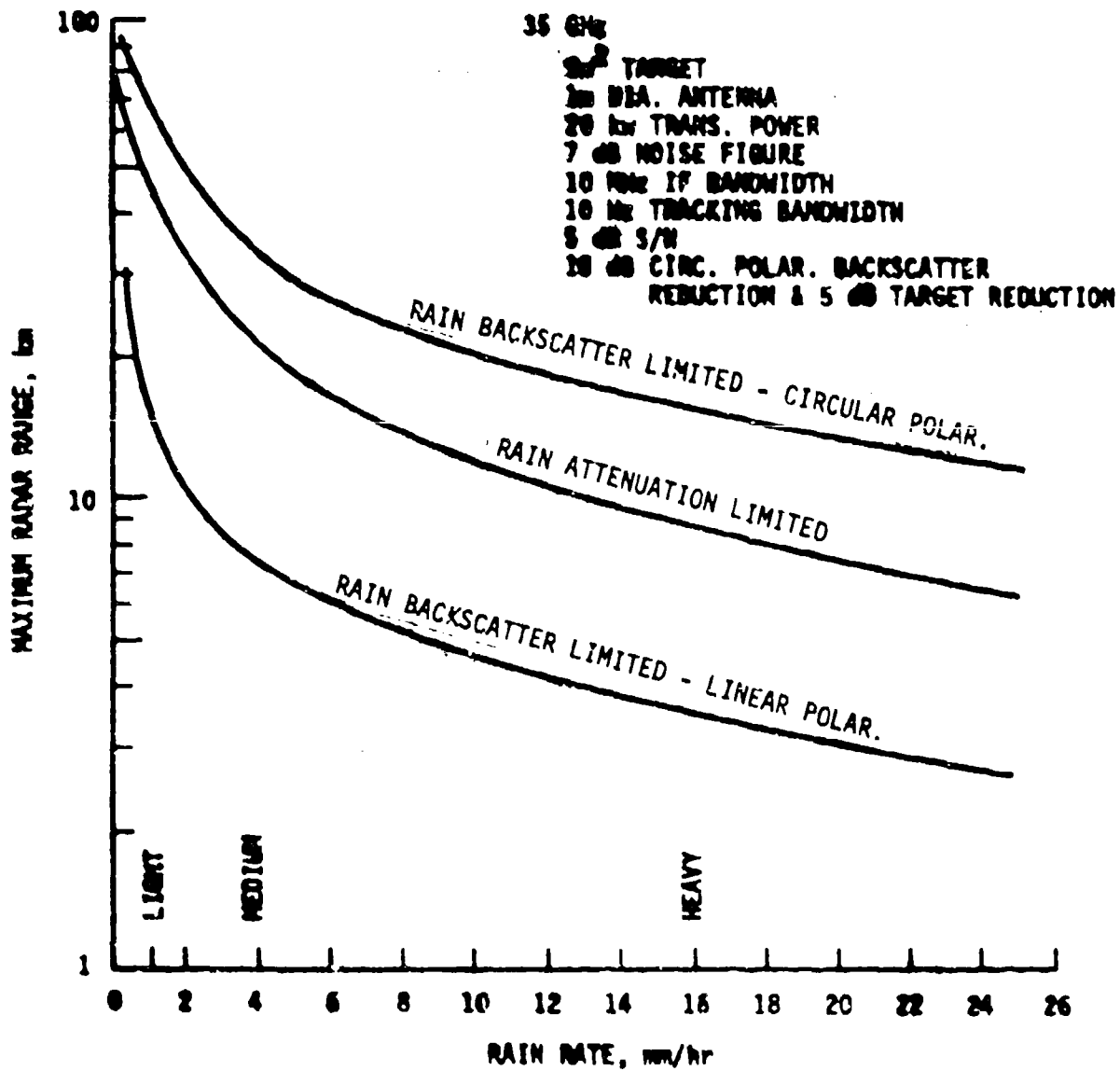


Figure 9. Calculated 35-GHz Radar Tracking Range in Rain

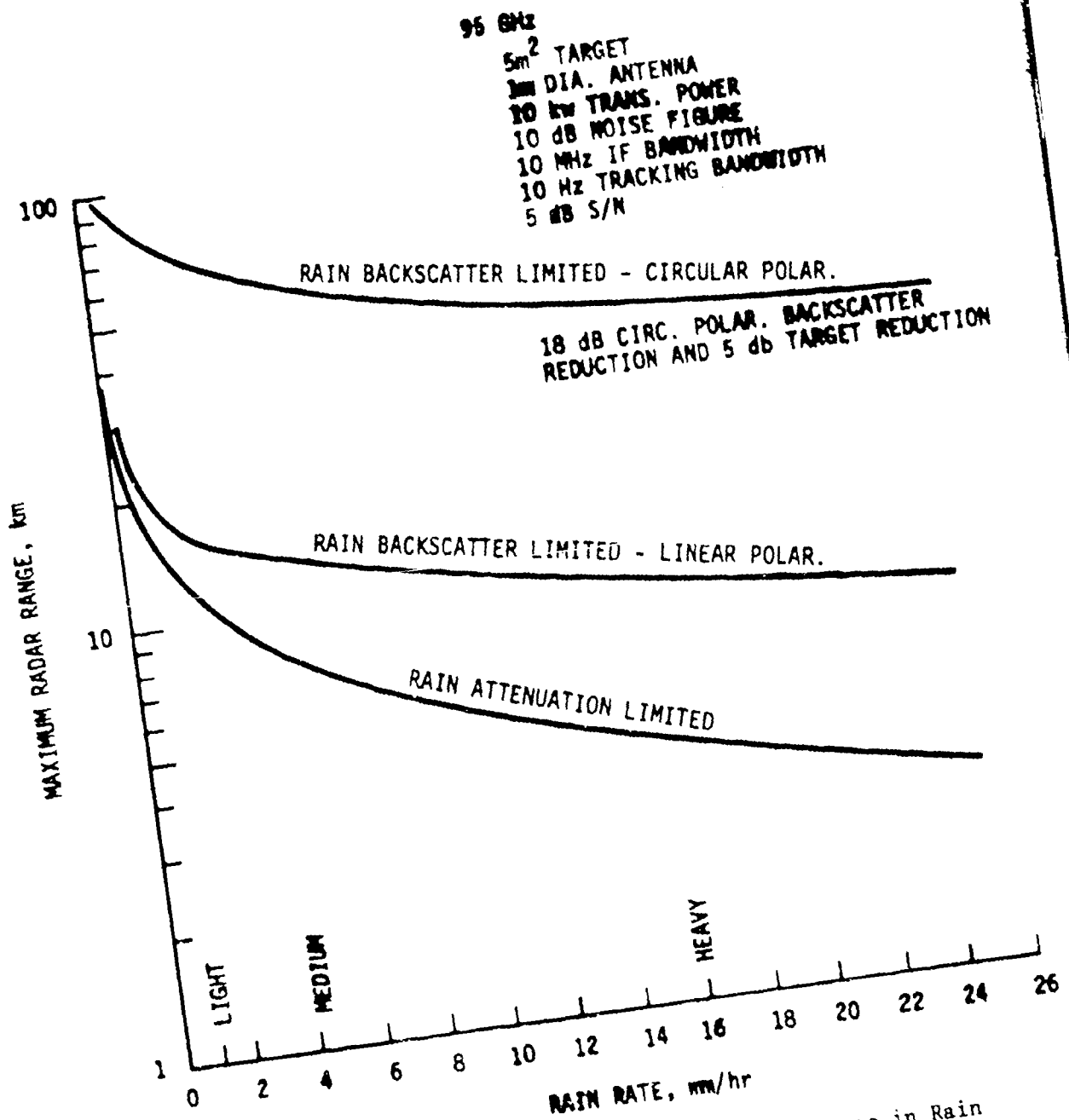


Figure 10. Calculated 95-GHz Radar Tracking Range in Rain

Transmitted power, kw	20	10
Receiver noise figure, dB	7	10
IF bandwidth, MHz	10	10
Tracking bandwidth, Hz	10	10
Signal-to-noise ratio, dB	5	5

Rain attenuation, dB/km, from  
Figure 2:

Rainfall rate, mm/hr	0	1	4	16
35 GHz attenuation, one-way, dB/km	0.16	0.25	0.95	3.6
95 GHz attenuation, one-way, dB/km	0.5	1.2	3.4	9.2

The backscatter-limited range data for linear polarization from Figures 6 and 8 are also shown in Figures 9 and 10 along with curves for circularly polarized operation based on a rain backscatter reduction of 18 dB with circular polarization and an associated 5 dB reduction of the target cross section.

At 35 GHz, for the radar and target parameters used in Figure 9, the range is severely limited by rain backscatter, with the range being about one-third of what it would be if limited by attenuation only. For moving targets, MTI would possibly reduce the effects of rain backscatter sufficiently to take the system to the rain attenuation limited range in most cases. For non-moving targets, circular polarization can be used to increase the range, provided that the radar has enough power and sensitivity to see the reduced target cross section that usually results when circular polarization is used. The effect of using circular polarization at 70 GHz to reduce rain clutter is shown in Figure 11 where the rain return is reduced below the receiver noise when circular polarization of the same sense for transmitting and receiving is used. Note also in this figure that the return from the trihedral and tree is also reduced when using circular polarization of the same sense. If neither MTI or circular polarization can be used with a 35-GHz radar system, the rain backscatter will impose a significant performance limitation unless a very large antenna can be used.

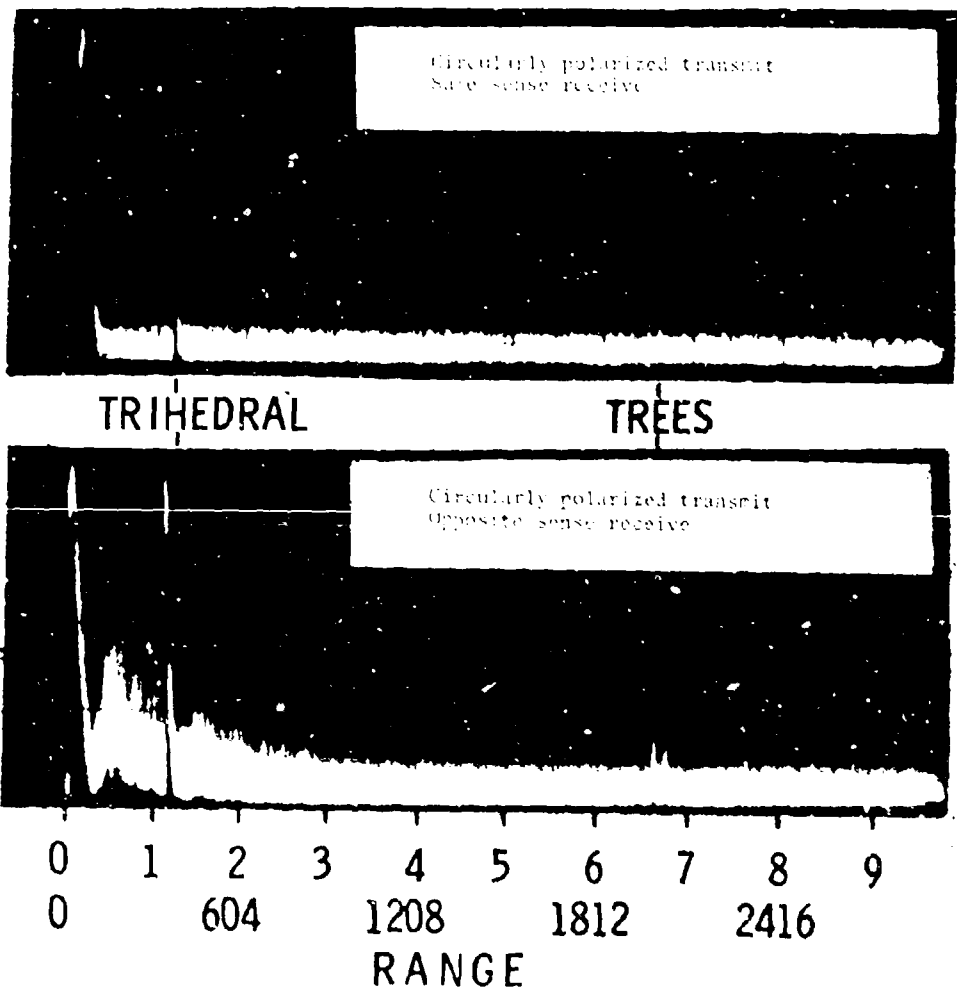


Figure 11. Reduction of Rain Backscatter and Target Return with Circular Polarization at 70 GHz

At 95 GHz, for the radar and target parameters used in Figure 10, the range is attenuation limited, which means that the range could be increased if more power or a more sensitive receiver was used. The use of circular polarization or MHI would not be absolutely necessary for the example chosen in Figure 10 to reduce rain clutter, unless ranges in excess of 10 km were desired.

These calculations of the range of millimeter wave radars operating in rain are given only as examples of the relative magnitudes of rain attenuation and backscatter effects. The calculated ranges do not necessarily represent the maximum performance attainable with higher performance components and the use of optimum modulation and data processing techniques.

### C. Optimum Radar Frequencies

Based on atmospheric propagation considerations alone, the choice of an optimum frequency for a weapons system radar would have to take into account the maximum range required under the types of adverse weather specified for the application. For example, rain backscatter can obscure small targets at very short ranges at certain frequencies. The optimum frequency to minimize rain clutter obscuration is a function of the antenna beamwidth and pulse length. In general, the attenuation by rain becomes more of a problem with increasing frequency, although attenuation can be overcome with increased antenna gain and transmitter power, and more sophisticated modulation and signal processing. Thus, it becomes necessary to consider the interaction between the radar system parameters and weather effects to obtain the required performance.

The choice of an optimum frequency for a wide range of radar applications has been very comprehensively treated by Strom.<sup>3</sup> The effects of propagation attenuation, rain and terrain clutter, and radar system parameters typically available at frequencies in the microwave and millimeter region are considered in these references.

---

<sup>3</sup>L.D. Strom, "Applications for Millimeter Radars," System Planning Corp., Arlington, VA, Report No. 108, for ARPA, 31 December 1973, (CONFIDENTIAL), AD 529566; "Adverse Weather Applications for Millimeter Radars on the Battlefield," Paper G.3, NELC/TD 308, 1974 Millimeter Wave  $\lambda$  Technical Conference, Naval Electronics Laboratory Center, San Diego, CA, 26-28 March 1974.

### III. MILLIMETER WAVE RADAR CHARACTERISTICS

#### A. General

The millimeter and sub-millimeter wave region of the electromagnetic spectrum between 10 millimeters and 1.0 millimeter wavelength (30-300 GHz) has unique quasi radio-optical propagation characteristics. The extremely high angular resolution and heavily degraded adverse weather properties of optical systems are approached at the high frequency end of this spectrum, and the all-weather propagation and broader resolution properties of radio waves are realized at the low frequency of this spectrum.

The use of very short wavelengths, in the millimeter and sub-millimeter region, and very narrow antenna beamwidths in radar designs offers a number of desirable features for Army weapons systems applications. These features include:

1. Narrow antenna beamwidth with small antenna, which provides
  - (a) high tracking and guidance accuracy,
  - (b) capability of tracking down to very low elevation angle before ground multipath and ground clutter become appreciable,
  - (c) good resolution of closely spaced targets,
  - (d) high angular resolution for area mapping and target surveillance,
  - (e) high immunity to jamming (narrow beamwidth makes jamming through the main beam difficult),
  - (f) high antenna gain, and
  - (g) capability of detecting and locating small objects such as wires, poles, and projectiles.
2. Wide frequency spectrum availability, which provides
  - (a) high information rate capability for obtaining fine structure detail of target signature with narrow pulses or wideband FM,
  - (b) wideband spread-spectrum capability for reduced multipath and clutter,
  - (c) high immunity to jamming,

- (d) multiple adjacent radar operation without interference, and
  - (e) very high range resolution capability for precision tracking and target identification.
3. High absorption around transmission windows, which provides
    - (a) secure operation, if required, by selecting a frequency with higher absorption, and
    - (b) difficulty of long-range jamming.
  4. Low scatter from terrain, which provides
    - (a) reduced multipath interference, and
    - (b) reduced terrain clutter.
  5. Penetration of dry contaminants in atmosphere, which provides good operation under limited visibility conditions of dust, smoke, and dry snow.
  6. Small targets become an appreciable part of a wavelength, which provides good capability of detecting wires, poles, trees, projectiles, birds, and insects.
  7. Doppler frequency is high from low radial velocity target, which provides good detection and recognition capability of slowly moving or vibrating target; doppler frequencies are typically conveniently in the audio range.

There are also limitations with millimeter wave radars which include the following:

1. Reduced range in adverse weather
  - (a) Rain, wet snow, and fog of high moisture content will reduce the range by attenuation that sometimes can be overcome with higher power, greater antenna gain and optimum modulation and data processing.
  - (b) Rain produces rain backscatter which can mask targets; the use of MTI, narrow antenna beamwidths, narrow pulse widths, and optimum operating frequencies will minimize rain backscatter effects.

## 2. Poor foliage penetration

- (a) There is little or no penetration of dense green foliage; which is also true at microwaves.
- (b) There is some penetration through the openings between leaves and branches which improves with increasing frequency. Visually obscured aircraft have been tracked behind trees at 70 GHz.

## 3. High cost of components

- (a) Currently most millimeter wave components are expensive, largely because of lack of high quantity production. Recent advances, such as the millimeter wave integrated circuit developments using microstrip and dielectric waveguides, show promise of greatly reducing the cost of components and assemblies.
- (b) Solid state sources are just becoming available from R&D laboratories, with attendant high cost and some limitations on reliability. Quality-controlled high-quantity production should solve these problems.

- 4. Lack of some components necessary for rugged, field model millimeter wave radar designs for operation above 35 GHz such as high-power ( $\geq 10$  kw) transmitters, high-power circulators ( $\geq 1$  kw), low-loss radomes, low-loss and compact receiver protectors, and monopulse antenna feeds. Some design and development work has been done on these items, but they have not been developed to a stage where they have been produced in quantity or ruggedized for field use.

## B. Ground-to-Air Millimeter Wave Radar Characteristics

1. General. A narrow beamwidth, millimeter wave radar is particularly well suited for tracking low-altitude aircraft since no appreciable ground clutter is intercepted and the sky background gives a high target-to-background contrast. When the aircraft is at tree-top level at very long ranges, the tree background return can present a problem in obscuring the aircraft return. However, the use of a narrow range gate will eliminate the obscuring problem except when the front edge of the tree line is at the range of the aircraft. The use of MTI and automatic tracking circuits with predicted aircraft velocity and acceleration will aid in keeping lock during short periods of high background and tree clutter.

2. Radar Return from Helicopter. To better assess the magnitude of the helicopter radar return and the ground and tree clutter problem, measurements were made of the radar return at 70 GHz while tracking a helicopter at low altitudes above and behind trees. The radars used are described in Tables II and III and are shown in Figures 12-14.

A UH-1 helicopter was flown above and behind trees and over water at an altitude of 30 meters in crossing courses and radial flight paths out to a maximum range of about 3 km. A video camera with a zoom telephoto lens was mounted on the radar antenna to record the aircraft position and its surroundings. A second video camera was trained on the A-scope of the radar to record the transmitted pulse and received echoes. The outputs of the two video cameras were mixed and recorded on a  $\frac{1}{4}$ -inch video tape recorder.

Example of flight records where manual tracking was used are shown in Figures 15 to 23; these are photographs of the video tape operating in the playback stop-action mode. The A-scope trace is shown in the lower portion of the photograph, with the transmitted ( $T_0$ ) pulse at the extreme left. The narrow, jitter-free quality of the original radar pulse returns is lost in these photographs taken of the video monitor, but the amplitude of the return and the absence of clutter can be seen. While viewing the tapes in motion, the rate and amplitude of the fluctuation of the radar returns can also be seen.

Figures 15 to 17 show the helicopter at a range of about 1.2 km and an altitude of 30 meters flying a crossing course just visible above the trees but beyond the front edge of the tree line, which is at a range of 240 meters. The strong aircraft return echo completely clear of ground and tree clutter can be seen. It is interesting to note that in Figure 17, where the main body of the helicopter is behind the trees and only the tail rotor is exposed, a strong echo is still received. In Figure 18, the entire helicopter is behind the trees and completely visually obscured, but a strong echo is still received by propagation through the openings among the leaves and branches. The tree return is also strong, but it is at a much shorter range since the radar reflection from trees is essentially all from the front edge of the tree line.

Figures 19 and 20 are from radial runs of the helicopter flying at an altitude of 30 meters with the line-of-sight just above the top of the trees. Since the antenna beam is only 6 meters wide at 1 kilometer, the helicopter must be very close to the trees and at the same range before the tree return will compete with the helicopter return. Figure 20 shows the propagation of the radar signal through a small gap between the trees. The helicopter at 0.91 km is giving a strong, clear radar return.

TABLE II

BRL 70-GHz TRACKING RADAR

Power, 10 kw peak, 5 watts average  
Pulse width, 50 nanoseconds  
PRF, 10 KHz  
Antenna, 0.92 m (3-foot) parabolic reflector  
Beamwidth, 0.34 degrees  
Beam scanning, conical  
Polarization, vertical  
Antenna Mount, automatic track and manually trainable via optical sight  
Transmitter-Receiver, from AN/MPS-29 Search Radar built by Georgia Institute of Technology for the U.S. Army Signal Corps.

TABLE III

UNITED AIRCRAFT CO., NORDEN DIV., 70-GHz RADAR

Power, 500 watts peak, 0.25 watts average  
Pulse width, 50 nanoseconds  
PRF 2-10 KHz  
Antenna, 0.92 m, (3-foot) parabolic reflector  
Beamwidth, 0.34 degrees  
Beam scanning, none  
Polarization, horizontal, vertical, right- or left-hand circular with any combination for transmit and receive  
Antenna mount, manually trainable

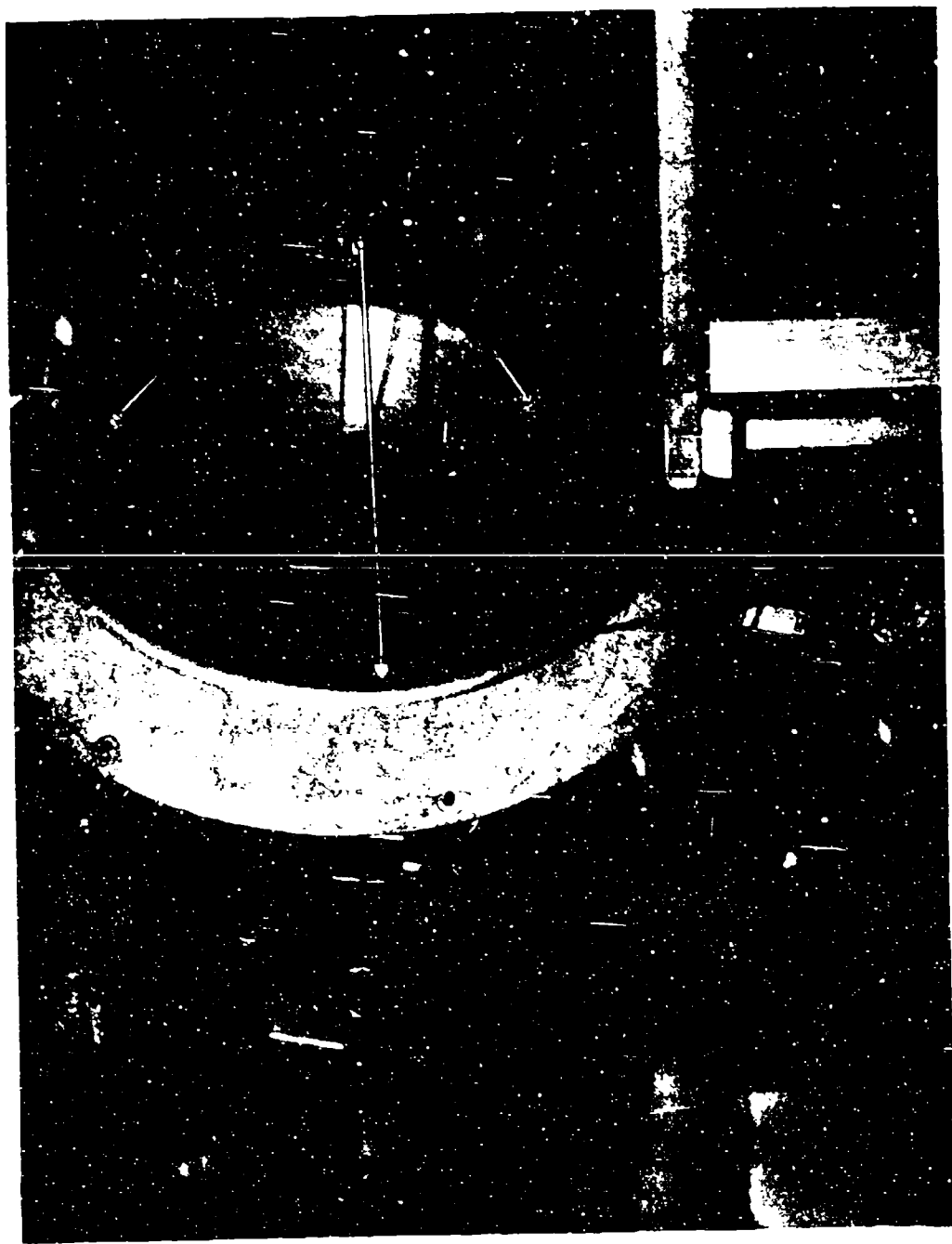


Figure 12. BRL 70-GHz Tracking Radar Antenna and Mount



Figure 13. BRL 70-GHz Tracking Radar Interior Showing A-Scope  
TV Recording

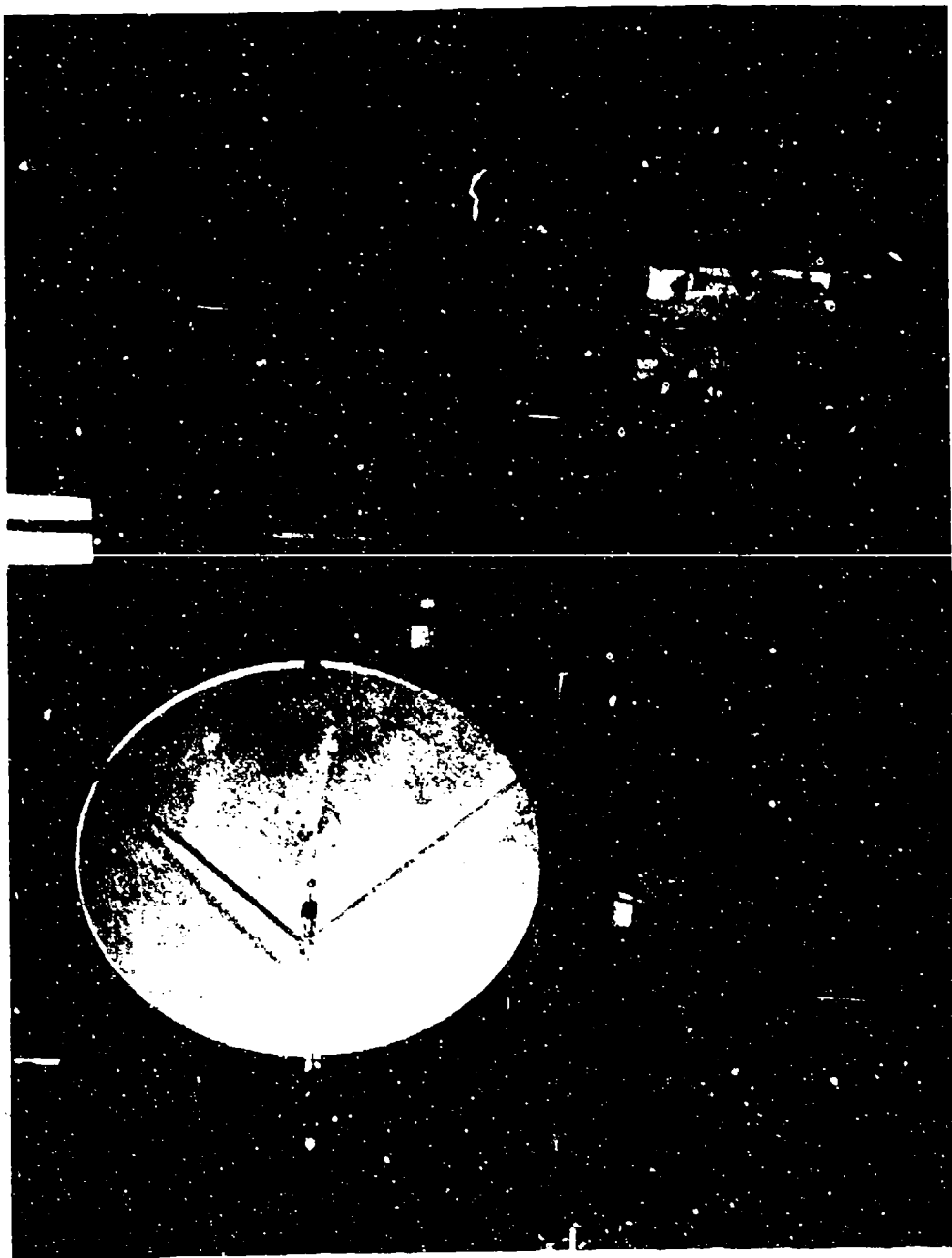
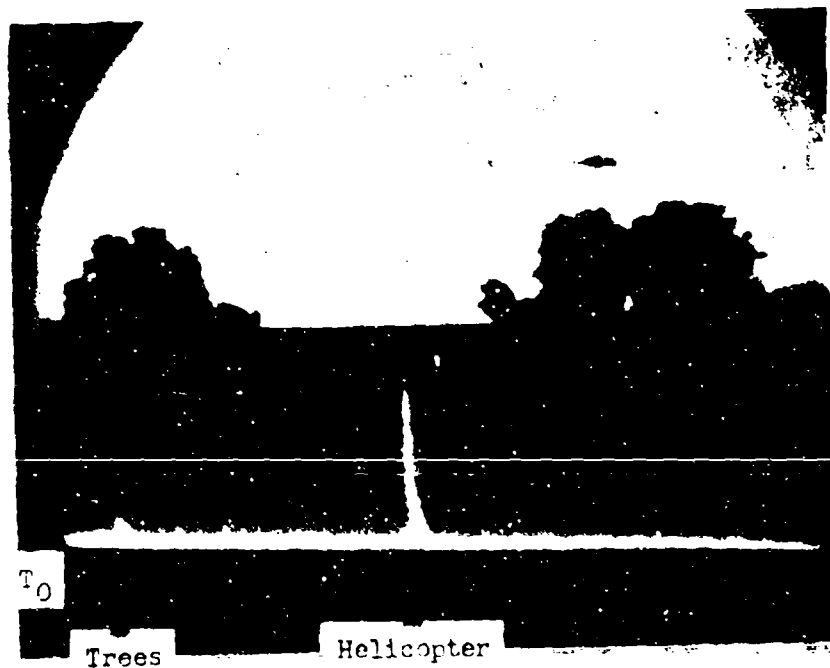


Figure 14. Norden 70-GHz All-Polarization Radar

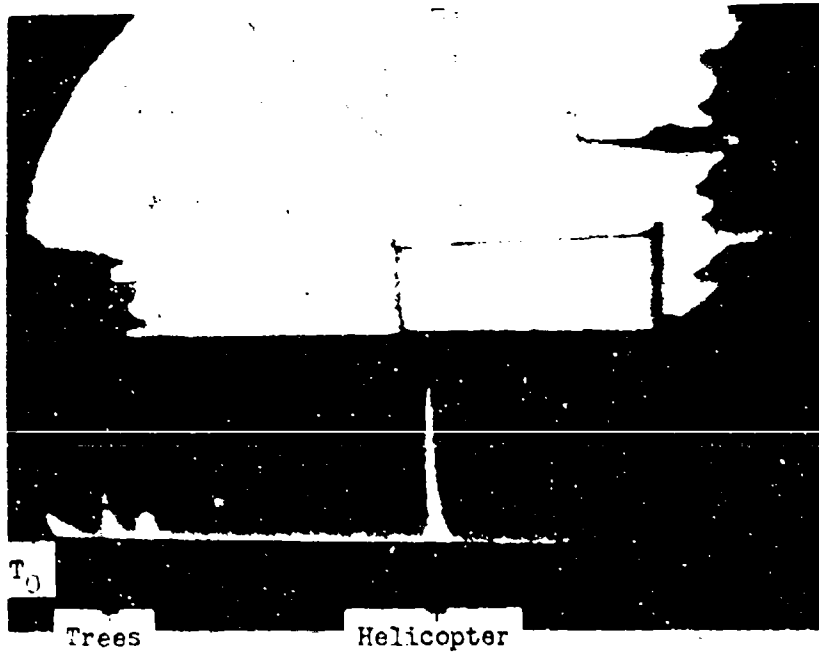


TARGET: UH-1B Helicopter

LOCATION: Flying Cross Course at 1.28 km, 30 meters  
Altitude, Close to Tree Top Level

RADAR: 70 GHz Norden

Figure 15. Helicopter Flying Crossing Course

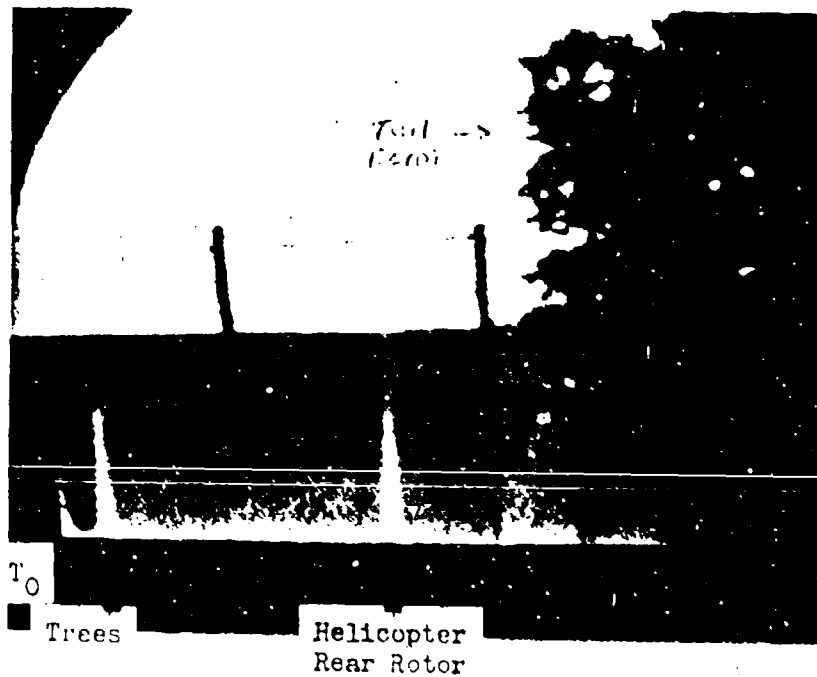


TARGET: UH-1B Helicopter

LOCATION: Flying Cross Course at 1.15 km, 30 meters  
Altitude, Going Behind Trees

RADAR: 70 GHz Norden

Figure 16. Helicopter Flying Crossing Course, Going Behind Trees



TARGET: UH-1B Helicopter

LOCATION: Flying Cross Course at 1.28 km, 30 meters  
Altitude, Main Body Behind Trees, Tail Rotor  
Exposed

RADAR: 70 GHz Norden

Figure 17. Helicopter Flying Crossing Course, Only Tail Rotor Exposed



Trees

Helicopter

TARGET: UH-1B Helicopter

LOCATION: Flying Cross Course at 1.28 km, 30 meters  
Altitude, Completely behind trees.

RADAR: 70 GHz Norden

Figure 18. Helicopter Flying Crossing Course, Completely Obscured by Trees



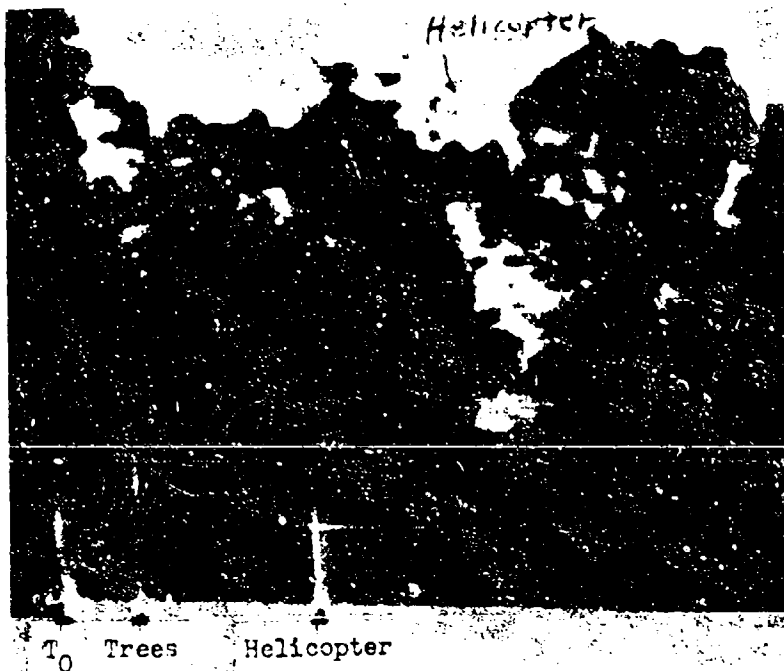
Trees Helicopter

TARGET: UH-1B Helicopter

LOCATION: Flying North-South Course, Range 455 meters,  
30 meters Altitude, Close to Trees

RADAR: 70 GHz Ballistic Research Laboratories

Figure 19. Helicopter Flying Radial Course, Just above Trees



TARGET: UH-1B Helicopter

LOCATION: Flying North-South Course, Range 910 meters,  
Between Gap in Trees

RADAR: 70 GHz Ballistic Research Laboratories

Figure 20. Helicopter Flying Radial Course, Behind Heavy Tree Cover  
but Visible Through Gap



T  
O

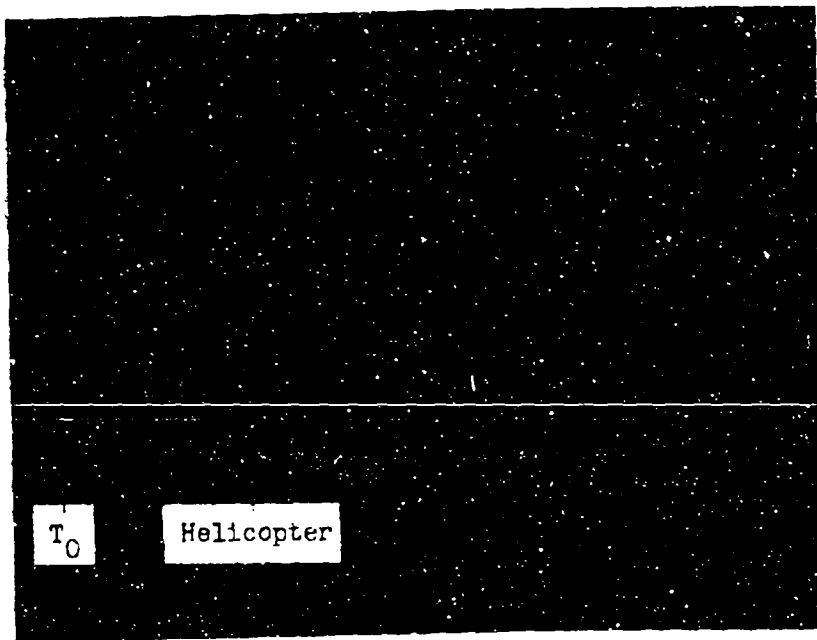
Bird Helicopter

TARGET: UH-1B Helicopter and Bird

LOCATION: Hovering at 670 meters Range, 7.5 meters  
Altitude. Bird at 400 meters.

RADAR: 70 GHz Ballistic Research Laboratories

Figure 21. Helicopter Hovering 7.5 Meters Above Water



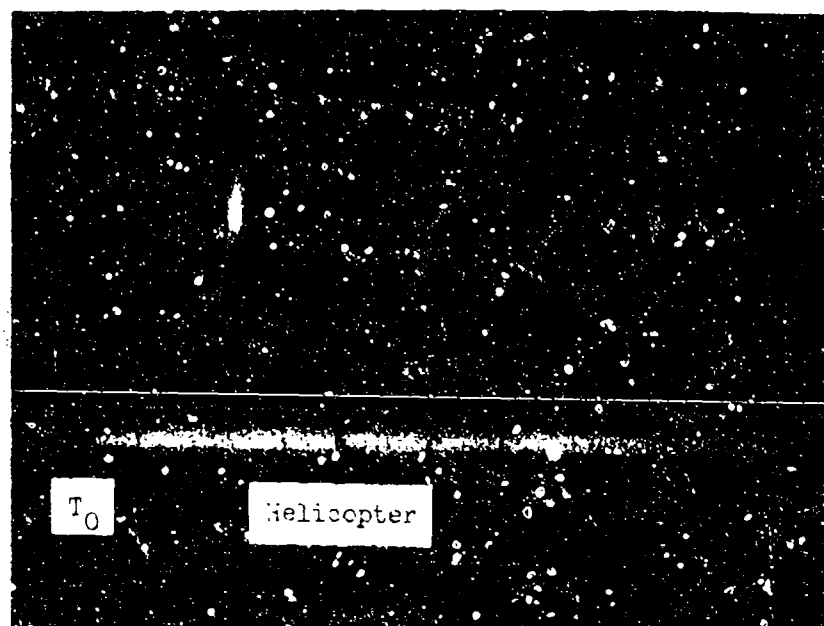
TARGET: UH-1B Helicopter

LOCATION: Hovering at 820 meters Range, 7.5 meters  
Altitude

RADAR: 70 GHz Norden

SWEEP: 2 microseconds/div; 1000 ft/div; 304 meters/div

Figure 22. Radar Return from Helicopter Hovering, Direct A-Scope Photograph



TARGET: UH-1B Helicopter

LOCATION: Flying Cross Course at 1.13 km, 30 meters  
Altitude just above Tree Top Level

RADAR: 70 GHz Norden

SWEEP: 2 microseconds/div; 1000 ft/div; 304 meters/div

Figure 23. Radar Return from Helicopter Flying Crossing Course over  
Trees, Direct A-Scope Photograph

Figure 21 shows the helicopter hovering 7.6 meters above the water at a range of 670 meters. The radar return is strong and clear without any clutter. The received signal was recorded as the helicopter slowly rotated in azimuth, presenting all aspects to the radar. A fortuitous circumstance happened while taping this run in that a bird flew across the beam, which shows up clearly as an echo at 460 meters.

Figures 22 and 23 show the radar pulse return from the helicopter as photographed directly from a fast-response oscilloscope. The narrow, jitter-free pulse and clutter-free return is more clearly shown in these photographs than in the previous photographs of the video tape playback. The signal-to-noise ratio is greater than 40 dB for an effective transmitter power to the antenna of about 200 watts peak and 0.1 watt average for this test.

3. Automatic Tracking Tests. Helicopter flight tests were made with the BRL 70-GHz radar operating in a conical scan, automatic tracking mode to assess (1) the tracking accuracy at low altitudes and close to trees, (2) target glint effects at close ranges, i.e., to determine the effective point of track as the aspect angle of the helicopter was changed, and (3) the acquisition and lock-on characteristics of a narrow beamwidth tracking system. A UH-1 helicopter was flown at an altitude of 30 meters in a circle of about 1.5-km diameter with part of the flight behind trees. Unfortunately the foliage was not very dense at the time of these tests and complete visual obscuration could not be obtained; also, safety limitations prevented flights to a greater range.

Figure 24a shows the field and wooded area over which the helicopter was flown. This photograph gives the general perspective of the test area as viewed with the unaided eye. The black horizontal lines on the photographs are transmitter pulses that leaked into the video camera circuits. A telescopic, zoom lens was used for Figures 24b, c and d to more accurately determine the point of track on the helicopter. The aiming circle has a 2-milliradian diameter and is boresighted to the radar antenna.

Figure 24b shows the helicopter being tracked while approaching the radar. The point of track was consistently the main rotor hub when the helicopter flew toward or away from the radar. Figure 24c shows the helicopter turning to make a crossing run; the radar is still tracking the main rotor hub. When the helicopter was exactly broadside to the radar, as shown in Figure 24d, the radar consistently moved back to track the tail rotor. Tracking accuracy was well within the aiming circle on each of the rotor hubs, with the only region of uncertainty occurring when the helicopter aspect was approaching the broadside orientation.

Acquisition and lock-on was not difficult. The radar antenna was pointed toward the helicopter with the aid of an optical sight to within roughly the dimension of the helicopter, and lock-on always occurred.

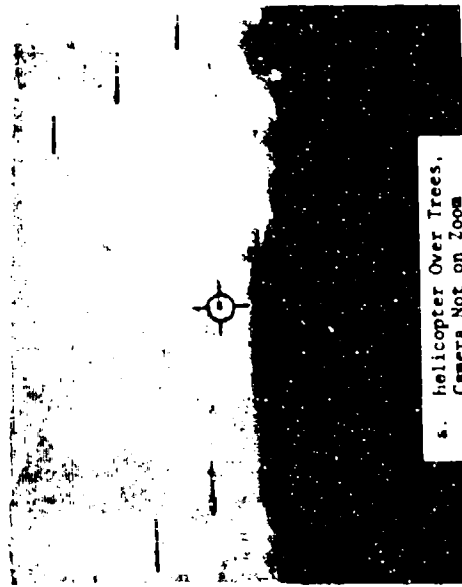
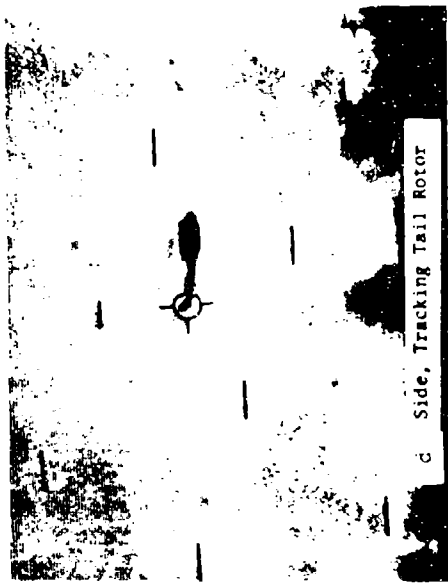
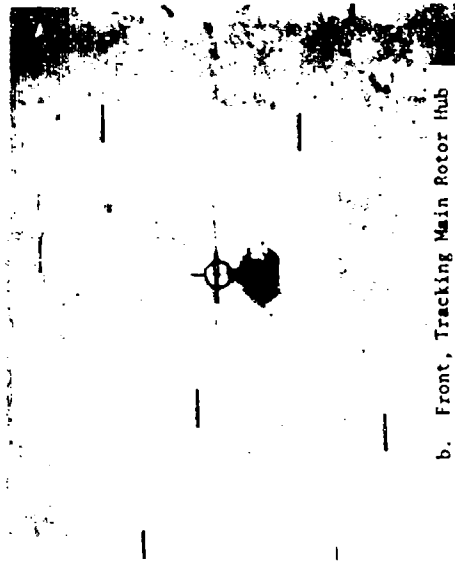
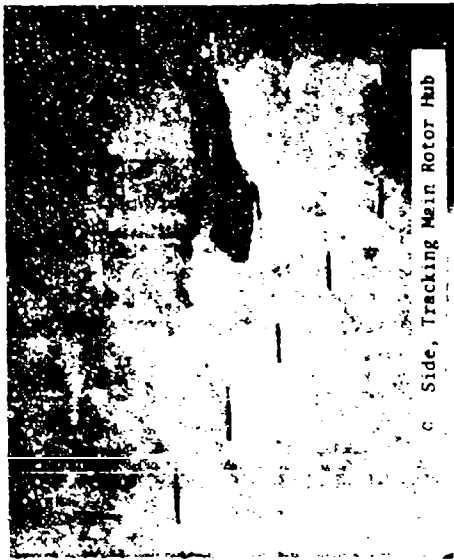


Figure 24. Automatic Tracking of Helicopter with BRL 70-GHz Radar

The radar antenna quickly moved toward the main or rear rotor hub, depending on the orientation of the helicopter.

The helicopter was also tracked while flying behind trees, as shown in Figure 25. Generally good tracking was maintained, although there was considerable modulation of the amplitude of the return caused by foliage obscuration and possibly multipath propagation from the trees. Tracking was much rougher than it was when the helicopter was away from the trees and there was an occasional loss of lock. There was no observable ground clutter multipath effects during any part of these tests.

4. Ground Multipath. When the tracking range is extended or the aircraft altitude is reduced over terrain that has little or no vegetation, a geometric condition will ultimately be reached where the lower portion of the antenna beam will illuminate the earth simultaneously with the target. The radar signal can then reach the target and return to the radar by a direct path and by way of reflection from the earth and/or scatterers on the earth. This multipath situation usually only becomes serious under geometrical conditions where the angular separation between the direct and reflected wave is comparable to or less than the antenna elevation beamwidth, e.g., a target altitude less than 20 meters at 5-km range when a 1-meter-diameter radar antenna is used at 95 GHz. The reflected wave is then not suppressed by the antenna directivity. The net effect of strong multipath propagation on radar performance is to cause errors in antenna pointing and ranging and to severely modulate the received signal amplitude, causing deep fades and possible loss of automatic track. The effect on tracking is to make the antenna point above and below the true target direction in a cyclic manner as the reflected wave goes alternately in and out of phase with the direct wave. The cyclic rate can vary from near zero to frequencies of many hertz. If the cyclic rate is within the antenna drive servo passband, the antenna will follow the apparently widely changing angle of arrival of the multipath signal. If the reflected signal is large and reaches a critical value, the swing of the antenna can approach the antenna beamwidth. If the reflected signal strength goes above this critical value, the antenna will swing down to the image direction and cycle above and below this point; however, this is not a stable condition and the antenna can swing erratically between the direction of the target and the image, usually causing loss of track.

One of the simplest techniques for reducing low-elevation-angle multipath tracking error is off-boresight tracking.<sup>4</sup> The antenna boresight is maintained at an elevation above the target with the exact

---

<sup>4</sup>W.H. Bockmiller and P.R. Dax, "Radar Low Angle Tracking Study," NASA Contract Report No. 1387, Westinghouse Electric Corp., Baltimore, MD, June 1969.

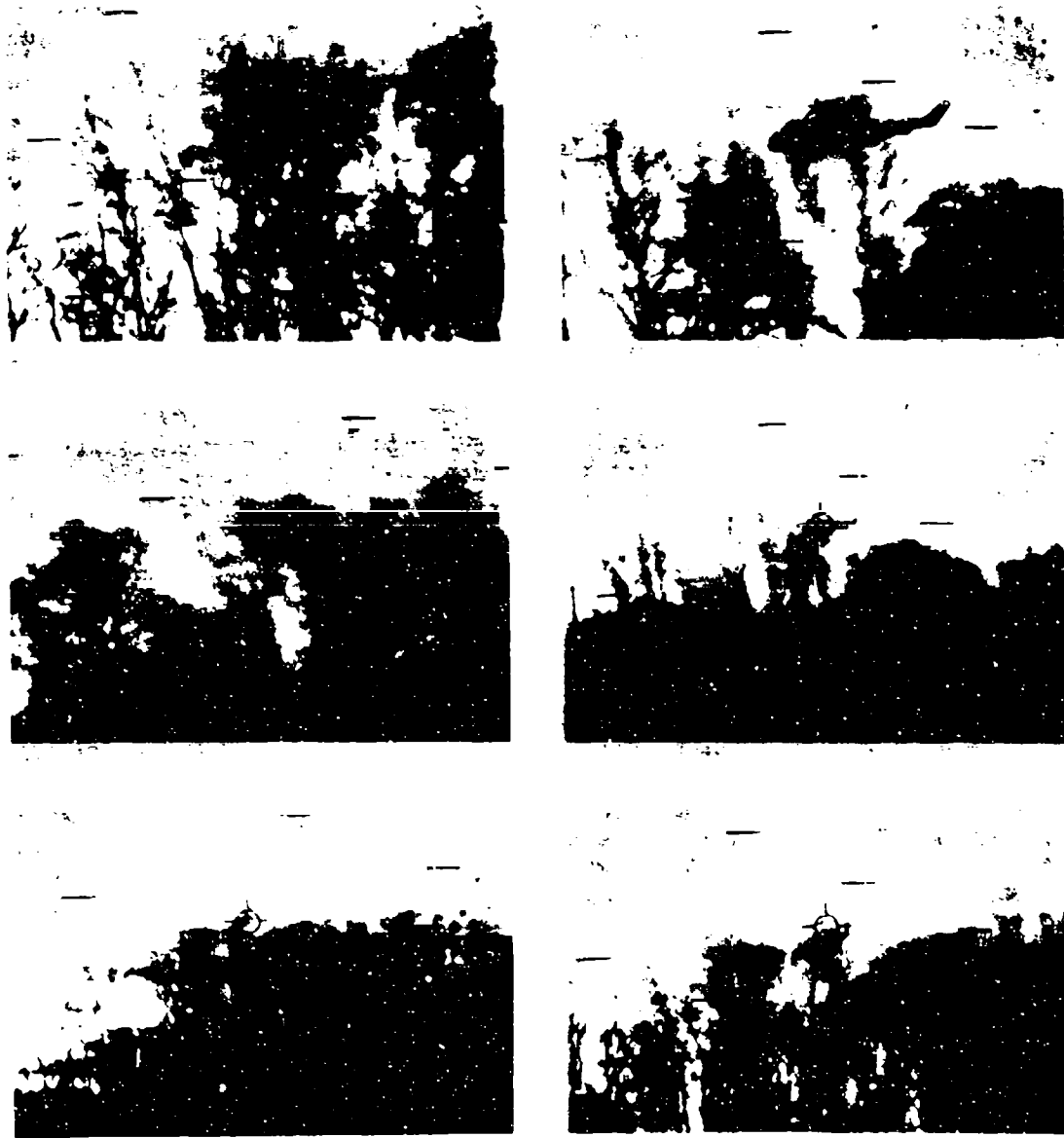


Figure 25. Automatic Tracking of Helicopter Behind Trees

elevation angle depending upon the radar antenna pattern shape and site conditions. This technique works on the principle that the multipath signal is reduced more than the target signal because of the steep falloff of the antenna pattern. Off-boresight tracking has been effective in preventing gross swings of the antenna and enables continuous automatic track until the target range is reduced enough to operate in the normal on-axis track mode.

Another very effective technique for reducing multipath effects is to change the frequency of the transmitted signal sufficiently to cause the error to go through a complete cycle during the time period of measurement. Thus, the multipath error can be averaged out. This technique is called either frequency agility, swept frequency, frequency diversity, or spread spectrum operation. The transmission frequency can be changed by different waveforms such as sinusoidal, triangular, or in random noise fashion. A theoretical study and experimental investigation of wideband swept frequency methods for reducing multipath effects have been made at BRL.<sup>5</sup> The results are very impressive not only in suppressing multipath but in increasing the target-to-background contrast ratio where the background clutter is caused by scintillation, target vibration, and wind-blown vegetation. Enhanced angular resolution and improved signal-to-noise ratios have been demonstrated.

### C. Ground-to-Ground Millimeter Wave Radar Characteristics

1. General. Ground-located microwave radars which operate against ground targets are typically subject to severe performance degradation from multipath propagation, foliage obscuration, terrain masking, clutter, and natural or man-made false targets. If an appreciable portion of the antenna beam intercepts the terrain, the radar performance can be limited because of one or more of the above factors. Ground multipath and clutter do not usually limit the performance of millimeter wave ground-to-ground systems as seriously as foliage obscuration, background clutter, and terrain masking. Operation in the millimeter wavelength region with a narrow beamwidth antenna and a short transmitted pulse or wide bandwidth frequency modulation aids sufficiently in operating successfully close to the ground.

---

<sup>5</sup>R. McGee, "Multipath Suppression by Swept Frequency Methods," Ballistic Research Laboratories Memorandum Report No. 1950, November 1968, AD 682728.

2. Multipath. Experimental studies have been made at BRL on millimeter wave multipath pointing errors when propagating very close to the ground.<sup>6-13</sup> Multipath pointing errors have also been measured with a 140-GHz bistatic radar.<sup>14,15</sup> In general, the maximum pointing error in elevation over grassy terrain was observed to be less than plus or minus one-tenth of the 3-dB beamwidth.

- 
- <sup>6</sup>K.A. Richer, "4.4 Mm Wavelength Near Earth Propagation Measurements (U)," Ballistic Research Laboratories Memorandum Report No. 1403, May 1962 (Confidential), AD 331098.
- <sup>7</sup>C.L. Wilson, "Antenna Pointing Errors in Simultaneous Lobing Antenna System," Ballistic Research Laboratories Technical Note No. 1453, June 1962, AD 608997.
- <sup>8</sup>C.L. Wilson, "Antenna Pointing Errors in Sequential Lobing Antenna System," Ballistic Research Laboratories Technical Note. 1463, May 1962, AD 609009.
- <sup>9</sup>T.W. O'Dell, "Final Report for Missile Guidance Subsystem Feasibility Program - Phase 1A (U)," General Precision Laboratories Report No. P0268 (Confidential).
- <sup>10</sup>T.W. O'Dell, "Final Report for Missile Guidance Subsystem Feasibility Program - Phase 2 (U)," General Precision Laboratories Report No. 14990-2, June 1962 (Confidential).
- <sup>11</sup>N. Leggett, "Final Report, Breadboard Feasibility Study of the Derringer Weapon Guidance System," Bendix Pacific Div. Report No. 91-139-1 (U), May 1963.
- <sup>12</sup>J.E. Kammerer and K.A. Richer, "4.4 Mm Near Earth Antenna Multipath Pointing Errors (U)," Ballistic Research Laboratories Memorandum Report No. 1559, March 1964 (Confidential), AD 443211.
- <sup>13</sup>J.E. Kammerer and K.A. Richer, "4.4 Mm Wavelength Precision Antennas and Mount," Ballistic Research Laboratories Memorandum Report No. 1576, July 1964, AD 449726.
- <sup>14</sup>J.E. Kammerer and K.A. Richer, "140 GHz Millimetric Bistatic Continuous Wave Measurements Radar," Ballistic Research Laboratories Memorandum Report No. 1730, January 1966, AD 484693.
- <sup>15</sup>J.E. Kammerer and K.A. Richer, "Pointing Errors of a 140 GHz Bistatic Radar System Illuminating U.S. Army Targets (U)," Ballistic Research Laboratories Memorandum Report No. 1755, June 1972 (Confidential), AD 375942.

Automatic tracking tests were made with the BRL 70-GHz radar tracking a pickup truck to study multipath and target glint effects. The truck was driven over an irregular course at a range of about 300 meters in a field covered with grass and high weeds. Figure 26a shows the radar tracking the rear edge of the truck as it was driven on a crossing course; this was a consistent tracking point when the truck was broadside to the radar. When the truck turned away from the radar, as shown in Figure 26b, the radar tracked the rear of the cab. Good tracking was maintained when the truck was driven right up to the edge of the woods, as shown in 26c. Figure 26d shows the truck as it is driven on a crossing course. The radar tracked the geometric center of the truck when it was coming toward or going away from the radar, as shown in Figures 26e and 26f.

Lock-on to the truck was easily accomplished either by orienting the antenna toward the truck and switching to automatic or by pointing the antenna ahead of the truck and letting it drive into the beam. Large targets in the field such as a corner reflector and a large wood pole would cause the radar to lose lock on the truck and stay on these targets if the truck was driven past them slowly. If the truck was driven past them at a high speed, the inertia of the antenna carried it past the other targets and the radar remained locked onto the truck. Tracking was generally very smooth and well within the 2-milliradian aiming circle, as can be seen in Figure 25. There was no evidence of multipath within the angular definition of observation using the aiming circle.

The pointing error caused by multipath is dependent upon the type and surface conditions of the terrain, the polarization of the transmitting and receiving antenna, the type of antenna scan, i.e., conical or monopulse, and the type of modulation and signal processing. Propagation over smooth, compacted, flat terrain causes the largest multipath pointing error, which under certain conditions can be as much as the antenna beamwidth; grassy terrain causes the smallest pointing error. The azimuth multipath pointing error is usually random in nature and small; however, if there are large irregularities in the composition or surface conditions in the region of the reflection area, the azimuth errors can also be large.

Monopulse and conical scan multipath pointing errors have been found to be quite similar in magnitude, although the monopulse system tested at 70 GHz had more regions of little or no pointing error as the height above ground was varied.<sup>11</sup>

The use of 140 and 240 GHz for anti-tank beam rider systems looks very promising. Very narrow beamwidths can be obtained with small antennas to obtain high tracking accuracy and avoid ground and back-ground multipath and clutter. The range obtainable in clear and moderately adverse weather appears adequate with the miniaturized, all-solid state transmitters and receivers that are becoming available.

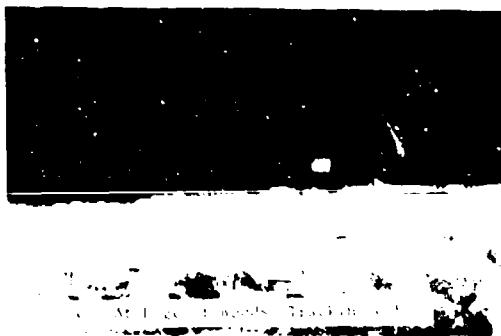
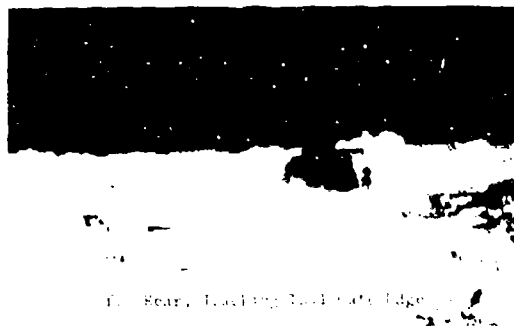
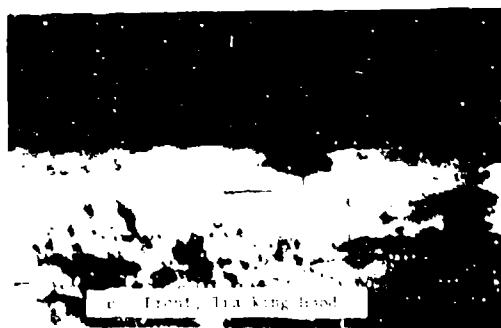


Figure 26. Automatic Tracking of Pickup Truck with BRL 70-GHz Radar

It is interesting to speculate that with a beam rider or a command guidance system, multipath errors might not be serious during the final phase of the flight since both the target and the missile being tracked would be seen by the tracking radar with approximately the same multipath errors. However, one potential problem is that the missile might strike the earth along the flight path if the multipath error has a large downward value.

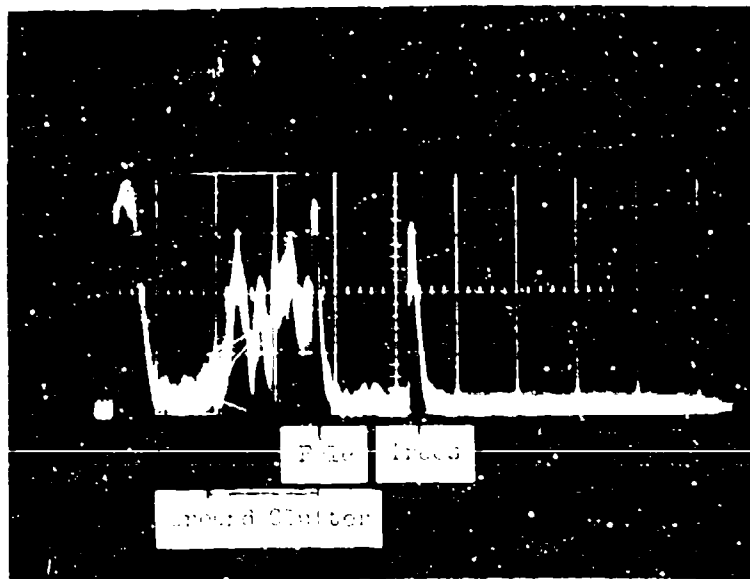
3. Ground Clutter. When narrow beamwidth antennas are used, the ground clutter return from flat terrain is not usually very large unless the antenna is directed downward to the ground. For example, at 70 GHz with a 0.34-degree antenna mounted 1.4 meters above the ground, no ground clutter was seen over flat terrain when the antenna was pointed horizontally; the antenna had to be pointed downward about a beamwidth to get appreciable ground clutter return. Figure 27 shows the clutter from a field of grass and weeds when the antenna was pointed downward 0.26 degree. The antenna was pointed toward the base of the trees at a range of 304 meters. The clutter has a peak value of about 25 dB above the peak receiver noise level.

The magnitude of ground clutter in a ground-to-ground radar application will depend strongly on the terrain features. If the terrain is flat with low vegetation, targets can be seen well above the clutter level. For example, a tank was manually tracked with a 70-GHz radar as an initial experiment to determine the relative magnitude of ground clutter and the tank return. Figure 28 shows the tank manually tracked with a 70-GHz radar whose antenna is about 1.4 meters above the ground. The A-scope trace is shown in the upper portion of the figure. When the beam was pointed at the junction of the turret and the tank body, the strongest signal was received and very little ground clutter was received at the tank range. In Figure 29, the tank has been moved to a low area among high weeds and the clutter is appreciable. A telescopic view of the tank is shown in Figure 29 where the high vegetation around the tank is causing some clutter close to the tank signal. The clutter signal scintillates rapidly and deeply and generally has a much longer risetime than the tank return pulse, which suggests a technique for discrimination of ground clutter from the desired target by pulse risetime gating.<sup>16</sup>

One of the most effective techniques in separating moving targets from background clutter is to use the doppler shift phenomenon where the frequency difference between frequency spectra of fluctuating clutter and doppler-shifted echoes from a moving target is used. The theory of the statistical nature of fluctuating clutter is given in Appendix B, and a description of MTI techniques is given in Appendix C.

---

<sup>16</sup>M.G. Stansbury and C.L. Wilson, "A Signal Processing Pulse Width Discriminator," Ballistic Research Laboratories Memorandum Report No. 2040, June 1970, AD 710230.



TARGET: Ground in Front of Trees

RADAR: 70 GHz Norden

POLARIZATION: Vertical

SWEEP: 0.5 microsecond/div; 200 ft/div; 76.2 meters/div

Figure 27. Ground Clutter at 70 GHz

T<sub>0</sub> Tank



TARGET: M 48 Tank

LOCATION: 365 meters Range, Woods Background

RADAR: 70 GHz Norden

Figure 28. 70-GHz Radar Return from Tank in Clear Field

Tank



TARGET: M 48 Tank

LOCATION: 260 meters; Telephoto Photograph showing  
High Grass

RADAR: 70 GHz Norden

Figure 29. 70-GHz Radar Return from Tank in High Grass

Other techniques for clutter rejection and/or target signal enhancement include the use of (1) a swept frequency radar as described earlier under ground-to-air systems, (2) pulse width and slope discrimination circuits,<sup>16</sup> (3) polarization discernment to identify the target by its polarization characteristics, and (4) target vibration and rotation-induced modulation. This fourth technique is particularly useful on stationary targets where either the engine is running or it is windy, since at short wavelengths small physical movement of a reflector causes a large fluctuation in received signal strength at the rate at which the reflector is vibrating or rotating or being blown about.

4. Foliage Obscuration. Foliage obscuration at millimeter wavelengths is quite high; there is essentially no penetration directly through dense green foliage. The propagation through the openings between foliage components has been studied at BRL with a 35-GHz radiometer where a comparison was made between the millimeter wave and the optical blockage.<sup>17,18,19</sup> Millimeter wave obscuration was found to be greater than originally predicted as based on the optical obscuration.

#### D. Air-to-Ground Millimeter Wave Radar Characteristics

Airborne radars operating against ground targets generally suffer from target acquisition problems, foliage obscuration, and ground clutter. Radars operating at millimeter wavelengths with narrow antenna beams will give high resolution of ground targets. A narrow antenna beamwidth will also reduce the ground clutter, but dense foliage obscuration will not be helped. However, where the foliage is sparse, the target might be seen because of the high resolution of angle and range.

Ground mapping for area surveillance and target acquisition can be done exceptionally well at millimeter wavelengths. The resolution obtained with narrow antenna beams is sometimes high enough for real-time, forward-aspect signal recording which is much simpler than the side-looking, synthetic aperture type system with its complex data processing and lack of coverage forward.

The use of millimeter wavelengths for Instrument Landing Systems (ILS) applications offers advantages of very high resolution and accuracy with acceptable aircraft antenna size.

---

<sup>17</sup>R. McGee, "Millimeter Wave Radiometric Detection of Targets Obscured by Foliage," Ballistic Research Laboratories Memorandum Report No. 1901, January 1968, AD 667962.

<sup>18</sup>R. McGee, W. Sacco and W. Lese, "Effects of Obscuration on Millimeter Wave Signatures of Targets," Ballistic Research Laboratories Memorandum Report No. 1962, February 1969, AD 684900.

<sup>19</sup>R. McGee, "A Foliage Obscuration for Passive Radiometric Detection System," Ballistic Research Laboratories Memorandum Report No. 1999, July 1969, AD 858380.

Given that the target is acquired and designated, a millimeter air-to-ground system should provide excellent gun-aiming accuracy or weapon delivery guidance and terminal homing. The multipath and terrain masking problems will not be as severe as in ground-to-ground applications.

#### E. Target Acquisition Millimeter Wave Radar Characteristics

The use of millimeter wave sensors for target acquisition holds promise for performing all the functions involved in acquisition such as the volume search; detection of presence of a target; discrimination of target from clutter and false targets; identification by gross category such as a moving tank, truck, rotary-wing or fixed-wing aircraft; location; automatic tracking for determination of range, radial velocity, and azimuth and elevation angles; assignment of target to a weapon for engagement; and assessment of the damage by the indication of cessation of movement or absence of signal return. The sensor could operate in either the pulse, FM/CW, or spread-frequency spectrum modes.

A millimeter wave target acquisition system will, of course, be limited by the handicaps already discussed (reduced performance in rain, foliage obscuration, terrain masking, clutter, and natural and man-made false targets) plus the inherent problem of a longer search time or more rapid scan rate requirement associated with searching a large volume with a narrow beamwidth. Some applications, such as an antiaircraft gun fire control search radar used against low-flying aircraft, require only limited elevation search, primarily at the horizon. These low-altitude search systems reduce the search volume appreciably and make the use of a narrow beamwidth search radar feasible. In addition, multiple-beam search antennas can be used to reduce the time required to search out a large volume. In view of the recent development of potentially low-cost integrated circuit receivers, the multiple-beam concept is becoming more feasible.

A millimeter wave target acquisition sensor would have a number of advantages and possibilities, such as:

1. Small targets can be detected since they will be an appreciable part of a wavelength.
2. Dry contaminants in the atmosphere such as smoke, dust, smog, and dry snow do not affect performance.
3. The absorption in the atmosphere and the narrow beams make detection and jamming by the enemy difficult at long ranges.
4. High angular resolution permits effective separation of the desired target from nearby scatters for effective target discrimination from natural and man-made objects.

5. A very narrow beam allows operation of the sensor close to the ground and acquisition of low-altitude targets with a minimum of ground multipath and ground clutter interference.

6. The combination of narrow beam and narrow transmitted pulse greatly improves the target-to-clutter ratio and permits design of a very effective MTI system for the detection of slowly moving targets hidden in clutter. At millimeter wavelengths, the doppler frequencies resulting from small radial velocities are in the audio frequency range and are convenient to process.

7. Stationary and moving targets have unique detectable signatures if there is some vibration or rotary motion of a component that is a millimeter wave reflector. It is possible to detect very small (millimeter) movements of reflectors since such movements are an appreciable part of a wavelength and cause a large change in the phase of the reflected signal. The phase-modulated reflected signal combines vectorially with the gross reflected signal from the main body of the target, resulting in an amplitude modulation at a rate proportional to the vibration or rotation rate. The success of this technique is dependent upon the difference in the spectra of the target and the clutter.

A millimeter wave radar used in conjunction with an acoustic sensing system (which has a good capability to detect and identify audio noise-emitting targets) would provide accurate target location and tracking information. The acoustic signature of the desired target would serve to aid the radar in acquiring the target by matching the spectrum of the acoustic signal with that of the rotation and/or vibration doppler modulation on the radar signal.

8. Wideband spread-spectrum operation provides good target-to-clutter enhancement by averaging out the clutter as described previously.

9. Extremely high range resolution techniques offer promise for the identification or recognition of spatial features of targets. For example, an FM/CW radar that has 15-cm resolution and a 4.5-mil, 3-db beamwidth has been investigated at BRL.<sup>20</sup> Good depth feature resolution is possible with this type of radar.

---

<sup>20</sup>J. E. Kammerer, "A 94 GHz FM-CW Radar with Six-Inch Range Resolution Capability," Ballistic Research Laboratories Memorandum Report No. 2235, September 1972, AD 908485L.

#### IV. MILLIMETER WAVE RADAR AND COMPONENT STATUS

##### A. Existing Radars

A number of radars operating at millimeter wavelengths have been built for military applications which are indicative of component availability and technology status. Most of them have been at the low frequency end of the millimeter wave band in the 33 to 36 GHz region, called the  $K_a$  band, and also called bands K-7(32-34 GHz) and K-8(34-36 GHz).

Following is a list of  $K_a$  band radars and applications:

<u>Application</u>	<u>Identification</u>
Weather Radars	AN/APQ-39 AN/APQ-70
Star Radars (Side-Looking Mapping)	AN/APQ-55, -56, -79, -86, -97 AN/APQ-7, -8, WX-50
Forward-Scanning Mapping Radars	AN/APQ-113( $K_a$ ), -144( $K_a$ )
Navigation Radars	AN/APQ-57, -58
Terrain-Avoidance and Terrain-Following Radars	AN/APQ-89
"MOTARDES" Doppler Airborne Radar	AN/APQ-137
Mapping and Search Radar	AN/APN-61
Carrier Landing Radars	AN/SPN-10, -41, -42
Sea Clutter Measurement	Instrumentation Radar, GIT Georgia Institute of Technology, Atlanta, GA
Cross Section Measurement	Instrumentation Radar, RATSCAT Air Force Special Weapons Command, Holloman AFB, NM
Lunar Radar	Experimental, MIT, Cambridge, MA
Low-Angle Tracking Over Water	Experimental, Naval Research Laboratory, Washington, DC
Anti-Tank Missile Terminal Homing, FM/CW and Noise/FM Solid State Radar	TGSM Project, BRL and Sperry for Missile Command, Redstone Arsenal, AL
Tracking and Cross Section Studies, Pulse/FM Solid State Radar	Experimental, BRL

Fewer military radars have been built for the higher frequency end of the millimeter wave band; most of them are in the experimental or prototype stage. Following is a list of radars operating between 70 and 140 GHz.

<u>Application</u>	<u>Freq.</u>	<u>Identification</u>	<u>Source</u>
Side-Looking Mapping Radar	70 GHz	AN/APQ-62	
Search Mapping Radar	70	JR-9	Raytheon
Search Radar	70	AN/BPS-8	
Search and Surveillance	70	AN/MPS-29	GIT
Search and Surveillance	70	Experimental	Harry Diamond Lab., Wash., DC
Aircraft Obstacle Avoidance Aircraft Instrument Landing Monopulse Tracking	70	Experimental	Norden Div. of United Aircraft, Norwalk, CT
Low-Altitude Aircraft Tracking	70	Experimental	BRL
Obstacle Avoidance Sea Clutter Measurement	95	"	NADC, Warminster, PA
Space Object Identification	95	"	Aerospace Corp., El Segundo, CA
Arctic Terrain Avoidance Airborne Obstacle Avoidance	95	"	Applied Physics Lab., Silver Spring, MD
Airborne Applications Terrain Imaging Instrument Landing Short Range Weapon Delivery Sensor Cueing	95	"	Goodyear Aerospace Corp., Litchfield Park, AZ
FM/CW and Noise/FM Radar for Clutter Suppression and Fine Range Resolution	95	"	BRL
Pulse/FM Solid State Radar for Tracking and Cross Section Measurement	95	"	BRL
Pulse/FM Solid State Radar for Beam Rider	140	"	BRL
Bistatic CW Radar for Cross Section and Propagation Measurements	140	"	BRL
Pulse/FM Solid State Radar Studies	220	"	BRL

A number of organizations outside the United States also have developed millimeter wave radars for military and commercial use.

#### B. Radar Components

At 35 GHz low-power, solid state transmitters, high-power transmitters up to 150 kw, and all of the other necessary system components and test instrumentation are commercially available to build and test radars.

At 95 GHz, low-power transmitters (1.5 watts peak), solid state sources, and a complete line of components and test instrumentation are available. For high-power transmitters in the 5- to 10-kw range, magnetrons and distributed interaction klystrons have been built. An extended interaction oscillator type tube has been proposed, but additional development, ruggedization, and reliability improvements are needed before any of these tubes can be put into field use. High-power circulators, compact receiver protectors, low-loss radomes, and monopulse tracking antennas are not now commercially available at 95 GHz.

At 140 GHz, low-power klystrons, solid state sources, Carcinotrons, and extended interaction oscillator type tubes are available, with the latter having an 80-watt CW output capability. In the 220- to 240-GHz region, klystrons, Carcinotrons, and extended interaction type oscillators are available, with the latter having a 10-watt CW output capability.

Mixers with very low noise figures are available; for example, noise figures of 4 dB at 35, 8 dB at 95, and 13 dB at 140 and 220 GHz are available. The Schottky barrier diodes used in these mixers are sensitive to burnout and, therefore, very high isolation receiver protectors are needed when they are used with high power transmitters.

Unfortunately, in general, currently available millimeter wave components are expensive, critical to use and generally have short life when they handle much power or are exposed to transients. This situation exists largely because of the newness of the field, the small volume of usage, and the small amount of reliability engineering being applied. A similar situation prevailed when microwave components were in their infancy. Today we have the advantage, however, that much of the technology for working to extremely small tolerances and with solid state devices is already well advanced.

#### V. TECHNOLOGY ADVANCES REQUIRED

The areas in which technology advances and basic data not now available are required in order to fully employ millimeter wave sensors are as follows.

#### A. Weather Effects

Additional experimental studies are needed at frequencies above 95 GHz to supplement the theoretical data that now exist. These data are needed to predict the maximum range of systems which must operate in adverse weather.

#### B. Target and Background Signatures

There is a great dearth of data on target cross sections and signatures with and without camouflage on the target and general terrain and background clutter data in the millimeter wave region. Particularly needed are power spectral density and probability density function data to optimally design radar systems for effective target acquisition and accurate tracking.

#### C. Basic Propagation Characteristics

Basic propagation data on foliage obscuration, multipath, clutter, multiple target, and glint effects are needed for very narrow beamwidth, short pulse, high range resolution FM/CW, and spread spectrum millimeter wave radars. Included in this study would be the effects and possible improvements of frequency and/or polarization agility in the conical scan and monopulse modes of operation. These data are needed to determine the tracking accuracy of these special types of radars where the beamwidth is so narrow and the range resolution is so high as to be comparable to the target or clutter source dimensions.

#### D. Target Acquisition Techniques

There is a need for practical, low-cost, and reliable techniques for the implementation of the complex data processing procedures required to acquire targets in difficult environments.

#### E. Component Improvement and Development

Improvements and new developments are needed on the following millimeter wave components:

1. Duplexers and mixer diode protectors for high-power ( $> 10$  kw) pulse radars that have low insertion loss, adequate isolation to prevent diode burnout, and fast recovery.
2. High-power ( $> 10$  kw) sources that have long life and high reliability.
3. Rapid antenna beam scan techniques, electronic or mechanical, with low loss, for target search and acquisition.

4. Radomes with low loss and low boresight shift.
5. High-power (1 to 10 kw) coherent sources or amplifiers for doppler systems.
6. Low-power (1-watt), pulsed, solid state sources at 140 and 240 GHz.
7. Low noise mixers at 140 and 240 GHz.

## VI. CONCLUSIONS

There are a number of possible military applications of millimeter wave technology where operation at these short wavelengths offers unique and distinct advantages. Following are suggested applications.

### A. Ground-to-Air

1. Target acquisition, particularly effective against low-altitude aircraft.
2. Gun fire control with complete solution radar and possibly closed-loop fire control, particularly effective against low-altitude aircraft.
3. Range-only radar with rapid data acquisition for very short time on the air operation for security.
4. Active seeker for terminal homing on projectile or missile.
5. Tracking radar for missile guidance in beam rider, command, or semi-active mode.
6. Firing error or miss-distance indication of projectiles or missiles with capability of rapidly providing trajectory and precision velocity data.
7. Weather radar, for acquisition of meteorological data with high spatial resolution at short ranges.

### B. Ground-to-Ground

1. Ground target acquisition, with best possibilities of working against targets that have some linear or rotary motion or vibration.
2. Anti-mortar radar where the small size and light weight of the antenna is a much needed advantage.

3. Bullet detector and incoming projectile sensor to quickly determine trajectory and source of incoming projectiles.

4. Anti-tank missile or projectile guidance by beam rider or command guidance technique.

5. Artillery rocket tracking immediately after launch to measure and correct for tipoff and ground wind effects.

C. Air-to-Ground

1. Target acquisition.

2. Side-looking and forward-scanning terrain-mapping radar for reconnaissance, target acquisition, and damage assessment.

3. Terrain-following and obstacle-avoidance radar.

4. Instrument landing monitor (ILM) system.

5. Anti-radiation missile (ARM) seeker head.

6. Anti-tank missile guidance by terminal homing of sub-missile (TGSM) or command guidance by sensor cueing.

7. Radar guided bomb.

8. Gun fire control radar against ground targets such as trucks, tanks, and missile launchers.

VII. ACKNOWLEDGEMENTS

The millimeter wave radar study described in this report is the result of group efforts of a number of persons in the Microwave Systems Branch of the Concepts Analysis Laboratory, BRL. In particular, John Kammerer, Harvey LaFon, Lt. Richard Aulroy, and Lt. Bruce Szypot made significant contributions.

The appendices were prepared for BRL by K. L. Koester, Dr. L. Kosowsky, and J. F. Sparacio of the Norden Division of United Aircraft, Norwalk, Connecticut.

#### REFERENCES

1. V.W. Richard and J.E. Kammerer, "Rain Backscatter Measurements and Theory at Millimeter Wavelengths," BRL Report No. 1838, October 1975, AD 800 8173L.
2. V.I. Rozenberg, "Radar Characteristics of Rain in Submillimeter Range," Radio Eng. and Elec. Physics, Vol. 15, No. 12, 2157-2163, 1970.
3. I.D. Strom, "Applications for Millimeter Radars," System Planning Corp., Arlington, VA, Report No. 108, for ARPA, 31 December 1973 (Confidential), AD 529566; "Adverse Weather Applications for Millimeter Radars on the Battlefield," Paper G.3, NELC/TD 308, 1974 Millimeter Wave  $\lambda$  Technical Conference, Naval Electronics Laboratory Center, San Diego, CA, 26-28 March 1974.
4. W.H. Bockmiller and P.R. Dax, "Radar Low Angle Tracking Study," NASA Contract Report No. 1387, Westinghouse Electric Corp., Baltimore, MD, June 1969.
5. R. McGee, "Multipath Suppression by Swept Frequency Methods," Ballistic Research Laboratories Memorandum Report No. 1950, November 1968, AD 682 728.
6. K.A. Richer, "4.4 Mm Wavelength Near Earth Propagation Measurements (U)," Ballistic Research Laboratories Memorandum Report No. 1403, May 1962 (Confidential), AD 331 098.
7. C.L. Wilson, "Antenna Pointing Errors in Simultaneous Lobing Antenna System," Ballistic Research Laboratories Technical Note No. 1453, June 1962, AD 608 997.
8. C.L. Wilson, "Antenna Pointing Errors in Sequential Lobing Antenna System," Ballistic Research Laboratories Technical Note No. 1463, May 1962, AD 609 009.
9. T.W. O'Dell, "Final Report for Missile Guidance Subsystem Feasibility Program - Phase 1A (U)," General Precision Laboratories Report No. P0268 (Confidential).
10. T.W. O'Dell, "Final Report for Missile Guidance Subsystem Feasibility Program - Phase 2 (U)," General Precision Laboratories Report No. 14990-2, June 1962 (Confidential).
11. N. Leggett, "Final Report, Breadboard Feasibility Study of the Derringer Weapon Guidance System," Bendix Pacific Div. Report No. 91-139-1 (U), May 1963.
12. J.E. Kammerer and K.A. Richer, "4.4 Mm Near Earth Antenna Multipath Pointing Errors (U)," Ballistic Research Laboratories Memorandum Report No. 1559, March 1964 (Confidential), AD 443 211.

REFERENCES (CONT.)

13. J.E. Kammerer and K.A. Richer, "4.4 Mm Wavelength Precision Antennas and Mount," Ballistic Research Laboratories Memorandum Report No. 1576, July 1964, AD 449 726.
14. J.E. Kammerer and K.A. Richer, "140 GHz Millimetric Bistatic Continuous Wave Measurements Radar," Ballistic Research Laboratories Memorandum Report No. 1730, January 1966, AD 484 693.
15. J.E. Kammerer and K.A. Richer, "Pointing Errors of a 140 GHz Bistatic Radar System Illuminating U.S. Army Targets (U)," Ballistic Research Laboratories Memorandum Report No. 1755, June 1966 (Confidential), AD 375 942.
16. M.G. Stansbury and C.L. Wilson, "A Signal Processing Pulse Width Discriminator," Ballistic Research Laboratories Memorandum Report No. 2040, June 1970, AD 710 230.
17. R. McGee, "Millimeter Wave Radiometric Detection of Targets Obscured by Foliage," Ballistic Research Laboratories Memorandum Report No. 1901, January 1968, AD 667 962.
18. R. McGee, W. Sacco and W. Lese, "Effects of Obscuration on Millimeter Wave Signatures of Targets," Ballistic Research Laboratories Memorandum Report No. 1962, February 1969, AD 684 900.
19. R. McGee, "A Foliage Obscuration for Passive Radiometric Detection System," Ballistic Research Laboratories Memorandum Report No. 1999, July 1969, AD 858 380.
20. J.E. Kammerer, "A 94 GHz FM-CW Radar with Six-Inch Range Resolution Capability," Ballistic Research Laboratories Memorandum Report No. 2235, September 1972, AD 908 485L.

March 1976

BIBLIOGRAPHY  
of  
MILLIMETER WAVE TARGET ACQUISITION AND GUIDANCE RESEARCH REPORTS

<u>NO.</u>	<u>AUTHORS</u>	<u>TITLE</u>
1. BRL MEMO 1403 (C) May 1962 (ASTIA No. AD 331 098)	K. A. Richer	4.4 MM Wavelength Near Earth Propagation Measurements
2. BRL TECH NOTE 1453 (U) June 1962 (AD 608 997)	C. L. Wilson	Antenna Pointing Errors in Simultaneous Lobing Antenna System
3. BRL TECH NOTE 1463 (U) May 1962 (AD 609 009)	C. L. Wilson	Antenna Pointing Errors in Sequential Lobing Antenna System
4. BRL RPT 1166 (C) April 1962 (AD No. 331 145)	L. P. Bolgiano	General Considerations Governing the Possible Use of Microwave Techniques for Missile Guidance
5. GPL Sec No. P0429-A (U) April 1962	S. M. Seelig	Final Technical Report on Radiometric Signatures of Battlefield Targets (BRL Contract DA 30-069-ORD-3507)
6. BRL MEMO 1454 (C) January 1963 (AD 336 243)	Compiled by D. Reuyl	Studies in the Support of the Development of Guidance Systems
7. GPL P-0268 (C)	T. W. O'Dell	Final Report for Missile Guidance Subsystem Feasi- bility Program - Phase 1A (BRL Contract DA 30-069-ORD- 3118)
8. GPL 14990-2 (C) June 1962 (AD 328 938)	T. W. O'Dell	Final Report for Missile Guidance Subsystem Feasi- bility Program - Phase 2, Nov 61-Jun 62 (BRL Contract DA 30-069-ORD-3118)
9. ECI RPT 62-45; FR-70 (C) November 1962 (AD 333 262)	F. L. Wentworth	High Sensitivity Millimeter Wave Receiver (BRL Contract DA-36-034-ORD-3509RD)

(U) Unclassified

(C) Confidential

(S) Secret

NOTE:

Obtain reports from DDC for all except the "Talk & Publications" reports which must be obtained from the sponsoring agency. For classified reports, a need-to-know and Government Contract must be cited. IMR reports have limited distribution and are not sent to DDC. However, IMR reports are later published as BRL Memorandum Reports.

<u>NO.</u>	<u>AUTHORS</u>	<u>TITLE</u>
10. BRL MEMO 1457 (U) March 1963 (AD 404 868)	C. L. Wilson J. E. Kammerer	70 Gc Klystron Stability and Spectrum
11. BRL TECH NOTE 1494 (U) March 1963 (AD 479 547)	K. A. Richer J. E. Kammerer	Optimizing Signal-to-Noise Ratio at 70 Gc
12. (Talk & Publication) Proceedings of the Electro- Magnetic Warfare Symposium on Millimeter Wave Techniques (S) Nov 14-15, 1963, Johns Hopkins University.	D. G. Bauerle C. L. Wilson K. A. Richer	Millimetric Wave Research for Guidance Applications
13. (Talk & Publication) Antitank Missile Guidance & Control Meeting. Tech- nical Working Panel D-7 of the Tripartite Technical Cooperation Project, 30 Sep-4 Oct 1963, USAMC, Redstone Arsenal, Ala. (S)	K. A. Richer	Supporting Research for Missile Guidance Millimeter Wave Research
14. BRL TECH NOTE 1516 (U) September 1963 (AD 426 009)	A. K. Gillis, Jr.	Installation and Operation of the 140 Gc Carcinotron with F- and G- Band Components
15. Sperry Microwave Elec- tronics Co., Rpt. S. J. 212-0042-14 (C) C-5495A- 1 (C). December 1963	D. L. Hornak R. E. Wilt	Millimeter Wave Radiometer Program (BRL Contract DA 01-009-AMC-1085X)
16. Sylvania Electronic Systems Rpt No. A103- 004-5-056 (U), 3 December 1963	A. DeAngelis	Final Report on the V-Band Harmonic Generator Program (BRL Contract DA 30-069- ORD-3705)
17. Sperry Microwave Elec- tronics Co., Ref. A02195 (C), 30 December 1963	H. F. Lamphears R. E. Wilt	Radiometric Temperature Measurement Program (BRL Contract DA 01-009-AMC-69R)
18. Bendix P. fic Div Rpt 91-13. i (U), May 1963	N. Leggett	Final Report. Breadboard Feasibility Study of the Derringer Weapon Guidance System (BRL Contract DA 04-495-ORD-3554)
19. BRL TECH NOTE 1525 (U) January 1964 (AD 434 047)	D. Bauerle	Millimeter Wave Diode Fabrication

<u>NO.</u>	<u>AUTHORS</u>	<u>TITLE</u>
20. BRL MEMO 1559 (U) March 1964 (AD 443 211)	K. A. Richer J. E. Kammerer	4.4 mm Near Earth Antenna Multipath Pointing Errors
21. BRL MEMO 1576 (U) July 1964 (AD 449 726)	K. A. Richer J. E. Kammerer	4.4 mm Wavelength Precision Antennas and Mount
22. (Talk & Publication) Proceedings of 1964 World Conference on Radio Meteor- ology Incorporating the 11th Western Radar Con- ference, Sep 14-18, 1964, C.R.P.L., National Bureau of Standards (U)	K. A. Richer D. G. Bauerle	Near Earth Millimeter Wave Radiometer Measurements
23. BRL RPT 1267 (U) December 1964 (AD 460 300)	K. A. Richer D. G. Bauerle	Near Earth Millimeter Wave Radiometer Measurements
24. General Precision, (C) Inc., Systems Div., GPI No. K20910 Oct 64	Myron Rosenthal Fred Biachi Sidney Lewinter	Final Rpt on a Millimeter Wave Radiometer Guidance Measurement Program (BRL Contract DA-30-064-AMC-621(R))
25. Advanced Technology Corp., March 1, 1965 (U)	J. Cotton M. Cohn	Research Study Into the Near Earth Application of Milli- meter Radio Waves as Applied to Certain Battlefield Problems (BRL Contract DA- 36-034-AMC-0102R)
26. BRL MEMO 1683 (C) Jun 1965 (AD 369 082)	K. A. Richer J. E. Kammerer	70 Gc Radar Characteristics Measurements for American and Russian Targets
27. BRL MEMO 1658 (C) June 1965 (AD 366 497)	D. G. Bauerle	Ground Radiometric Measurements at 2.17 Millimeters
28. TRG/A Subsidiary of Control Data Corp. TRG No. S-302 March 18, 1965 (U)	A. Kay	The Relationship of Antenna Performance and Contrast Temperatures in Radiometers with Application to Ground Targets in the Near and Far Fields (BRL P.O. 1095)
29. BRL MEMO 1667 (C) June 1965 (AD 368 867)	J. W. Roberts	Radiometric Pointing Errors & Target Isotherms
30. BRL MEMO 1730 (U) January 1966 (AD 484 693)	J. E. Kammerer K. A. Richer	140 GHz Millimetric Bistatic Wave Measurements Radar

<u>NO.</u>	<u>AUTHORS</u>	<u>TITLE</u>
31. BRL RPT 1322 (U) May 1966 (AD 640 009)	R. B. Patton C. L. Wilson	The VARR Method - A Technique for Determining the Effective Power Patterns of Millimeter Wave Radiometric Antennas
32. BRL MEMO 1755 (C) June 1966 (AD 375 942)	J. E. Kammerer K. A. Richer	Pointing Errors of a 140 GHz Bistatic Radar System Illumi- nating U.S. Army Targets
33. North American - Tulsa Space & Information Systems Div., June 1966(S) (AD 375 794)	W. Hill R. Stratton	The Design, Fabrication and Testing of a Flexible Radar Absorptive Blanket for Army Application (BRL Contract OI- 18-001-66-01303(X))
34. BRL MEMO 1785 (C) August 1966 (AD 378 097)	J. E. Kammerer K. A. Richer	Cross Section Measurements of U.S. Army Targets by 140 GHz Radar
35. Advanced Technology Corp., Nov 30, 1966 (AD 648 732)	J. Cotton J. Dozier	Research Study Into Near Earth Application of Millimeter Radiowaves as Applied to Certain Battlefield Problems (BRL Contract DA 18-001-AMC-829(X)) Interim Technical Report
36. BRL RPT 1331 (U) July 1966 (AD 643 770)	C. L. Adams	The Electromagnetic Propagation Range Facility at the Ballistic Research Laboratories
37. BRL MEMO 1820 (S) May 1967 (AD 383 424)	J.E. Kammerer K. A. Richer	Wide Angle Bistatic Measure- ments of Surfaces and Di- electrics at 140 GHz
38. BRL TECH NOTE 1637 (U) November 1966 (AD 650 318)	C. L. Wilson	70 Gc Pulse Radar
39. BRL MEMO 1805 (U) November 1966 (AD 813 377)	J. Freidhoffer	Scattering of Electromagnetic Waves from Rough Surfaces
40. BRL MEMO 1835 (C) March 1967 (AD 381 943)	D. Bauerle M. Stansbury	Near Earth Radiometric Measure- ments at 4.38 Millimeters
41. BRL MEMO 1890 (C) December 1967 (AD 389 050)	S. Talbot	Target Versus Background Clutter Measurements with 70 GHz Radar
42. BRL MEMO 1836 (S) April 1967 (AD 381 886)	C. Wilson	Millimeter Wave Camouflaging

<u>NO.</u>	<u>AUTHORS</u>	<u>TITLE</u>
43. Gen Prec Inc. (C) Document SN641S001A 31 March 1967 (AD 381 676)	A. Lyons M. Rosenthal	Radiometric Target Tracking System Model 401, Final Rpt (BRL Contract DA 18-001-AMC-975(X)
44. Advanced Technology Corp (U) September 19, 1967 (AD 386 162)	Andrew F. Eikenberg	Imaging Radar Target Signatures Contract DAAD05-67-C-0550
45. Advanced Technology Corp (U) December 15, 1967 (AD 664 120)	John Cotton	Research Study Into the Near Earth Application of Millimeter Radio Waves as Applied to Certain Battle- field Problems (W. A. 4, Scanning Antenna), BRL Contract DA-18-001-AMC- 829(X)
46. Advanced Technology Corp (U) December 15, 1967 (AD 664 175)	John Cotton	Research Study Into the Near Earth Application of Millimeter Radio Waves as Applied to Certain Battle- field Problems (W.A. 5, 35 GHz Solid State Source), BRL Contract DA-18- 001-AMC-829(X)
47. BRL MEMO 1901 (U) Jan 68 (AD 667 962)	R. McGee	Millimeter Wave Radiometric Detection of Targets Obscured by Foliage
48. BRL TECH NOTE 1701 (U) Aug 68 (AD 840 077)	C. Wilson	Bearing Angle Errors in Inter- ferometer Antenna System Used for Short Range Vertical Angle Measure- ments
49. BRL MEMO 1912 (U) Jan 68 (AD 669 241)	K. Richer	Radiometric Tracking of Small Islands
50. BRL MEMO 1922 (U) April 1968 (AD 834 975)	C. Weigel	Millimeter Wave Radiometric Tunnel Detection Measurements
51. BRL MEMO 1950 (U) November 1968 (AD 682 728)	R. McGee	Multipath Suppression by Swept Frequency Methods
52. BRL MEMO 1962 (U) February 1969 (AD 684 900)	R. McGee W. Sacco W. Lese	Effects of Obscuration on Millimeter Wave Signatures of Targets
53. BRL MEMO 1940 (U) October 1968 (AD 843 138)	J. Roberts	Electromechanical Boresight Align- ment of Conical Scan Radiometer Antenna

<u>NO.</u>	<u>AUTHORS</u>	<u>TITLE</u>
54. BRL MEMO 1984 (C) June 1969 (AD502 837)	C. Wilson K. Richer	Detectability of Aircraft Radiating Systems
55. Penn State Univ (U) November 1968 (AD 687 391)	Louis Winkler	Radio Astronomy Observatory Study of Millimeter Propagation in the Earth's Atmosphere - Contract DA- 18-001-AMC-905(X)
56. BRL MEMO 1999 (U) July 1969 (AD 858 380)	R. McGee	A Foliage Obscuration Model for Passive Radiometric Detection System
57. Talk & Publctn (U) 1969 Int. Microwave Symposium-IEEE-PGMITT Dallas, Texas 5-7 May 1969	K. A. Richer	Near Earth Millimeter Wave Radar and Radiometry
58. BRL MEMO 2003 (U) August 1969 (AD 859 949)	K. A. Richer	Radiometric Vs Radar Camouflage
59. Geological Society of America Bulletin February 1970	K. A. Richer	Comments on a Microwave Radiometric Study of Buried Karst Topography
60. Talk & Publctn (U) 1969 Technical Symposium on Navigation & Positioning USAECOM-AAAA-ION Ft. Monmouth, NJ 23-25 Sep 69	C. L. Wilson	Radiometric Navigation
61. Talk & Publctn (U) 1970 Int. Submillimeter Wave Symposium IEEE-PGMITT, Optical Society of America, MRI Polytechnic Inst of Brooklyn, 31 Mar-2 Apr 70, New York, NY	K. A. Richer	Environmental Effects On Radar and Radiometric Systems at Millimeter Wavelengths
62. BRL MEMO 2040 (U) Jun 1970 (AD 710 230)	M.G.Stansbury C.L. Wilson	A Signal Processing Pulse Width Discriminator
63. BRL MEMO 2052 (C) Aug 1970 (AD 511 301)	D.G.Bauerle K.A. Richer	Modeling of L Band Helicopter Radar Cross Section
64. BRL MEMO 2050 (C) Aug 1970 (AD 511 684)	D.G. Bauerle K.A. Richer	Modeling of L Band Tank Cross Section

<u>NO.</u>	<u>AUTHORS</u>	<u>TITLE</u>
65. BRL MEMO 2157 (U) March 1972 (AD 893 229L)	J.E.Kammerer	A Millimeter Wave Frequency Scanned Radiometer Having a 25 GHz Tuning Range
66. BRL MEMO 2088 (C) January 1971 (AD 513 920)	K. A. Richer	Radiometric Terminal Guidance
67. BRL MEMO 2051 (U) August 1970 (AD 875 828)	C. L. Wilson	Dynamic Armor Radar Sensors
68. Talk & Publctn (S) 6-7 June 1970, Advanced Sensors Lab, R&D Directorate, USAMICOM, Redstone Arsenal 35809, pp 140-172	K. A. Richer	Program for the President's Scientific Advisory Committee Ground Warfare Panel (U) "Radiometric Terminal Guidance"
69. BRL MEMO 2162 (C) March 1972 (AD 519 976L)	D.G.Bauerle	Modeling of S Band Tank Radar Cross Section
70. BRL MEMO 2163 (C) March 1972 (AD 520 112L)	D.G.Bauerle	Modeling of S Band Helicopter Radar Cross Section
71. Vought Missiles & Space Co. Rpt VMSC-M-52/00/71R- 4(C), 22 Feb 1972, under BRL Sponsored Contract DAA401-71-C-1364	J.Mayersak R. Roder et al.	Microwave Radiometer Terminally Guided Sub-Missile Design and Evaluation
72. BRL MEMO 2202 (C) July 1972 (AD 522 396L)	K.A.Richer	35 GHz Radiometer High Incident Angle Propagation
73. BRL MEMO 2222 Sept 1972(AD 906718L)	C. L. Wilson	Radiometric Guidance Signals by Antenna Positioning Sampling
74. BRL MEMO 2224 Sept 1972 (AD906474L)	R. A. McGee	Signal Processing In a Conically Scanned Millimeter Wave Radiometer
75. BRL MEMO 2223 Sept 1972 (AD 905 736L)	K. A. Richer	Rain and Fog Range For a 35 GHz Radiometer
76. BRL Interim MEMO 61 (U) October 1972	V. Richard	Millimeter Wave Radar Applications to Weapons Systems
77. BRL MEMO 2235 Sept 1976 (AD 908485L)	J.E. Kammerer	A 94 GHz FM-CW Radar with Six-Inch Range Resolution Capability

<u>NO.</u>	<u>AUTHORS</u>	<u>TITLE</u>
78.	USAMICOM, Redstone Arsenal, Ala., Army Terminal Homing Proceedings (C) pp 65-73, 24-75, April 1973	A. Hammond Green, Jr. & K. A. Richer Millimeter Wave Measurements for Terminal Homing
79.	Vought Missiles & Space Co., Rpt 7-52100 (73R-13), 31 Aug 1973, under BRL Contract DAAD05-73-C-0028 (C)	S.C. Lambert et al Stabilization and Control Sub-system Design and Evaluation For a Microwave Radiometric Sensor
80.	BRL MEMO 2318, August 1973 (AD 913938L)	R. McGee The General Optimum Digital Filter in Millimeter Wave Radiometric Signal Processing
81.	BRL MEMO 2327C, Sept 1973 (AD 527927L)	K. A. Richer Maximum Range of a 35 GHz FM-CW Active Radiometer
82.	BRL Contract Report 121, Sept 1973 (AD 914690L)	Sperry Microwave Elec., Clearwater, Florida Millimeter Wave Conical Scan Radiometer Flight Tests
83.	BRL Contract Report 131C, Jan 1974 (AD 528814L)	Honeywell, Inc., Systems Res Center, Minn, MI Millimeter Wave Radiometer Signal Processing
84.	1974 Millimeter Wave Techniques Conference, 26-28 Mar 74, Naval Elec Lab Ctr, San Diego, CA, Vol. 3 (C) NELC/TD 308	J. Knox Airborne Tank Signature Measurements with a 35 GHz Active Radiometer
85.	1974 Millimeter Wave Techniques Conference, 26-28 Mar 74, Naval Elec Lab Ctr, San Diego, CA, Vol. 1 (U) NELC/TD 308	V. W. Richard Millimeter Wave Rain Backscatter Measurements
86.	BRL MEMO 2371, April 1974 (AD 920133L)	R. McGee Analysis of an FM-CW Radar
88.	BRL MEMO 2401, July 1974 (AD 5313971.)	K. A. Richer D. G. Bauerle Millimeter Wave Pulsed IMPATT Seeker

<u>NO.</u>	<u>AUTHORS</u>	<u>TITLE</u>
88. BRL Contract Report 168, July 1974 (AD 923101L)	Sperry Micro- wave Elec Clearwater, Fla.	Microwave Radiometric Sub- system (MRSS)
89. BRL Contract Report 170 (C), July 1974 (AD 531 729L)	Honeywell, Inc., Sys Res Center, Minn., MI	Millimeter Wave Radiometer Signal Processing
90. BRL IMR 295 (C) Sept 1974	D. G. Bauerle	SADARM Millimeter Wave Radiometer Data - Vol. I
91. BRL IMR 296 (C) Sept 1974	D. G. Bauerle	SADARM Millimeter Wave Radiometer Data - Vol. II
92. BRL MEMO 2433 (C) Jan 1975, C001046L	K. A. Richer	SADARM Millimeter Wave Radiometer Measurements
93. BRL MEMO 2467 Mar 1975, A 009699	A. R. Downs	A Model for Predicting the Rain Backscatter from a 70 GHz Radar
94. BRL IMR 365 (U) Apr 1975	R. McGee L. Puckett	Radiometer Antenna Pattern Invariant Contour
95. BRL MEMO 2391 (C), Jun 1975, AD-C002505L	K. A. Richer D. G. Bauerle J. Knox	94 GHz Radar Cross Section of Vehicles
96. BRL MEMO 2525 (U), Sept 1975, AD B00 7284L	H. Raub C. Wilson	An Automatic DC Nulling Circuit for Radiometric Signal Processing
97. BRL IMR 445 (C), Oct 1975	H. B. Wallace	35 GHz Radiometric Signatures of Artillery Pieces and Their Application of HOWLS
98. BRL Report 1838 Oct 1975, AD B00 8173L	V. W. Richard J. E. Kammerer	Rain Backscatter Measurement and Theory at Millimeter Wavelengths

APPENDIX A\*  
MILLIMETER WAVE PROPAGATION

I. INTRODUCTION

The propagation of microwave energy through the atmosphere results in a reduction in intensity of the primary beam. This attenuation is the result of two phenomena - absorption and scattering. The absorption arises from both free molecules and suspended particles such as dust and water droplets condensed in fogs and rains. In addition to the attenuation, the energy scattered back in the direction of incidence is of prime interest for radar applications since it contributes additional noise to the system.

This section summarizes the available theoretical and experimental data on millimeter wave (35-94 GHz) propagation in rain and fog. In addition, an analysis of clear attenuation in the 60 to 75 GHz region is presented.

II. CLEAR AIR ATTENUATION

The gases that absorb microwave energy in a noncondensed atmosphere are oxygen, which has a magnetic interaction with the incident radiation, and water vapor, which contributes because of the electric polarity of the water molecule. In each case, there are resonance frequency regions where the absorption is abnormally large.<sup>1</sup> For oxygen, the resonance occurs at wavelengths of approximately 0.5 and 0.25 cm. In the case of water vapor, the resonance occurs at approximate wavelengths of 1.35, 0.27, 0.16 and 0.09 cm.

The clear air attenuation coefficient is given as a function of frequency by Rosenblum<sup>2</sup> for sea level and an altitude of 4 kilometers, as reproduced in Figure A-1. Examination of the figure shows regions of relatively low attenuation at wavelengths of approximately 8.6, 3.2, 2.1, and 1.3 millimeters. These clear weather windows are usually chosen as the operating frequency of sensors when optimum range performance is required.

---

\*Appendices A-D were prepared for BRL under Contract DAAD05-72-C-3059 by K. L. Koester, L. Kosowsky, and J. F. Sparacio of Norden Division, United Aircraft, Norwalk, Connecticut.

<sup>1</sup>J.H. Van Vleck, "Theory of Absorption by Uncondensed Gases," in D.E. Kerr (ed.), Propagation of Short Radio Waves, pp. 646-664, Boston Technical Publishers, Massachusetts, 1964.

<sup>2</sup>E.S. Rosenblum, "Atmospheric Absorption of 10 to 400 KMCPS Radiation," Microwave Journal, pp. 91-96, March 1961.



Further examination of Figure A-1 shows that the attenuation falls off quite rapidly as the frequency increases from 60 to 94 GHz. Because of the rapid variation in attenuation in this frequency region, a study of clear air propagation at sea level was conducted by Norden and is summarized below.

Tables of theoretical values of absorption by oxygen and water vapor at several discrete wavelengths were presented by Van Vleck.<sup>1</sup> Measurements have been made of the clear air attenuation into the 60 to 75 GHz region by several authors.<sup>3-6</sup> Their experimental results were combined with Van Vleck's to obtain the clear attenuation coefficient of 64 to 80 GHz energy shown in Figure A-2. It should be noted that the water absorption is dependent on the water vapor content of the air. In a temperate climate, approximately one percent of the molecules in the atmosphere are H<sub>2</sub>O; this corresponds to a vapor content of 7.5 g/m<sup>3</sup>. Figure A-2 is plotted for this vapor content. At saturation at 20°C at sea level, the water vapor content is 17 g/m<sup>3</sup>. Under tropical conditions the water vapor content can be even higher.

An examination of the figure indicates that the attenuation decreases rapidly from 6.7 dB/km at 64 GHz to 0.27 dB/km at 76 GHz. In the 76 to 94 GHz frequency range, there is only a slight decrease in attenuation.

---

<sup>3</sup>D.C. Hogg, "Millimeter-Wave Communication through the Atmosphere," Science, pp. 39-46, 5 January 1968.

<sup>4</sup>C.W. Tolbert, and A.W. Straiton, "Experimental Measurement of the Absorption of Millimeter Radio Waves Over Extended Ranges," IRE Transactions on Antennas and Propagation, pp. 239-241, April 1957.

<sup>5</sup>A.W. Straiton, and C.W. Tolbert, "Anomalies in the Absorption of Radio Waves by Atmospheric Gases," Proceedings of the IRE, pp. 898-903, May 1960.

<sup>6</sup>A.G. Kislyakov, V.N. Nikonov and K.M. Strezknew, "An Experimental Study of Atmospheric Absorption on a 4.1 mm Wave as Function of the Height above Sea Level," translated from Russian by the Foreign Technology Division, WPAFB, Ohio, Report FTD-MT-24-339-68, 30 October 1968, (AD 685 996).

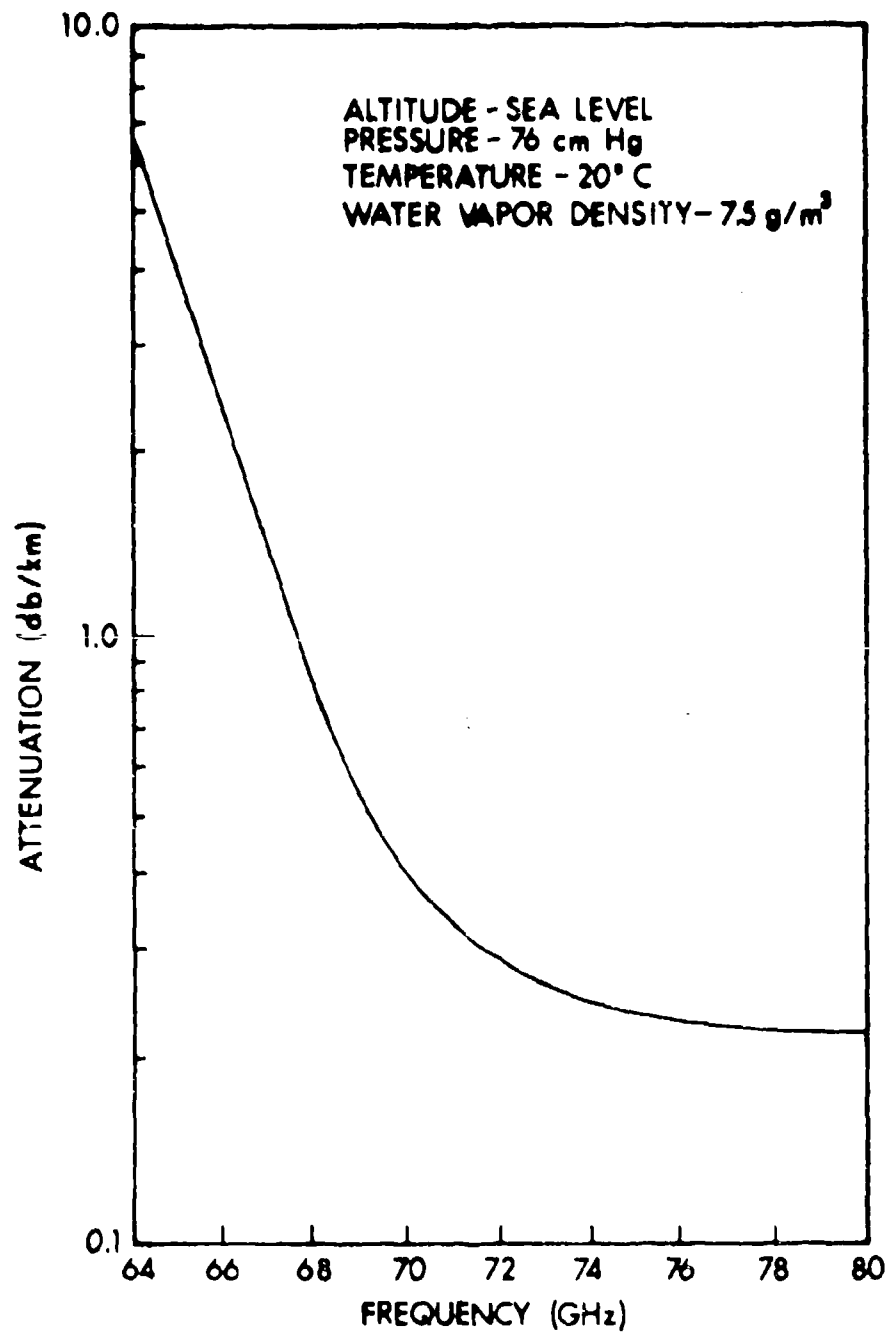


Figure A-2. One Way Attenuation per Kilometer for Horizontal Propagation in Clear Air

### III. PROPAGATION IN RAIN

The study of the attenuation and scattering in a medium such as rain is based upon the knowledge of the effects of the individual particles. The complete theory for spherical particles of any material in a non-absorbing medium was developed by Gustav Mie.<sup>7</sup> This work was extended by Stratton<sup>8</sup> and is outlined in Kerr.<sup>9</sup> A comprehensive study of the theory of electromagnetic scattering from small particles is also offered by Van de Hulst.<sup>10</sup> A detailed examination of this theory is beyond the scope of this report. However, a brief discussion of the basic is summarized in Section III-A.

#### A. Cross Sections of Single Spheres

A single dielectric sphere in the path of a plane wave will scatter and absorb some of the incident energy. These effects are characterized by several quantities called cross sections and have the dimensions of area. The Gunn and East<sup>11</sup> definitions of the scattering, absorption, extinction, and backscatter cross-sections are:

$$\text{Scattering Cross Section } (Q_s) = \frac{\text{Total Power Scattered (over } 4\pi \text{ steradians)}}{\text{Incident Power Density}} \quad (\text{A-1})$$

$$\text{Absorption Cross Section } (Q_a) = \frac{\text{Total Power Absorbed (as heat)}}{\text{Incident Power Density}} \quad (\text{A-2})$$

$$\text{Extinction Cross Section } (Q_e) = \frac{\text{Total Power Lost (to the incident wave)}}{\text{Incident Power Density}} \quad (\text{A-3})$$

---

<sup>7</sup>G. Mie, Ann Physik, Vol. 25, p. 377 et. seq., 1908.

<sup>8</sup>J.A. Stratton, Electromagnetic Theory, McGraw-Hill, New York, 1941.

<sup>9</sup>H. Goldstein, "Attenuation in Condensed Water," in D.E. Kerr (ed.), Propagation of Short Radio Waves, pp. 641-692, Boston Technical Publishers, Boston, Massachusetts, 1964.

<sup>10</sup>H.C. Van de Hulst, Light Scattering by Small Particles, Wiley, New York, 1957.

<sup>11</sup>K.L.S. Gunn and T.W.R. East, "The Microwave Properties of Precipitation Particles," Quarterly Journal of the Royal Meteorological Society, Vol. 80, pp. 533-545, October 1954.

The term extinction is used to describe the energy lost by the incident wave to a single particle; attenuation is the energy lost to a continuous volume of particles.

It should be noted that the conservation of energy requires that<sup>10</sup>

$$Q_e = Q_a + Q_s \quad (A-4)$$

$$\text{Backscatter Cross Section } (\sigma) = \frac{\text{Total Power Scattered Backward (along the direction of incidence)}}{\text{Incident Power Density}} \quad (A-5)$$

The scattering and absorption properties of single particles are complex functions of the size, shape, and index of refraction of the particles as well as the wavelength of the incident energy. The scattering cross sections for water spheres ranging from 0.04 to 6.0 millimeters in diameter in 0.04 millimeter increments were calculated by SRI<sup>12</sup> for various temperatures. The various cross sections at 18°C are shown in Figure A-3.

#### B. Mie Scattering Theory

Our interest lies in the backscatter and attenuation cross sections associated with a continuous distribution of particle sizes within a given volume. The relationships for a single particle were described in Section III-A. If the particle size distribution is known, the reflectivity and attenuation can be determined, using the appropriate scattering theory.

The scattering theory to be used in the determination of the backscatter and attenuation of rain and fog depends on the size of the drops in the medium and the wavelength of the radiation. Mie scattering theory must be used for drops larger than 0.06 wavelength in diameter. For drops smaller than 0.06 wavelength the Rayleigh theory approximations are applicable.

---

<sup>12</sup>"Study of Atmospheric Propagation Factors for 70 GHz Energy," Stanford Research Institute, 26 August 1969 (Supplied by SPI under Norden FO 0016146 - not available for distribution).

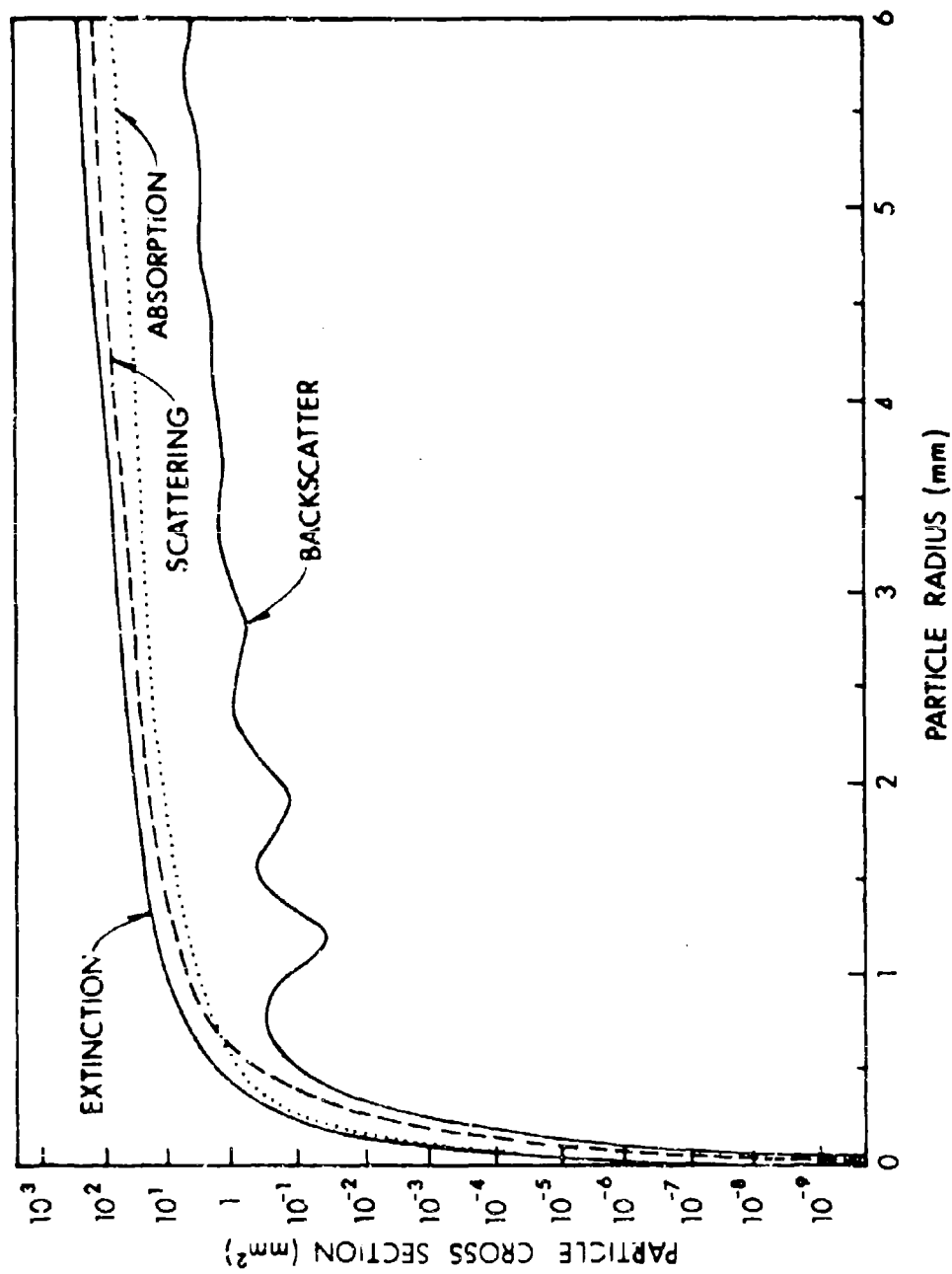


Figure A-3. Cross Sections of Water Spheres at 18°C for 4.3 mm Wavelength Energy [1]

Lukes<sup>13</sup> describes the size of the drops present under various atmospheric conditions. The ranges of drop size diameters for several atmospheric conditions are given in Table A-1.

Table A-1  
Drop Diameters for Various Atmospheric Conditions<sup>13</sup>

ATMOSPHERIC CONDITION	DROP SIZE RANGE Micrometers
Haze	0.01 - 3
Fog	0.01 - 100
Clouds	1 - 50
Drizzle (0.25 mm/hr)	3 - 800
Moderate Rain (4.0 mm/hr)	3 - 1500
Heavy Rain (16.0 mm/hr)	3 - 3000

Since rain is comprised of drops 258 micrometers (0.258 mm) and larger, Mie scattering theory must be used for millimeter wavelength radiation. The smaller drops in haze and clouds allow the use of the Rayleigh approximation. Rain is investigated in Section III-D and fog is discussed in Section IV.

The reflectivity or backscatter cross section per unit volume in the Mie Scattering Region is defined by Mitchell<sup>14</sup>

<sup>13</sup>G.D. Lukes, "Penetrability of Haze, Fog, Clouds and Precipitation by Radiant Energy Over the Spectral Range 0.1 Micron to 10 Centimeters," The Center for Naval Analyses of the University of Rochester, Report No. 61, May 1968, AD 847658.

<sup>14</sup>R.L. Mitchell, "Radar Meteorology at Millimeter Wavelengths," Aerospace Corporation, Report TR-669 (6236-46)-9, June 1966.

$$\eta = \int_{D_{\min}}^{D_{\max}} \sigma(D)N(D)dD, \quad (A-6)$$

where  $\sigma(D)$  = backscatter cross section of particle with diameter  $D$ ,  
 $N(D)dD$  = the number of particles with diameter between  $D$  and  $D + dD$  per unit volume.

Similarly the attenuation is defined as

$$\alpha = 4.343 \int_{D_{\min}}^{D_{\max}} Q_e(D)N(D)dD, \quad (A-7)$$

where  $Q_e(D)$  = extinction cross section of particle with diameter  $D$ .

Note that the integral is multiplied by 4.343 to give the units of decibels per unit length as in standard radar practice.

### C. Drop Size Distributions

The relation of raindrop size to intensity was first investigated by Laws and Parsons<sup>15</sup> in 1943. Their experimental study indicated that the median drop size was a fairly strict function of rain intensity. The change in median drop size over the range of intensities covered was quite small, increasing by only three diameters while the intensity increased by a factor of four hundred. Tolbert and Gerhardt<sup>16</sup> presented the drop size distribution for the Laws and Parsons data shown in Figure A-4. Additional raindrop measurements

<sup>15</sup>O.J. Laws and D.A. Parsons, "The Relation of Raindrop-Size to Intensity," Transactions of the American Geophysical Union, Vol. 24, pp. 452-460, 1943.

<sup>16</sup>C.W. Tolbert and J.R. Gerhardt, "Measured Rain Attenuation of 4.3 Millimeter Wavelength radio Signals," University of Texas, Report No. 83, 31 May 1956.

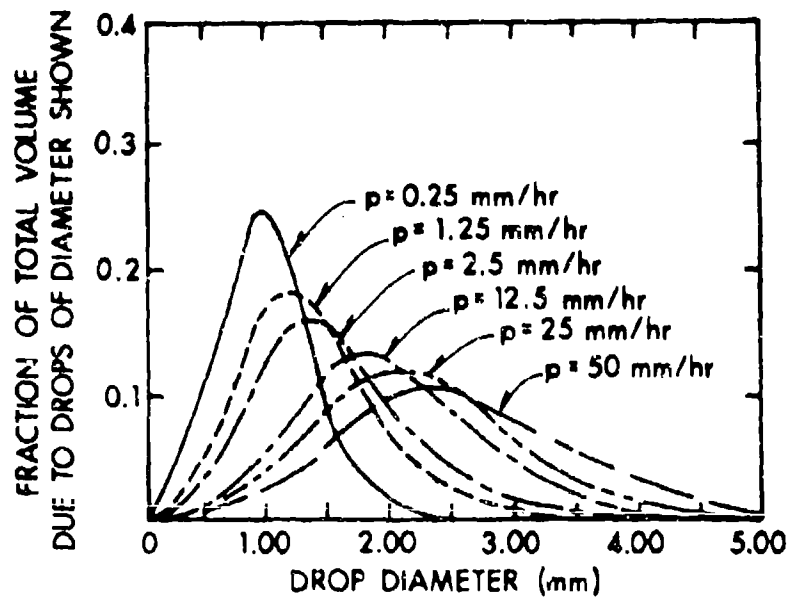


Figure A-4. Rainfall Drop Size Distribution as a Function of Rain Rate for Laws and Parsons Data with 0.25 mm Diameter Interval [16]

were performed by Marshall and Palmer<sup>17</sup> in 1948. The distribution of drops with size was found to be in agreement with that of Laws and Parsons.

Cantaneo and Stout<sup>18</sup> studied raindrop size distributions in several locations and found the distributions to be quite similar. A difference was found between warm and cold frontal rains with the cold rain having smaller drops. Despite the existing differences in rain of a given intensity, the drop size distributions described are valid for a general study of propagation through rain.

#### D. Attenuation Due to Rain

The first extensive investigation of attenuation in rain was performed by Ryde and Ryde<sup>19</sup> in 1945. Their calculations, which are presented in Kerr,<sup>9</sup> were performed for wavelengths ranging from 3 millimeters to 10 centimeters. A form of equation (A-7) was used with the Laws and Parsons drop size distribution and the extinction cross section determined from Mie scattering theory. The one-way attenuation in rain at 18°C for 4.3 millimeter energy is shown in Figure A-5.

Mie theory was also used to determine the rain attenuation at 70 GHz at 0°C by Crane<sup>20</sup> and at 10° and 30°C by SRI.<sup>12</sup> Their results are also shown in Figure A-5.

Experimental confirmation of these results was provided by Tolbert and Gerhardt<sup>16</sup> and Hogg.<sup>21</sup> The latter's results are also shown in Figure A-5. Examination of this illustration indicates general agreement on the attenuation in rain at 70 GHz.

---

<sup>17</sup>J.S. Marshall and W.McK. Palmer, "The Distribution of Raindrops with Size," Journal of Meteorology, Vol. 5, pp. 165-166, August 1948.

<sup>18</sup>R. Cantaneo and G.E. Stout, "Raindrop-Size Distributions in Humid Continental Climates, and Associated Rainfall Rate-Radar Reflectivity Relationships," Journal of Applied Meteorology, Vol. 7, pp. 901-907, October 1968.

<sup>19</sup>J.W. Ryde and D. Ryde, "Attenuation of Centimeter and Millimeter Waves by Rain, Fog, and Clouds," British General Electric Co., Report No. 8670, 1945.

<sup>20</sup>R.K. Crane, "Microwave Scattering Parameters for New England Rain," Technical Report 426, Lincoln Laboratories, MIT, 3 October 1966.

<sup>21</sup>D.C. Hogg, "Millimeter-wave Communication through the Atmosphere," Science, Vol. 159, pp. 39-46, 5 January 1968.

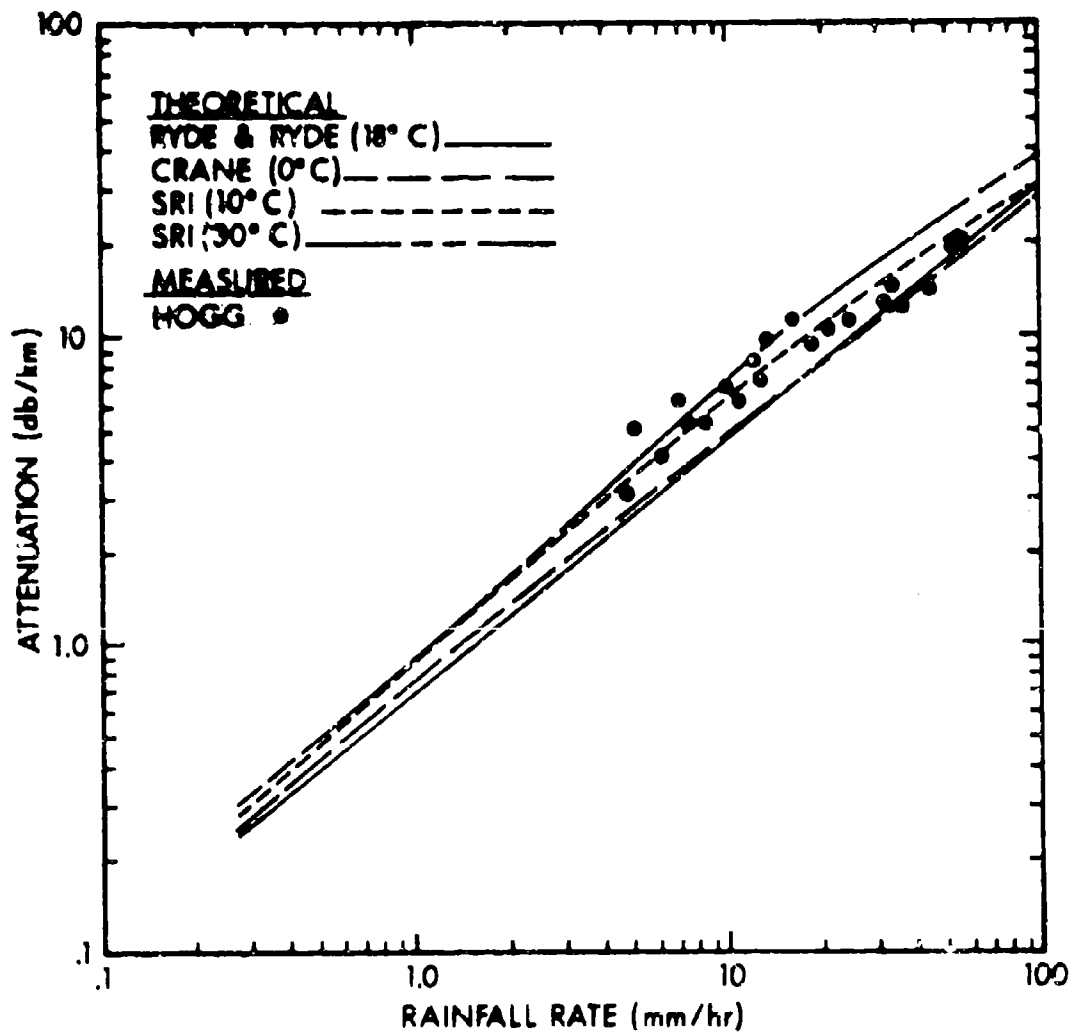


Figure A-5. One-Way Attenuation in Rain at 70 GHz

Figure A-6 shows the attenuation coefficient for 35, 70 and 94 GHz, the "millimeter" frequencies. Also shown for comparison is the attenuation at 15.5 GHz. These curves were derived from data presented by Crane.<sup>20</sup>

#### E. Backscatter Cross Section of Rain

Until recently, the study of radar meteorology at millimeter wavelengths has largely been ignored. The Rayleigh scattering approximations used at lower frequencies are not applicable above X-band. The exact, but more difficult, Mie theory was not utilized because as Skolnik<sup>22</sup> points out, "...the larger attenuations at the higher frequencies preclude the making of measurements conveniently." As components were developed, interest in millimeter radar systems increased because of their high resolution capability. At the relatively short ranges of less than 5 nautical miles where the resolution would be most useful, the rainfall attenuation is small. Since backscatter data were not available, many people incorrectly extrapolated lower frequency results.

The Rayleigh approximation of the backscatter cross section of rain at 35, 70 and 94 GHz is shown in Figure A-7. Also shown is the backscatter cross section predicted by Crane, using Mie scattering theory. At 70 and 94 GHz the difference between the Mie and Rayleigh values increases with rainfall rate. It is interesting to note the crossover of the 35, 70 and 94 GHz Mie curves at a rain rate of 9 millimeters per hour.

Crane's backscatter curve for 70 GHz energy is repeated in Figure A-8 for comparison with the SRI 70 GHz curves, which show the temperature dependence of the backscatter coefficient. (Both used a form of equation (A-6) to obtain the volume backscatter coefficient in units of  $\text{km}^{-1} \text{ster}^{-1}$ . The radar backscatter coefficient, plotted in Figure A-8, is defined as  $4\pi$  times the volume backscatter coefficient).

The measurement of the backscatter cross section of rain was included in the Norden experimental program. The results for rains of 2 and 3.8 millimeters per hour are shown in Figure A-8. They compare favorably with the predicted values.

---

<sup>22</sup>M. Skolnik, Introduction to Radar Systems, pp. 521-569, McGraw-Hill, New York, 1962.

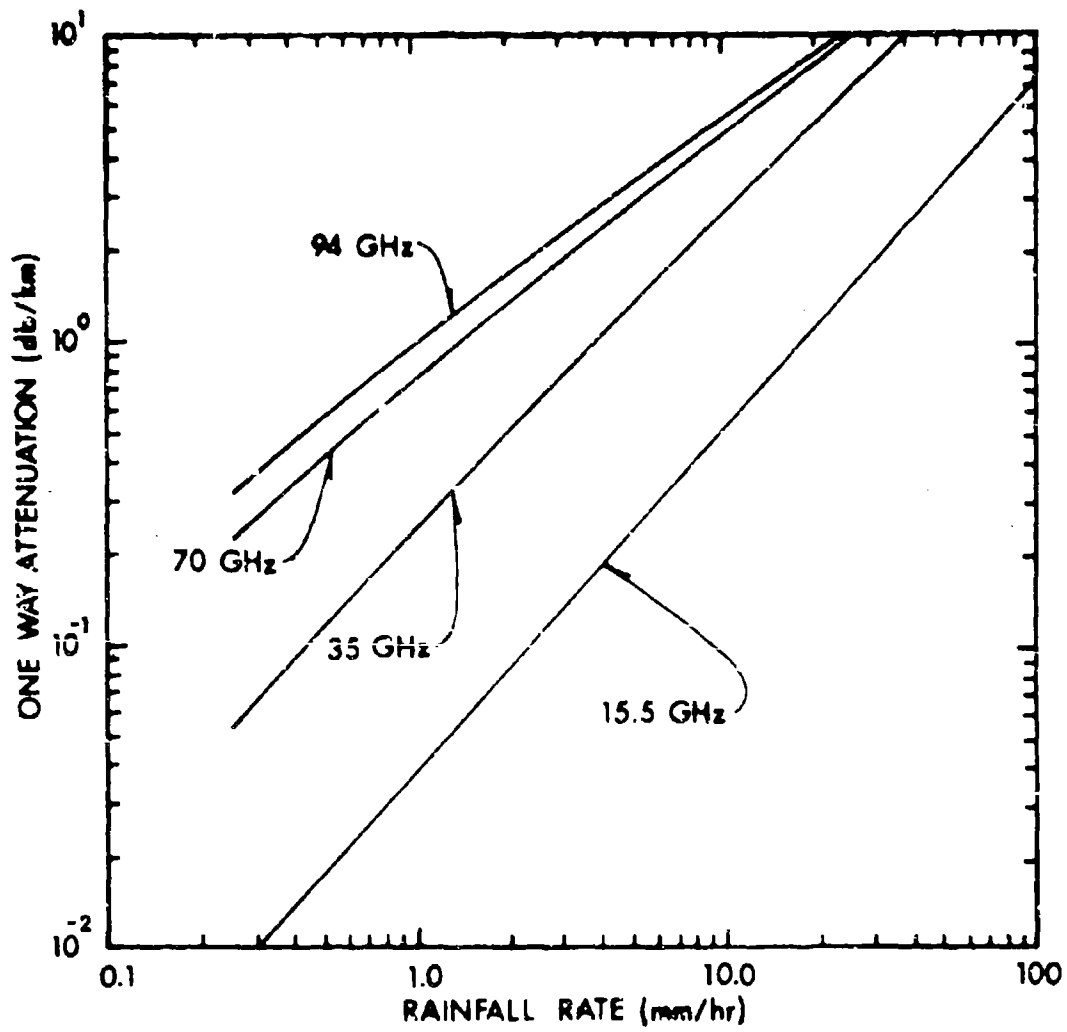


Figure A-6. One-Way Attenuation in Rain [20]

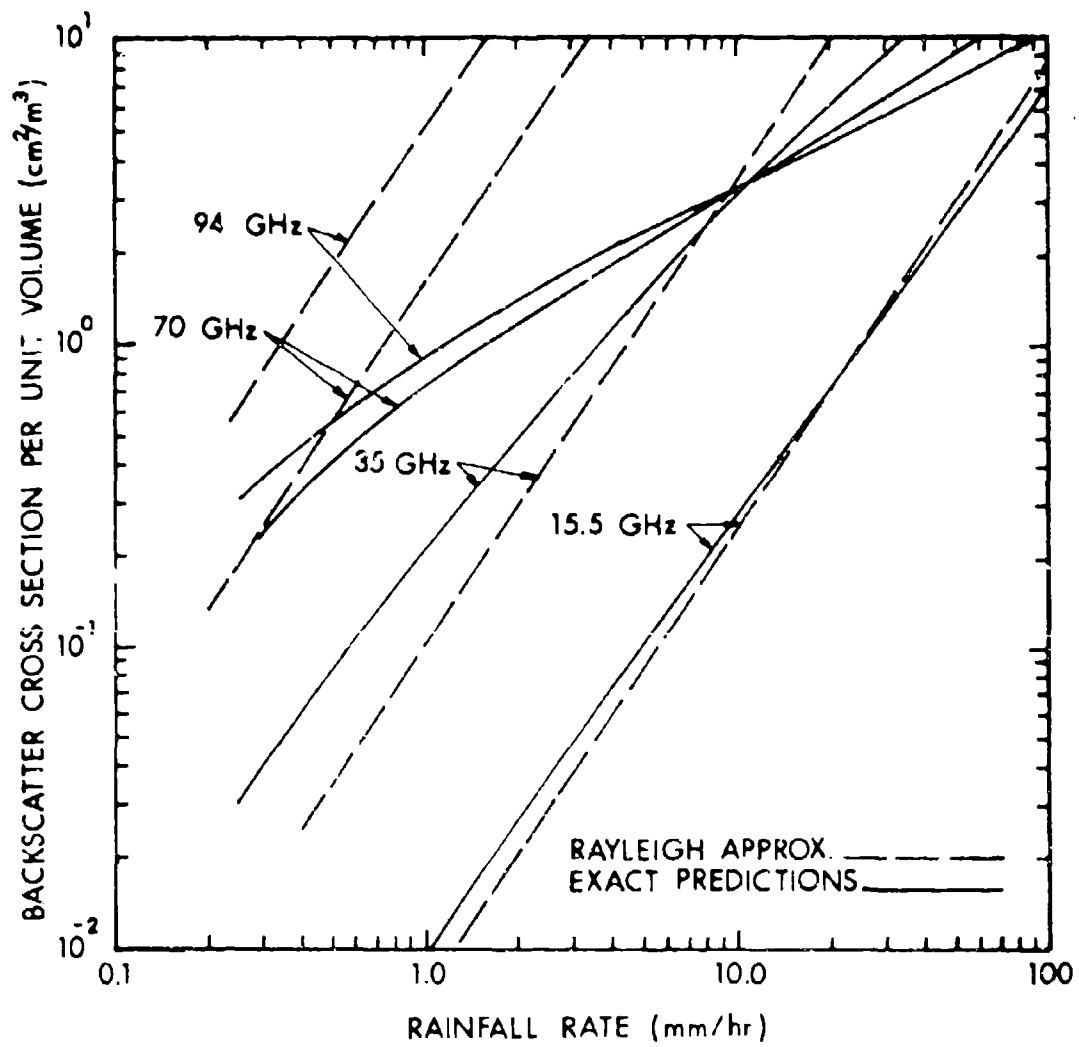


Figure A-7. Backscatter Cross Section Per Unit Volume of Rain at 0°C [20]

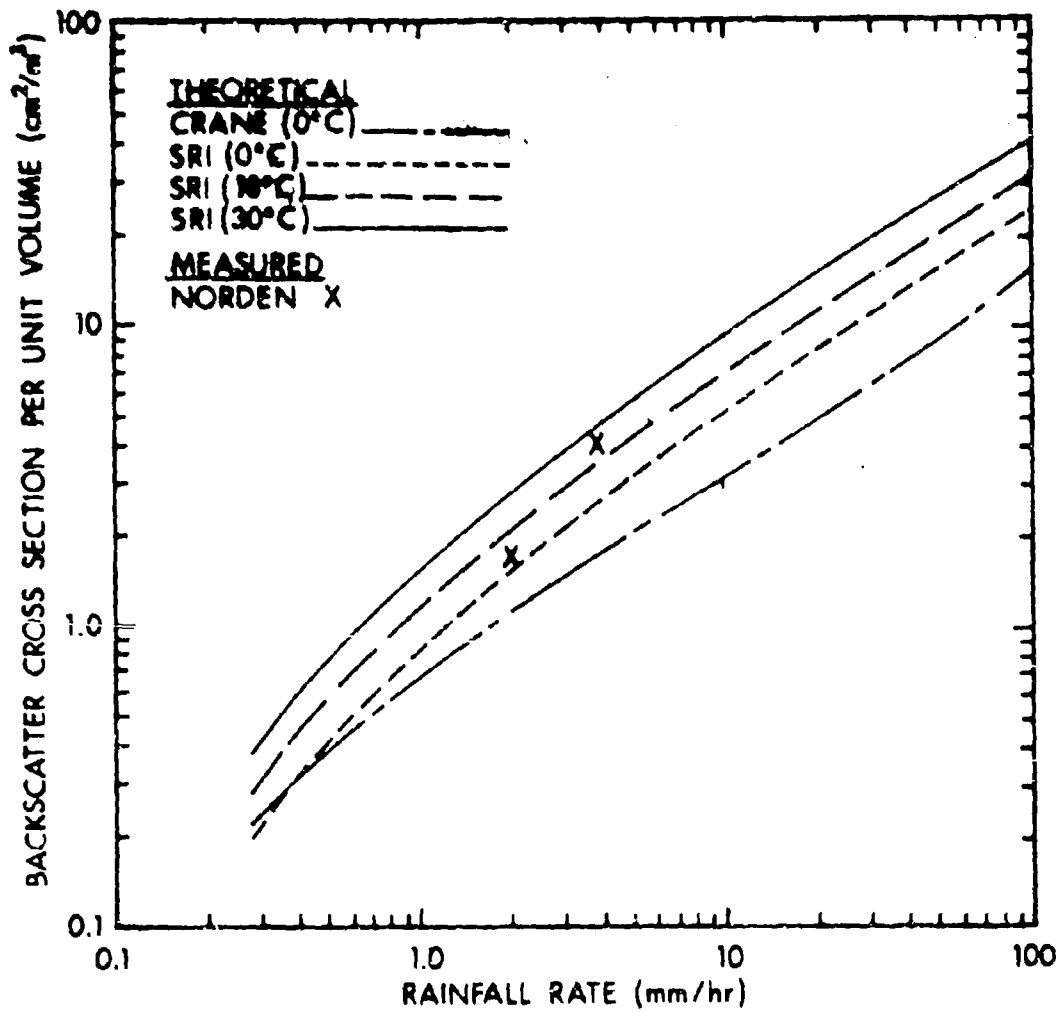


Figure A-8. Backscatter Cross Section Per Unit Volume of Rain at 70 GHz

#### IV. FOG

##### A. Characteristics of Fog

Fog results from the condensation of atmospheric water vapor into water droplets that remain suspended in the air.<sup>23</sup> When the resulting cloud or water droplets or ice crystals envelop an observer and restrict his horizontal visibility to one kilometer or less, the international definition of fog has been satisfied.<sup>24</sup> Evaporation and cooling are the principal physical processes which contribute to the formation of fog. Of the various fog classifications used by meteorologists, the two basic types of interest in radar applications are advection fog and radiation fog.

Advection is the horizontal movement of an air mass that causes changes in temperature or other physical properties. An advection (or coastal) fog is one which forms over open water as a result of the advection of warm moist air over colder water.

Radiation (or inland) fog forms in air that has been over land during the daylight hours preceding the night of its formation. Fogs which form in low, marshy land and along rivers on calm, clear nights are also considered radiation fogs.

The characteristics of these two fogs are given in Table A-2:

Table A-2  
Fog Characteristics<sup>12</sup>

	RADIATION (INLAND) FOG	ADVECTION (COASTAL) FOG
Average Drop Diameter	10 microns	20 microns
Typical Drop Size Range	5-35 microns	7-65 microns
Liquid Water Content	0.11 g/m <sup>3</sup>	0.17 g/m <sup>3</sup>
Droplet Concentration	200 cm <sup>-3</sup>	40 cm <sup>-3</sup>
Visibility	100 m	200 m

<sup>23</sup> J.F. O'Connor, "Fog and Fog Forecasting," Handbook of Meteorology, pp. 727-736, McGraw-Hill, New York, 1945.

<sup>24</sup> J.J. George, "Fog," Compendium of Meteorology, pp. 1179-1189, American Meteorological Society, Boston, 1951.

Note that the advection fog has a higher liquid water content, but greater visibility than the radiation fog. The correlation of visibility in fog to liquid water content is shown in Figure A-9 for both advection and radiation fogs.

There is considerable variation in the water content of clouds and water fogs, but in general, stratus (or low) clouds and typical radiation or advection fogs have water contents on the order to  $0.25 \text{ g/m}^3$  or less.<sup>12</sup> Mason<sup>25</sup> reports that the maximum liquid water content of an advection fog approaches  $0.4 \text{ g/m}^3$  when there is a strong temperature inversion. On rare occasions, the liquid water content can become as large as  $0.5$  to  $1.0 \text{ g/m}^3$  in very dense radiation fogs (with 20 to 30 meters visibility).<sup>12, 19, 26, 27</sup>

### B. Fog Attenuation

The small size of water droplets comprising a fog allows the use of the Rayleigh approximations in the determination of the reflectivity and attenuation at 70 GHz. Atlas<sup>28</sup> shows that in the Rayleigh scattering region the one-way attenuation coefficient,  $\alpha$ , is given by

$$\alpha = \frac{81.86 M \text{Im}(-K)}{\lambda \rho} \text{ dB/km,} \quad (\text{A-8})$$

where  $M$  = liquid water content per unit volume of fog in  $\text{g/m}^3$ ,

$\text{Im}(-K)$  = absorption coefficient,

$$K = \frac{m^2 - 1}{m^2 + 2},$$

$m$  = complex index of refraction,

$\lambda$  = wavelength in mm,

$\rho$  = density of water in  $\text{g/cm}^3$ .

<sup>25</sup>R.J. Mason, The Physics of Clouds, p. 97 et. seq., Clarendon Press, Oxford, 1957.

<sup>26</sup>P.N. Tverskoi, "Physics of the Atmosphere," Translated from Russian for the National Aeronautics and Space Administration and the National Science Foundation, NASA TTF-288 TT65-50114, 1965.

<sup>27</sup>Ralph G. Eldridge, "Haze and Fog Aerosol Distributions," Journal of the Atmospheric Sciences, Vol. 23, September 1966.

<sup>28</sup>D. Atlas, "Advances in Radar Meteorology," Advances in Geophysics, Vol. 10, pp. 317-478, Academic Press, New York, 1964.

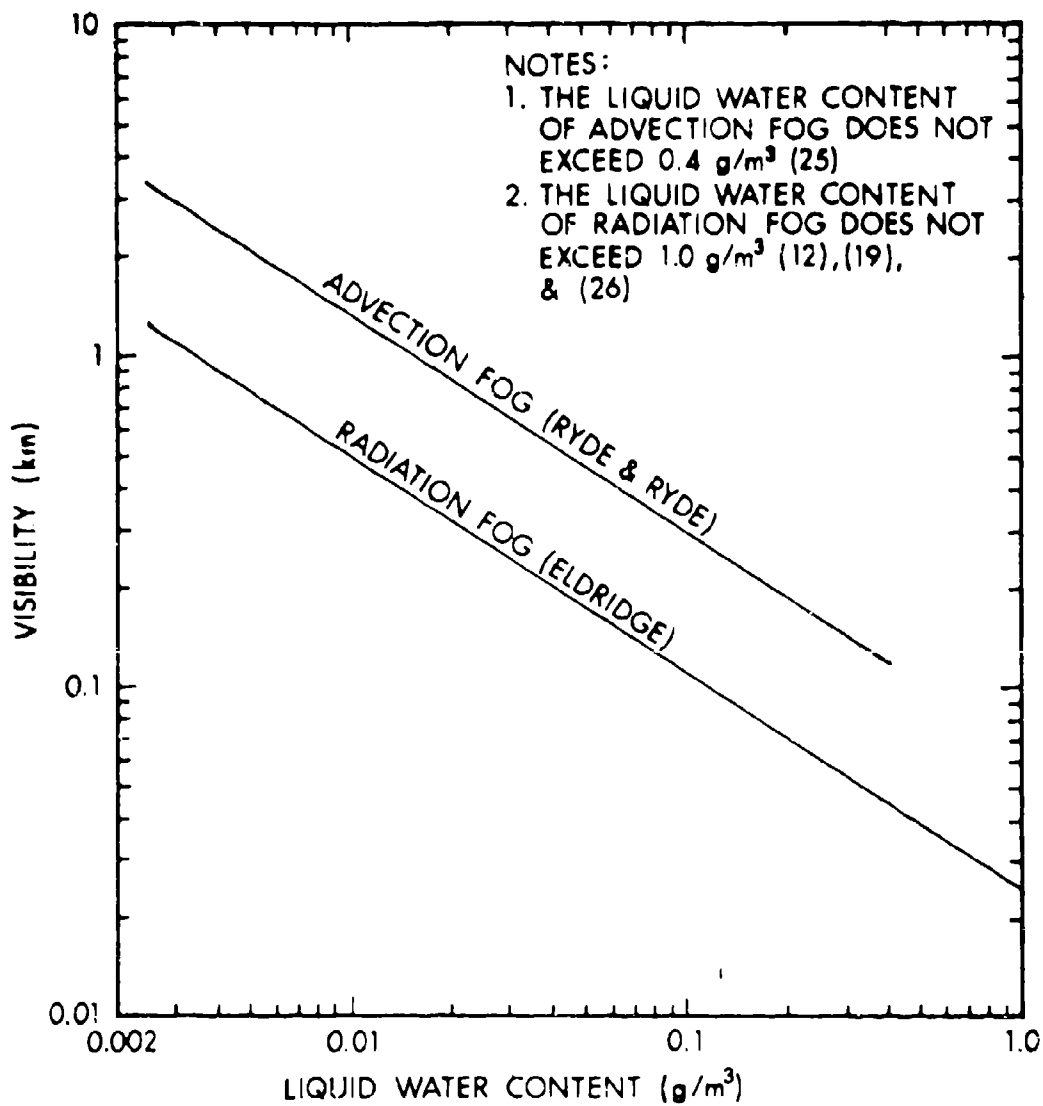


Figure A-9. Correlation of Visibility in Fog to Liquid Water Content

A density of 1 g/cm<sup>3</sup> for water is generally assumed for all temperatures, since the density varies no more than 0.78% over the 0°C to 40°C temperature range.<sup>29</sup>

In the Rayleigh scattering region, attenuation is due mainly to absorption. To calculate the absorption coefficient for fog, the index of refraction for water must be determined for the frequencies of interest. The complex index of refraction,  $m$ , is given in terms of the complex dielectric constant,  $\epsilon_c$ , by<sup>11</sup>:

$$m^2 = \epsilon_c = \epsilon_1 - j\epsilon_2, \quad (\text{A-9})$$

where  $\epsilon_1$  and  $\epsilon_2$  are the real and imaginary parts of the dielectric constant.

The dielectric constant may be evaluated by the Debye formula<sup>9</sup>:

$$\epsilon_c = \frac{\epsilon_0 - \epsilon_\infty}{1 + j\frac{\Delta\lambda}{\lambda}} + \epsilon_\infty, \quad (\text{A-10})$$

where  $\epsilon_0$ ,  $\epsilon_\infty$ , and  $\Delta\lambda$  are empirically derived constants. The Debye constants for water over the 0°C to 40°C temperature range are presented in Table A-3.

Table A-3  
Constants for the Debye Formula

T(°C)	$\epsilon_0$	$\epsilon_\infty$	$\Delta\lambda$ (cm)
0	88.0	5.5	3.59
10	84.0	5.5	2.24
18	81.0	5.5	1.66
20	80.0	5.5	1.53
30	76.4	5.5	1.120*
40	73.0	5.5	0.857*

\* These constants have been rederived and differ from those published in Reference 9. The derivation of these new values will be presented in a forthcoming paper.

<sup>29</sup>D.E. Gray, American Institute of Physics Handbook," McGraw-Hill, New York, 1957.

The complex indices of refraction of liquid water for 8.6, 4.3, and 3.2 mm energy were evaluated from equations (A-9) and (A-10) and are shown in Table A-4 as a function of water temperature.

Table A-4  
Complex Index of Refraction of Water

Temp. (0°C)	8.6 mm 35 GHz	4.3 mm 70 GHz	3.2 mm 94 GHz
0	3.947-j2.367	3.039-j1.603	2.801-j1.302
10	4.802-j2.735	3.543-j2.059	3.173-j1.732
20	5.607-j2.838	4.077-j2.380	3.596-j2.076
30	6.266-j2.733	4.608-j2.574	4.031-j2.323
40	6.748-j2.501	5.108-j2.649	4.457-j2.477

Using the complex indices of refraction listed in Table A-4, the absorption coefficients for 35, 70 and 94 GHz radiation were determined for the 0°C to 40°C temperature range. These values are given in Table A-5.

Table A-5  
Absorption Coefficients for Water

TEMPERATURE (0°C)	ABSORPTION COEFFICIENT		
	35 GHz	70 GHz	94 GHz
0	0.114	0.172	0.183
10	0.079	0.137	0.162
20	0.058	0.107	0.133
30	0.044	0.085	0.109
40	0.036	0.069	0.090

Examination of Table A-5 indicates that the absorption coefficient of water is highly sensitive to temperature in the 0°C to 40°C range. Assuming the density of water to be 1 g/m<sup>3</sup>, the attenuation coefficient of fog at 35, 70 and 94 GHz may be computed using equation (A-8), and is given by:

$$\alpha_{35} = 9.52 M \operatorname{Im}(-K) \text{ db/km}, \quad (\text{A-11})$$

$$\alpha_{70} = 19.04 M \operatorname{Im}(-K) \text{ db/km}, \quad (\text{A-12})$$

$$\alpha_{94} = 25.58 M \operatorname{Im}(-K) \text{ db/km}. \quad (\text{A-13})$$

The attenuation coefficient has been computed as a function of liquid water content using equations (A-11), (A-12), and (A-13) at 0°C and 40°C. These results are shown graphically in Figure A-10. An examination of the figure shows that the attenuation is substantially greater at 0°C than it is at 40°C.

Fog is generally described by its apparent optical visibility. This, however, is an inadequate characterization of fog in that similar visibility conditions may result from various meteorological conditions.

Visibility restrictions result from fog or low clouds with or without precipitation. These natural conditions occur in wide variety as a result of different weather conditions with seasonal and geographical variations. The detailed physical nature of the phenomena varies considerably even when producing comparable effects on vision. Reduced visibility can result from widely different distributions of water substance in terms of numbers of droplets of different dimensions.

As discussed in Section IV-A advection fogs have a higher liquid water content, but greater visibility than radiation fogs. The small number of large drops in an advection fog attenuates light, and hence visibility, much less than the large number of small drops in a radiation fog. The larger liquid water content of advection fogs causes greater attenuation of millimeter wave energy.

It is possible, however, to obtain representative values of attenuation based on the apparent visibility in each of the two basic fogs by combining the advection and radiation fog visibility curves from Figure A-9 with the attenuation curves of Figure A-10. However, the most meaningful description of the attenuation coefficient is obtained from the liquid water contents.

### C. Fog Backscatter

The backscatter cross section of fog can be determined from the Rayleigh scattering theory approximation given by Atlas<sup>28</sup> as

$$\eta = \frac{\pi^5}{4} \frac{|K|^2}{\lambda} Z, \quad (\text{A-14})$$

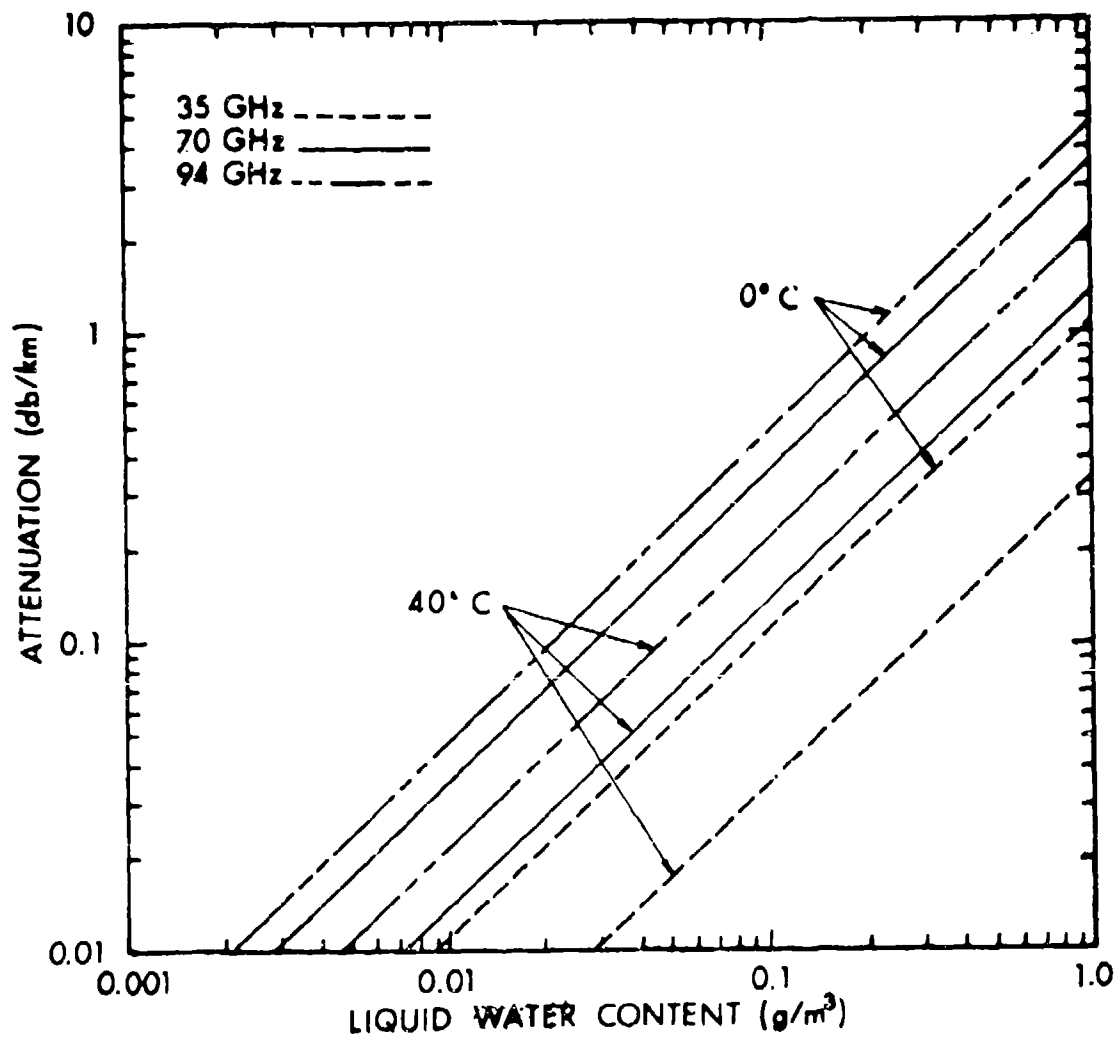


Figure A-10. One-Way Attenuation in Fog As a Function of Liquid Water Content

where

$|K|^2$  = backscatter coefficient,

$\lambda$  = wavelength in mm,

Z = reflectivity factor.

Atlas<sup>28</sup> gives the reflectivity factor in terms of the liquid water content for radiation fog as

$$Z_R = 0.48M^2 \quad (A-15)$$

and for advection fogs as

$$Z_R = 8.2M^2. \quad (A-16)$$

For M in units of g/m<sup>3</sup>, Z is in units of mm<sup>6</sup>/m<sup>3</sup>. It is obvious from the above relationships that the largest backscatter cross section would be found in advection fogs. However, in the millimeter wavelength region (35 to 94 GHz) the largest cross section was found to be less than 1.0 mm<sup>2</sup>/m<sup>3</sup>. Inasmuch as the cross section is more than two orders of magnitude smaller than that of rain, it has a negligible effect on radar system performance. Consequently, it will not be considered further.

## V. SYSTEM CONSIDERATIONS

### A. Introduction

The primary considerations in the selection of frequency relate to the antenna size, transmission properties of the atmosphere, and the state of component technology. Since radar systems must be designed to operate under adverse weather conditions, such as rain and fog, close examination must be made of attenuation and backscatter in these media, as a function of radar wavelength.

From an installation point of view, selection of a higher frequency would be advantageous in reducing antenna swept volume, with a corresponding reduction in radome size and the attendant structural, cost, and weight problems. Since swept volume varies approximately as the cube of the antenna size, any reduction in antenna size would prove quite beneficial. However, an increase in frequency to achieve this benefit must be carefully weighed against possible deleterious effects of weather.

### B. Clear Air Performance

The attenuation of millimeter energy in clear air was discussed in Section II. The clear air attenuation coefficient for the frequencies of interest is shown in Table A-6.

Table A-6  
Clear Air Attenuation Coefficient

Frequency GHz	New Band Designation	Old Band Designation	Attenuation Coefficient dB/km
35	K	K <sub>A</sub>	0.18
70	M	V	0.41
94	M	W	0.24

If the system is designated for clear air operation only, the frequency at which the attenuation is smallest should be chosen. However, any operational radar would be used under adverse weather conditions, such as rain and fog. The effect of rain and fog on system performance must be analyzed.

### C. Rain Performance

The performance of a radar operating in the rain is degraded by the absorption and scattering of the energy by the raindrops. For analysis purposes, the attenuation coefficient for light and heavy rain is given in Table A-7 for the three millimeter frequencies of interest. These values are taken from Figure A-6. (An attenuation coefficient of 1 dB/km would reduce the radar range of a system from 10 nautical miles in clear air to approximately 6.5 nautical miles; 7 dB/km reduces the range to approximately 1.1 nautical miles.)

Table A-7  
Rain Attenuation and Backscatter Coefficient

Frequency GHz	Light Rain (1 mm/hr)		Heavy Rain (16 mm/hr)	
	Attenuation (dB/km)	Backscatter (cm <sup>2</sup> /m <sup>3</sup> )	Attenuation (dB/km)	Backscatter (cm <sup>2</sup> /m <sup>3</sup> )
35	0.24	0.21	4.0	4.9
70	0.73	0.72	6.9	4.1
94	0.95	0.89	7.4	3.9

In addition to the attenuation, the energy reflected back to the radar is of interest since it contributes additional noise to the system. The backscatter coefficients are also presented in Table A-7 based on the curves of Figure A-7.

As can be seen, the backscatter cross section of heavy rain is comparable for V- and W-band radars and is actually less than at Ka-band. Thus, a V- or W-band radar operating in heavy rain would have less rain clutter than a Ka-band system. A W-band system would have slightly less rain backscatter than a V-band system at the heaviest rain rates, but the higher attenuation at all rain rates would tend to discourage the use of frequencies higher than V-band.

Even though rain attenuates V-band more than Ka-band, it does not preclude its choice as the frequency of an operational radar. Consider the target-to-rain clutter ratio for a given radar.

The return from a target is given by

$$P_{TGT} = \frac{P_T G^2 \lambda^2 \sigma_T}{(4\pi)^3 R^4 \exp(2\alpha R)} \quad (A-17)$$

The return due to rain is given by

$$P_{RAIN} = \frac{P_T G^2 \lambda^2 \sigma_i \theta \phi \left(\frac{cT}{2}\right)}{(4\pi)^3 R^2 \exp(2\alpha R)} \quad (A-18)$$

where  $P_T$  = peak power,

$G$  = antenna gain,

$\lambda$  = wavelength,

$\sigma_T$  = target cross section,

$R$  = range,

$\alpha$  = one way attenuation coefficient,

$\sigma_i$  = rain backscatter cross section per unit volume,

$\theta$  = azimuth beamwidth,

$\phi$  = elevation beamwidth,

$c$  = speed of light in free space,

$\tau$  = transmitted pulse width.

The target-to-clutter ratio is given by

$$\frac{P_{TGT}}{P_{RAIN}} = \frac{\sigma_T}{R^2 \left(\frac{c\tau}{2}\right) \sigma_i \theta \phi}$$

For a parabolic antenna of dimension  $\ell$

$$\theta = \phi = \frac{65 \lambda}{\ell}$$

Substituting,

$$\frac{P_{TGT}}{P_{RAIN}} = \left[ \frac{\sigma_T \ell^2}{R^2 \left(\frac{c\tau}{2}\right) (65)^2} \right] \frac{1}{\lambda^2 \sigma_i}$$

For a fixed target cross section at a given range, the term in brackets is a constant. It is now possible to define a figure of merit,  $F_m$ , for system performance in rain which is a function only of frequency; namely,

$$F_m = \frac{1}{\lambda^2 \sigma_i} \quad (A-19)$$

This factor gives an indication of the effect of rain backscatter on system performance.

Figure A-11 shows the "figure of merit" as a function of radar frequency. An examination of the curve indicates that a frequency in the Ka-band region would provide the poorest performance under all rain conditions. Consequently, a frequency other than 35 GHz should be chosen. Inasmuch as a frequency in the V- or W-band region offers acceptable performance in rain, it will be considered further. Before a frequency is chosen, its performance in fog must be investigated.

#### D. Fog Performance

The attenuation coefficient for millimeter propagation in fog was derived in Section IV-B. As shown in Figure A-10, the attenuation is linearly dependent on the liquid water content of the fog. In addition, there is a significant temperature dependence. The attenuation coefficient is given in Table A-8 for a liquid water content of  $0.1 \text{ g/m}^3$ .

Table A-8  
Attenuation Coefficient of Fog  
Liquid Water Content -  $0.1 \text{ g/m}^3$

Frequency GHz	Attenuation Coefficient dB/km	
	0°C	40°C
35	0.11	0.034
70	0.36	0.138
94	0.47	0.22

The attenuation increases with frequency. Thus the lowest frequency (35 GHz) should be chosen for adequate fog performance.

#### E. Frequency Choice

Consideration of clear air and fog attenuation would lead to the choice of 35 GHz as the frequency for an operational system. However, once the effect of rain backscatter is considered, a frequency in M-band (70 or 94 GHz) would offer the best performance under all weather conditions. A choice between 70 and 94 GHz requires a careful examination of component technology, noise, and ECM. There has been sufficient development of 70 GHz components to allow the design of practical systems at this frequency band.

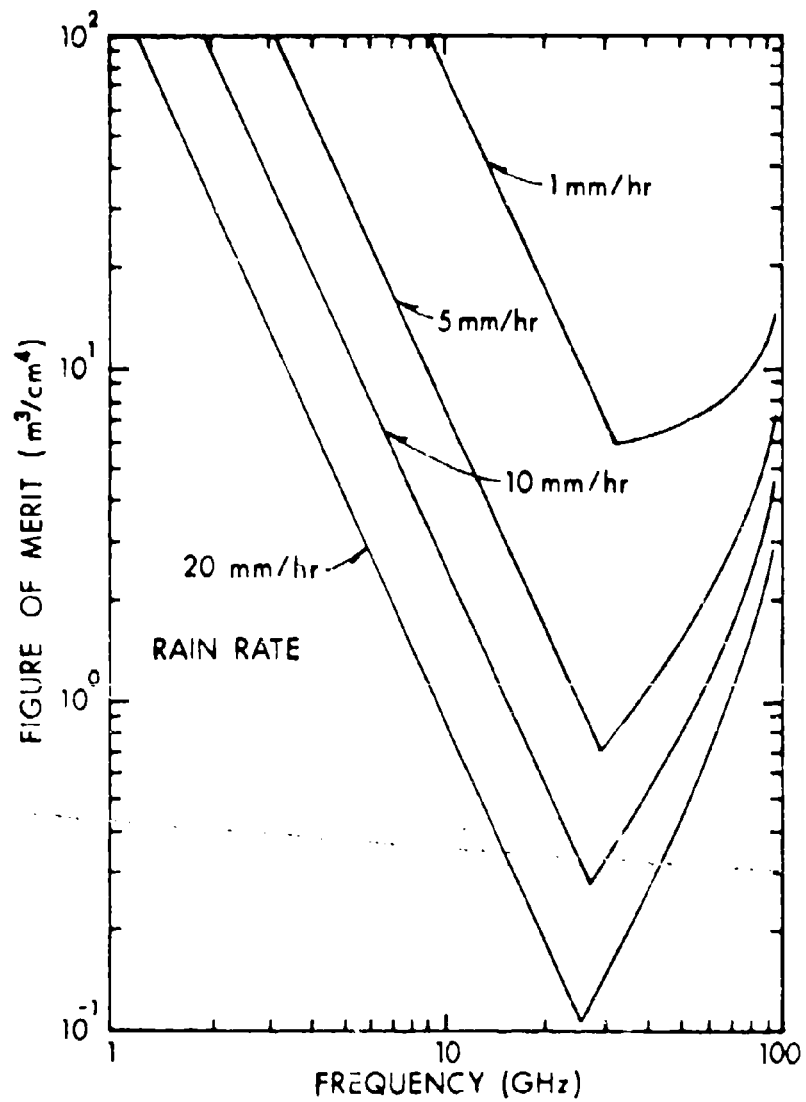


Figure A-11. Figure of Merit of Radar Performance in Target Cross Section = 1 Square Meter

## APPENDIX B FLUCTUATING CLUTTER

### I. INTRODUCTION

In this section we shall be concerned with the reradiation characteristics of terrain at millimeter wavelengths where the short wavelength permits operation of small lightweight radar systems capable of operation in adverse weather over ranges of several nautical miles.

Because of the short wavelength, the clutter environment plays a very significant role in obstacle detectability in that small variations in clutter position cause large fluctuations in the strength of the background signal. A terrain clutter model is presented whose output is characterized by its power spectral density and its probability density function. A comparison with experimental data indicates that the model may confidently be used for signal detection studies at these wavelengths.

### II. STATISTICAL NATURE OF CLUTTER

The signal radiated by a large group of scatterers has been studied on a statistical basis for many years. The theoretical models which have served to describe observed phenomena generally consist of an infinite number of independent scatterers, each free to move at a different velocity. The description of the signal emanating from such an array forms a branch of the general theory of random processes dating back to Rayleigh.<sup>1</sup>

The received electric field strength can be shown to be of the form<sup>2</sup>

$$E(t) = R(t) \cos [\omega_0 t + \phi(t)], \quad (B-1)$$

---

<sup>1</sup> Lord Rayleigh, Theory of Sound, Second Edition, Volume 1, MacMillian, 1894.

<sup>2</sup> D. Kerr, Propagation of Short Radio Waves, Radiation Laboratory Series, Volume 13, McGraw-Hill Book Company, 1951.

where  $\omega_0$  is the transmitted frequency and  $R(t)$  and  $\phi(t)$  are functions of scatterer motion. If we define a vector,  $R(t)$ , whose magnitude is equal to  $R$  and whose phase is  $\phi$ , then the probability density function of  $R$ , i.e., the probability that  $R$  lies between  $R$  and  $R + dR$ , is given by the well-known Rayleigh distribution<sup>2</sup>

$$P(R) = \frac{2}{P_0} R \exp\left(-\frac{R^2}{P_0}\right), \quad (B-2)$$

where  $P_0$  is a parameter of the distribution. A plot of equation (B-2) is given in Figure B-1. The mean value of  $R$  is  $\frac{\sqrt{\pi P_0}}{2}$ , and the rms value is  $\sqrt{P_0(4 - \pi)/2}$ .

Extending the discussion to the case of a fixed target return plus clutter, Schwartz<sup>3</sup> has shown that the probability density function of  $R$ ,  $q(R)$ , is given by

$$q(R) = \frac{2R}{P_0} \exp\left[-\left(\frac{R^2}{P_0} + m^2\right)\right] I_0\left(\frac{2mR}{\sqrt{P_0}}\right), \quad (B-3)$$

where  $I_0$  is the modified Bessel function,  $m^2$  is the signal-to-noise power ratio. For  $m^2 \gg 1$ , equation (B-3) reduces to the Gaussian function,

$$q(R) = \frac{1}{\sqrt{\pi P_0}} \exp\left[-\left(\frac{R}{P_0} - \left(\frac{R}{\sqrt{P_0}} - m\right)^2\right)\right]. \quad (B-4)$$

Thus, for high signal-to-noise ratios, the probability density function of the magnitude of the composite return approaches a Gaussian distribution with mean,  $m\sqrt{P_0}$ , and standard deviation,  $\sqrt{P_0}/2$ .

<sup>3</sup>M. Schwartz, Information Transmission, Modulation, and Noise, McGraw-Hill Book Company, 1959.

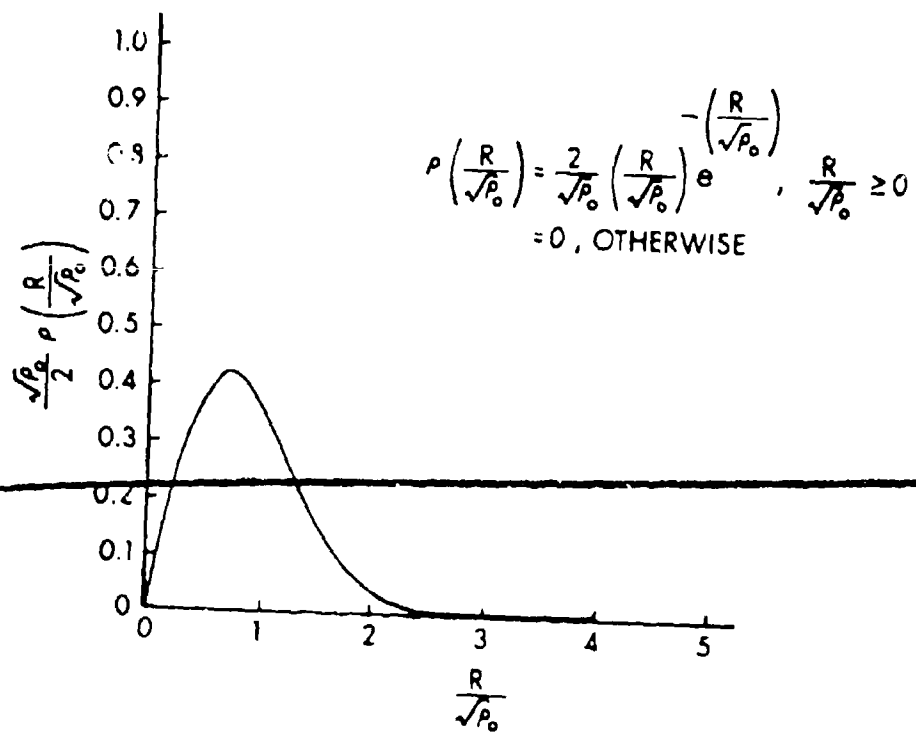


Figure B-1. The Rayleigh Probability Density Function

Up to this point we have been concerned with the long-term statistics of the clutter which essentially determine the "betting curve" of the noise process. Now let us examine the correlation between samples of the clutter signal spaced at second intervals, i.e., the autocorrelation function of the clutter process. This problem has not been solved analytically for the model discussed previously, although much experimental data has been obtained for a wide variety of scatterer mobilities and forcing functions, such as wind. The Fourier transform of the autocorrelation function is the power spectral density, and it is with this function that we shall be concerned. Figure B-2 is a plot of experimental data obtained for various types of terrain when observed at the frequency 70 GHz. Barlow<sup>4</sup> suggests that a good approximation to the power spectral density is given by

$$W(f) = \exp \left[ -a \left( \frac{f}{f_0} \right)^2 \right], \quad (\text{B-5})$$

where "a" is a spectrum parameter dependent on the composition of the area being observed and  $f_0$  is the frequency of operation. Shown on Figure B-2 is a plot of equation (B-5) for values of "a" obtained by Barlow at 1 GHz.

It is evident that in each case observed data at 70 GHz has a broader spectrum than that which would have been predicted using Barlow's parameters. A possible explanation for this discrepancy is that at low frequencies the smaller structures such as leaves and grass play a more prominent role.

In Figures B-3 and B-4 are shown the probability density functions for tree-covered terrain with the mean value removed. For the cases considered, the mean values were large compared to the fluctuating component and produced a Gaussian distribution as predicted by equation (B-4), where noise is replaced by the fluctuating component and  $m \gg 1$ .

### III. PROBABILITY DENSITIES OF FLUCTUATING CLUTTER

The problem of describing the radar video return from a fixed target immersed in clutter is analogous to that of describing a signal composed of a sine wave plus narrow band noise. This problem has been extensively treated in the literature.<sup>5,6</sup>

<sup>4</sup>E. J. Barlow, "Doppler Radar," Proc. IRE, Vol. 37, April 1949.

<sup>5</sup>S. O. Rice, "Mathematical Analysis of Random Noise," BSTJ, Vol. 24, pp. 98-107.

<sup>6</sup>D. Middleton, Introduction to Statistical Communication Theory, McGraw-Hill Book Company, 1960.

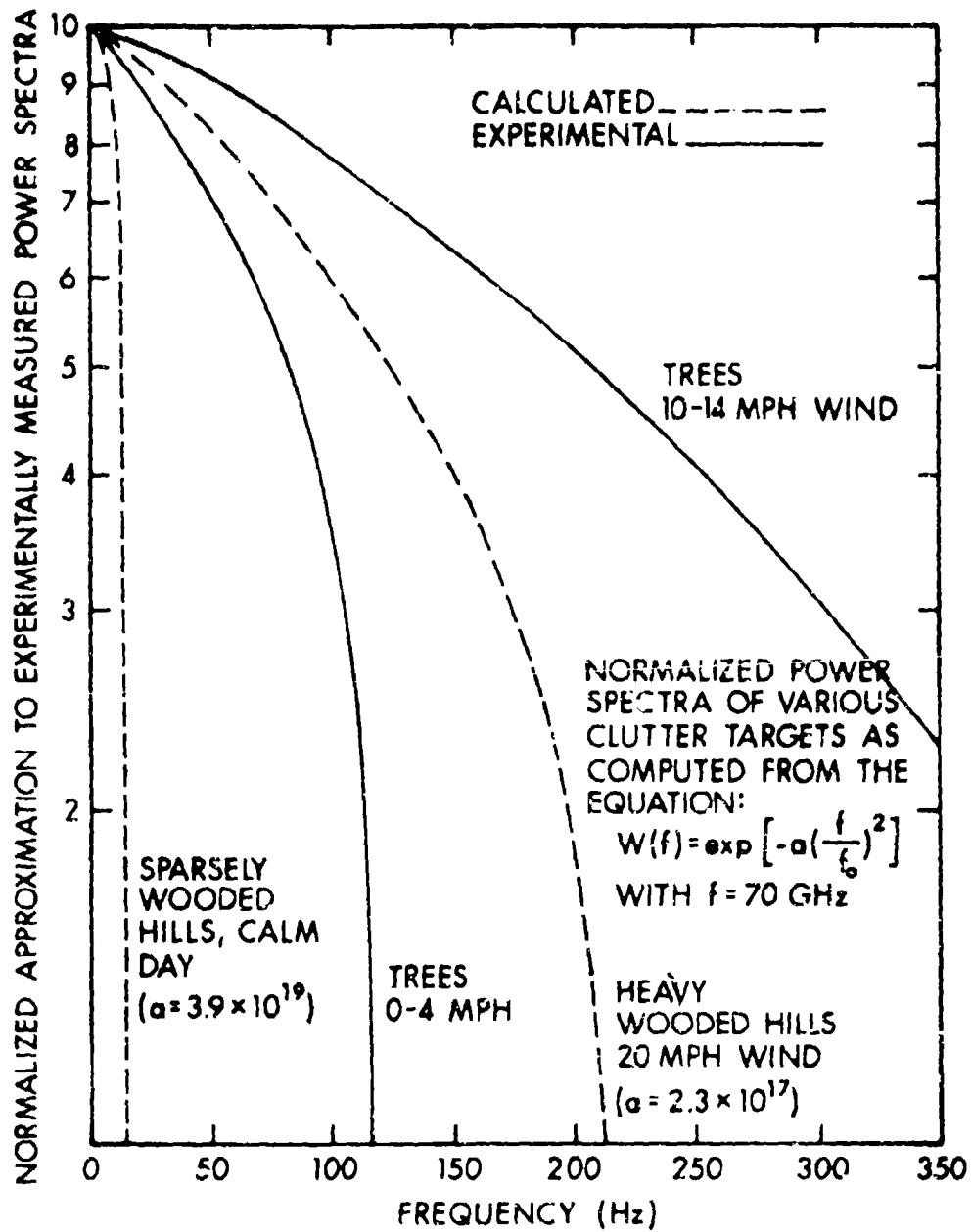


Figure B-2. Clutter Spectrum of Wooded Ground at Millimeter Wavelengths

PATCH OF TREES, 0-4 MPH WIND

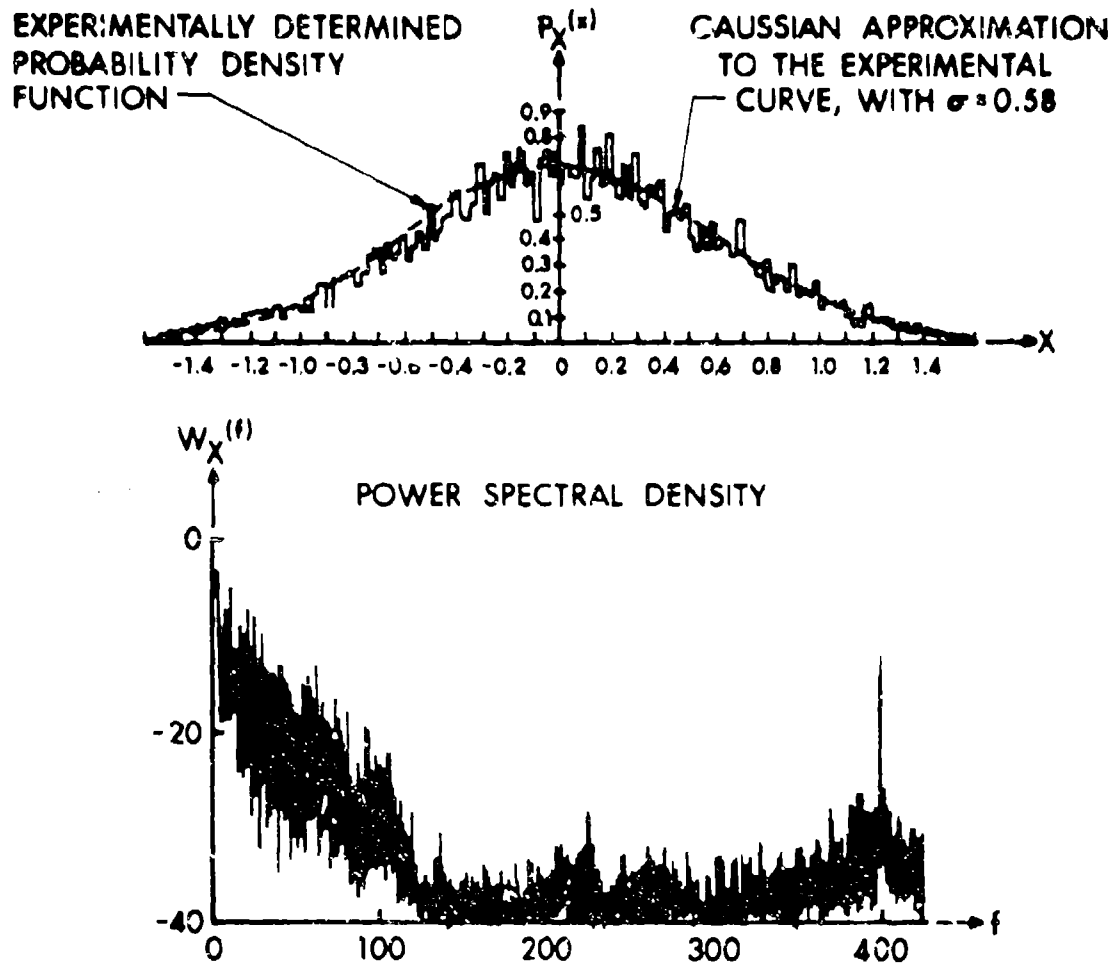


Figure B-3. Characteristics of the Radar-Video Return From A Fluctuating Target

PATCH OF TREES, 10-14 MPH WIND

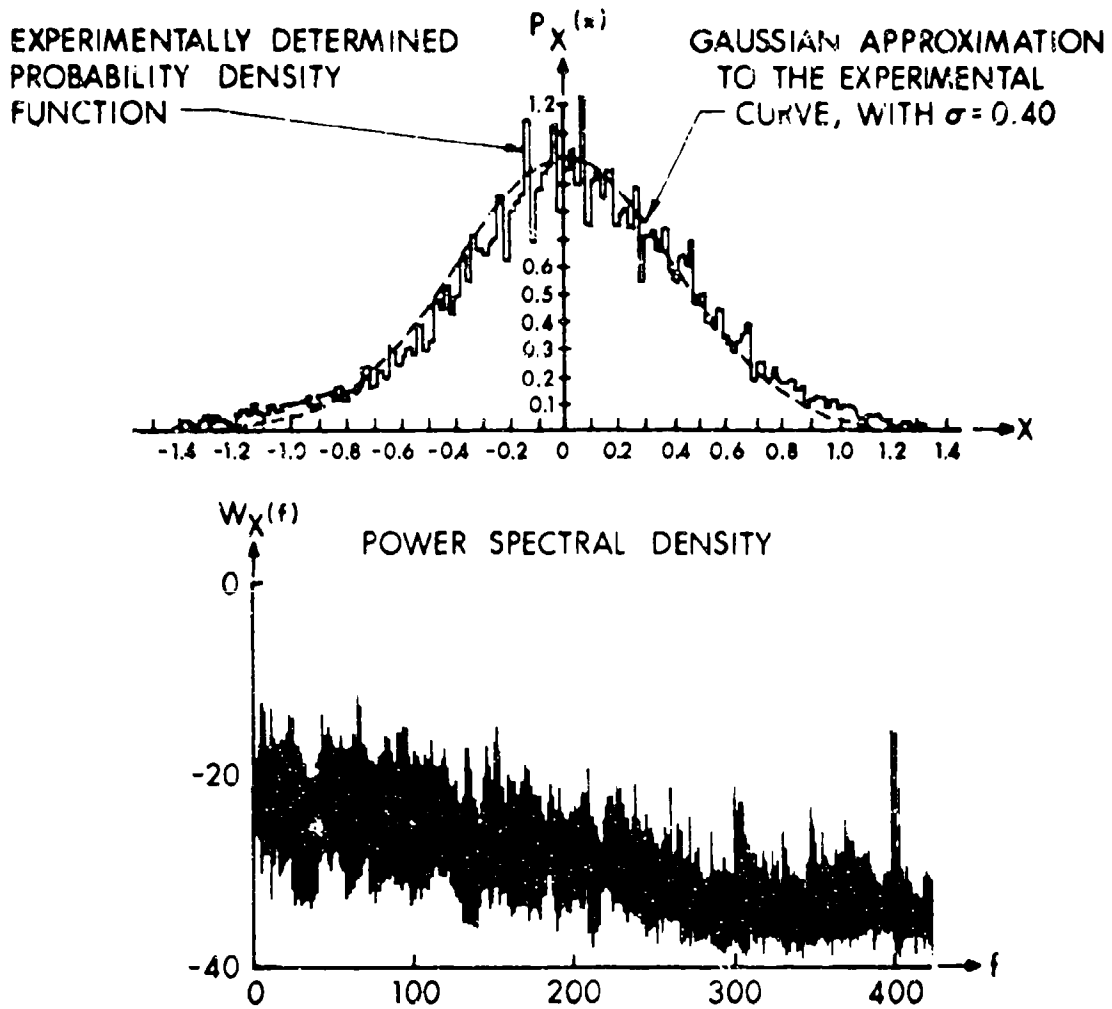


Figure B-4. Characteristics of the Radar-Video Return From A Fluctuating Target

The instantaneous signal voltage,  $v(t)$ , in the receiver prior to detection can be written as the superposition of the return from a large number of independent scatterers, representing clutter, and an unmodulated sine wave at the radar frequency,  $f_0$ , corresponding to the return from the fixed target. Rice<sup>5</sup> has shown that

$$v(t) = [x_c(t) + A] \cos 2\pi f_0 t - x_s(t) \sin 2\pi f_0 t, \quad (\text{B-6})$$

where  $x_c$  and  $x_s$  are normally distributed random variables related to the clutter process. Their probability density functions are given by<sup>5</sup>

$$p(x_c) = \frac{1}{2\pi C} e^{-\frac{x_c^2}{2C}}, \quad (\text{B-7})$$

$$p(x_s) = \frac{1}{2\pi C} e^{-\frac{x_s^2}{2C}}, \quad (\text{B-8})$$

where  $C$ , the variance of the distributions, is equal to the mean clutter power, and  $A$  is the constant amplitude of the return from the fixed target. As the clutter spectrum is narrow band,<sup>4</sup> it is appropriate to write

$$v(t) = r(t) \cos [2\pi f_0 t + \theta(t)] \quad (\text{B-9})$$

with

$$\theta = \tan^{-1} \frac{x_s}{x_c + A} \quad (\text{B-10})$$

and

$$r = x_s^2 + (x_c + A)^2. \quad (\text{B-11})$$

For a radar receiver employing a linear envelope detector, envelope  $r(t)$  of instantaneous voltage  $v(t)$  is equal to the radar video return. It is known that the probability density function of  $r$ ,  $p(r)$ , is given by<sup>5</sup>

$$p(r) = \frac{1}{C} e^{-s^2 r} e^{-\frac{r^2}{2C}} I_0 \left( r s \sqrt{\frac{2}{C}} \right), \quad r \geq 0$$

(B-12)

$$= 0 \quad r < 0$$

where  $p_R(r)$  is zero for negative values of  $r$  as the radar video is not allowed to make negative excursions.  $I_0$  is the modified Bessel function of the first kind and zero order,<sup>7</sup> and

$$s^2 = \frac{A^2}{2C} \tag{B-13}$$

is the target-to-clutter power ratio.

---

<sup>7</sup> Handbook of Mathematical Functions, U.S. Department of Commerce, National Bureau of Standards, Applied Mathematics Series 55, 1964, pp. 374-377.

## APPENDIX C

### CLUTTER DISCRIMINATION TECHNIQUES (MOVING TARGET INDICATION)

#### I. INTRODUCTION

It is possible to distinguish between fixed and moving objects on the basis of the doppler shift in the frequency of transmission which occurs when radar signals are reflected from moving objects. The doppler shift is proportional to the radial velocity of the moving target with respect to the radar and inversely proportional to the wavelength of the radar. Detection of this frequency shift makes it possible to discern moving targets in the presence of unwanted fixed or scintillating targets whose returns may be many times stronger than those of the moving targets.

Detection of the doppler shift in frequency requires a knowledge either of the phase and frequency of the transmitted signal or of an external reference with respect to which the shifted frequency can be compared.

The three types of MTI radar most frequently used today are the coherent, coherent-on-receiver, and clutter-coherent systems. Coherent and coherent-on-receiver systems measure the doppler shift with respect to the transmitted frequency, whereas clutter-coherent systems measure the doppler shift with respect to the essentially time-invariant clutter return. Depending upon the system, the frequency shift produced by the moving target may be detected as a phase or as an amplitude fluctuation. In coherent and coherent-on-receiver systems, the phase information is processed to yield moving target indication. In clutter-coherent MTI systems, amplitude information is used to detect the doppler component produced by a moving target. Highly stable oscillators are not required although a moving target can be detected only when viewed against a fixed or scintillating background. For this reason, a clutter-coherent processor offers a simple approach to the detection of targets moving along the ground, an approach that is attractive where space and weight are limited, as in an aircraft or portable ground system.

The video output of both coherent and clutter-coherent pulsed radar systems is a superposition of the familiar "butterfly" signal, whose amplitude varies at the doppler frequency, and the extraneous lower frequency clutter signals against which the doppler signal must compete for detection. Discrimination between fixed and moving targets on the basis of differences in their frequency spectra is made more difficult by the motion of the radar platform. Although the relative velocity between the radar and the clutter will usually differ from the relative velocity between the radar and the moving target,

their frequency spectra tend to overlap due to spectral broadening of both the target and the clutter returns. Spectral spreading of the clutter is minimal when the antenna points in the same direction as the aircraft velocity vector. As the antenna moves off this position, however, the spectral spreading increases. Additional spectral broadening results from the processing of a finite pulse train and from the use of a noncoherent second detector as well as from instabilities in the radar itself.

However, with special attention to frequency, amplitude, and time jitter, a conventional radar may be used in a clutter-coherent MTI mode. The only requirement is that an MTI video processor be added to the conventional radar. The function of this processor is to reduce the clutter returns that are present in the detected video output of the radar while preserving the moving target information. The rejection of the low-frequency clutter echoes and transmission of the higher frequency, doppler shifted, target returns can be achieved by a number of filtering techniques, including delay line cancellation and the use of range-gated filters.

Delay line cancellation involves the subtraction of the radar return on successive pulses. The residue is indicative of the speed and magnitude of the moving target. Range information is preserved, but the filter characteristics necessary for good clutter discrimination require the use of more than one delay line for realization. Size and weight are problems, as is the requirement for maintaining stability between the delay line length and the interpulse period.

Filter characteristics yielding superior clutter discrimination, while avoiding the problems peculiar to the use of delay lines, e.g., the interpulse period stability requirement, can be achieved by quantizing the range into discrete, contiguous intervals. This process, known as range gating, preserves the range information. Associated with each range interval is a sample and hold circuit (boxcar detector) that operates into its own filter network. By properly designing the filter, an MTI is obtained which has far greater moving target detection capability than a single delay line canceller.

## II. RANGE-GATED DOPPLER PROCESSOR

Figure C-1 is a simplified block diagram of a range-gated doppler signal processor. The video signal is applied to the range channels through a buffer stage that provides both isolation and a convenient means of shifting the dc level of the input. The system contains N channels, each corresponding to a discrete contiguous range element. Each channel consists of a boxcar, bandpass filter, rectifier and low pass filter, and threshold gate. Information is gated into each channel at a time coinciding with a prescribed range

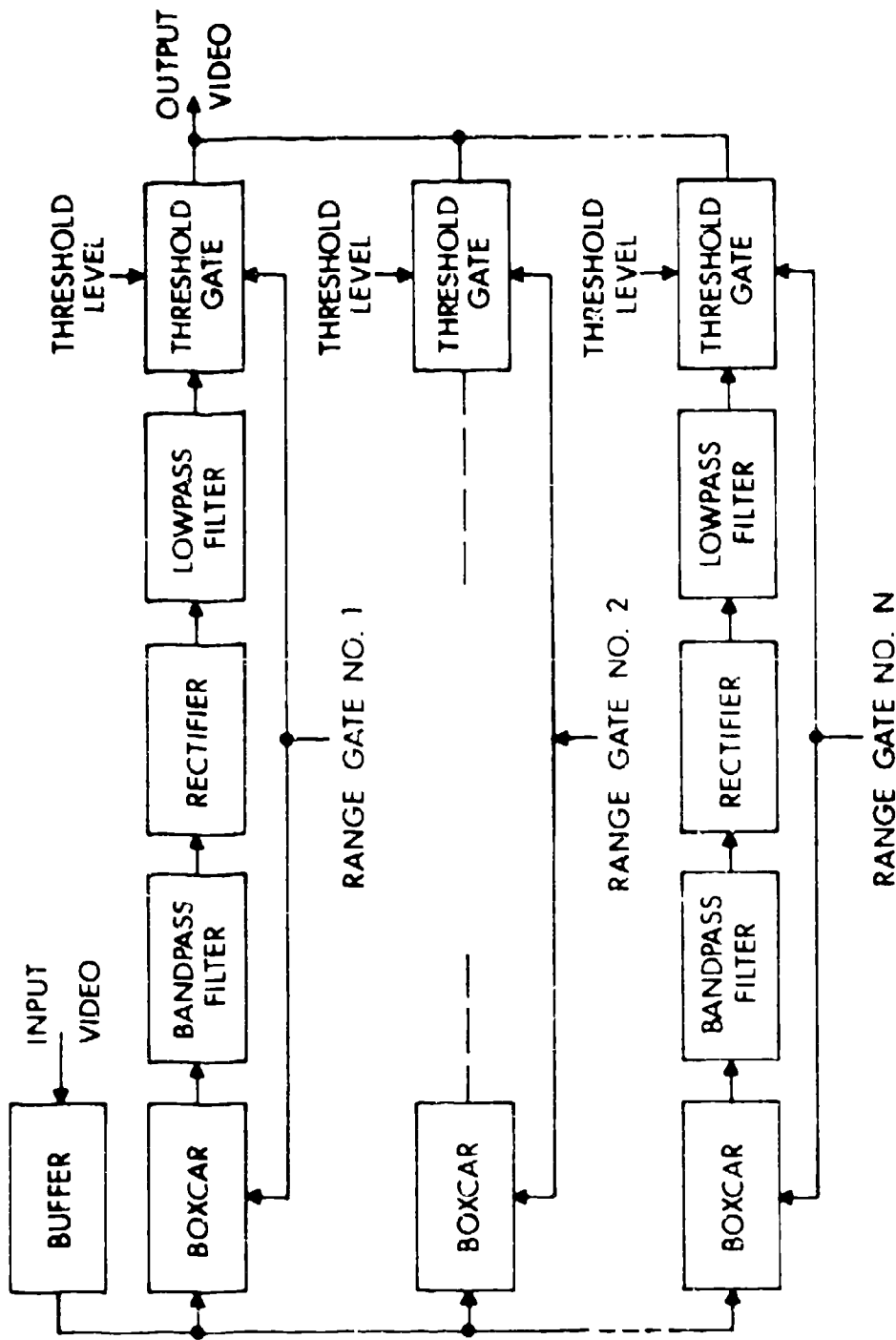


Figure C-1. Range-Gated Doppler Signal Processor

and is held by the boxcar circuit until the next sample value is obtained, one PRF interval later. The output of the boxcar is applied to a bandpass filter which serves to reject the clutter components of the radar return while passing the doppler frequencies. The doppler returns are rectified and integrated in a low-pass filter that improves the signal-to-noise ratio by averaging the signal over the beamwidth of the antenna pattern. The processed video is then threshold detected and gated onto a common line.

The timing pulses (range gates) are derived from an integrated circuit timing generator to sequentially gate the range channels once each pulse repetition interval. The width of the range gates depends upon the range accuracy desired. If the range gate is made equal to the width of the transmitted radar pulse, then maximum range resolution is achieved. The moving target competes only against clutter within its range interval, thereby permitting maximum clutter attenuation. The number of gates is determined by the desired range coverage, and in turn determines the complexity of the gating circuitry and the number of data processing channels required. Because this number can become large if extended range coverage is desired, careful attention must be given to using circuits that can be fabricated in thin-film or integrated circuit form. To this end, pulse transformers have been eliminated by redesigning boxcar detector circuits and by replacing blocking oscillators with diode-transistor micro-logic elements. Similarly, inductors have been eliminated by using active RC networks, rather than LC filters, to achieve the sharp cutoff frequency characteristics required for good clutter discrimination.

DISTRIBUTION LIST

<u>No. of Copies</u>	<u>Organization</u>	<u>No. of Copies</u>	<u>Organization</u>
2	Commander Defense Documentation Center ATTN: DDC-TCA Cameron Station Alexandria, VA 22314	1	Commander US Army Aviation Systems Command ATTN: DRSAV-E 12th and Spruce Streets St. Louis, MO 63166
1	Director of Defense Research and Engineering Engineering Technology ATTN: Mr. L. Weisberg Washington, DC 20301	1	Director US Army Air Mobility Research and Development Laboratory Ames Research Center Moffett Field, CA 94035
1	Director Defense Advanced Research Projects Agency ATTN: Dr. L. Strom 1400 Wilson Boulevard Arlington, VA 22209	5	Commander US Army Electronics Command ATTN: DRSEL-RD DRSEL-TL-I, Dr. Jacobs DRSEL-CT DRSEL-CT-R, Mr. Pearce DRSEL-VL, Mr. Post Fort Monmouth, NJ 07703
1	Director Institute for Defense Analyses 400 Army-Navy Drive Arlington, VA 22202	1	Office of the Test Director Joint Services LGW/CM Test Program ATTN: DRSEL-WL-MT Mr. R. Murray White Sands Missile Range NM 88002
1	Director Defense Nuclear Agency ATTN: STRA (RAEL), LTC Brown Washington, DC 20305	1	Commander US Army Electronics Command ATTN: DRSEL-BL-RD Atmos. Sci. Rsch. Fort Huachuca, AZ 85613
1	Commander US Army Materiel Development and Readiness Command ATTN: DRCDMA-ST 5001 Eisenhower Avenue Alexandria, VA 22333	1	Director US Army Night Vision Laboratory Visionics Technical Area ATTN: DRSEL-NV-VI Mr. J. Russell Moulton Fort Belvoir, VA 22060
1	Commander US Army Materiel Development and Readiness Command ATTN: DRCDE-W 5001 Eisenhower Avenue Alexandria, VA 22333		

DISTRIBUTION LIST

<u>No. of Copies</u>	<u>Organization</u>	<u>No. of Copies</u>	<u>Organization</u>
7	Commander US Army Missile Command ATTN: DRSMI-R, Mr. Pittman DRSMI-RBL DRSMI-RES DRSMI-RER, Mr. H. Green DRSMI-RF, Mr. C. Hussey DRSMI-RFC, Mr. A. Michetti DRSMI-RFE, Mr. Salonimer Mr. Duvall Redstone Arsenal, AL 35809	4	Commander US Army Frankford Arsenal ATTN: SARFA-FCW Mr. R. Phielsticker (2 cys) SARFA-FCS, Mr. J. Schmitz SARFA-FCD-M Mr. S. Greenberg Philadelphia, PA 19137
1	Commander US Army Missile Command Redstone Scientific Information Center ATTN: Chief, Document Station Redstone Arsenal, AL 35809	3	Commander US Army Picatinny Arsenal ATTN: SARPA-DW12, T. Malgeri SARPA-ND-C Mr. Rosenbluth SARPA-V Dover, NJ 07801
1	Commander US Army Tank Automotive Development Command ATTN: DRDTA-RWL Warren, MI 48090	1	Commander US Army White Sands Missile Range ATTN: STEWS-TE, Mr. J. Flores White Sands Missile Range NM 88002
3	Commander US Army Mobility Equipment Research & Development Command ATTN: DRSME-RZT SMEFB-EM Mr. K. Steinback Tech Doc Cen, Bldg 315 Fort Belvoir, VA 22060	3	Commander US Army Harry Diamond Laboratories ATTN: DRXDO-TD/002 DRXDO-TI DRXDO-RA, J. Salerno 2800 Powder Mill Road Adelphi, MD 20783
5	Commander US Army Armament Command ATTN: DRSAR-RD, Dr. J. Brinkman DRSAR-RDF DRSAR-RDT-F, Dr. R. Moore DRSAR-RDT-L DRSAR-RDT-S, Mr. C. Erwin Rock Island, IL 61202	1	Commander US Army Foreign Science and Technology Center Federal Office Building 220 7th Street, NE Charlottesville, VA 22901
		1	Commander US Army Training and Doctrine Command Fort Monroe, VA 23351

DISTRIBUTION LIST

<u>No. of Copies</u>	<u>Organization</u>	<u>No. of Copies</u>	<u>Organization</u>
1	Commander US Army Combined Arms Combat Development Activity Fort Leavenworth, KS 66027	1	Commander US Naval Air Systems Command ATTN: AIR-2324, Mr. C. Francis Washington, DC 20360
1	Commander MASSTER ATTN: Dr. P. C. Dickinson Scientific Advisor Fort Hood, TX 76544	1	Chief of Naval Research Department of the Navy Washington, DC 20360
1	Director US Army TRADOC Systems Analysis Activity ATTN: ATAA-SA White Sands Missile Range NM 88002	2	Commander US Naval Air Development Center ATTN: AETD, Radar Division Mr. M. Foral Warminster, PA 18974
1	Office of Assistant Secretary of the Army for R&D Assistant for Electronics ATTN: Mr. Victor L. Friedrich Washington, DC 20310	1	Commander Center for Naval Analysis ATTN: Document Control 1401 Wilson Boulevard Arlington, VA 22209
1	HQDA (DAMA-CSM-CA/LTC N. Conner) Washington, DC 20310	2	Commander US Naval Electronics Lab Center ATTN: Code 2330 Mr. J. H. Provencher Technical Library San Diego, CA 92152
1	HQDA (DAMA-DDZ-C) Washington, DC 20310	2	Commander US Naval Surface Weapons Center Dahlgren Laboratory ATTN: Library Code DF34 Dahlgren, VA 22448
1	Commander US Army Research Office ATTN: Dr. D. Van Hulsteyn P.O. Box 12211 Research Triangle Park NC 27709	3	Commander US Naval Weapons Center ATTN: Mr. F. Essig Mr. R. Higuera Dr. J. Battles Code 6014 China Lake, CA 93555
1	US Army Research and Development Group (Europe) ATTN: Electronics Branch Box 15 FPO New York, NY 09510		

DISTRIBUTION LIST

<u>No. of Copies</u>	<u>Organization</u>	<u>No. of Copies</u>	<u>Organization</u>
3	Director Naval Research Laboratory ATTN: Code 5300, Radar Division, Dr. Skolnik Code 5370, Radar Geophysics Branch Code 5460, Electro- magnetic Prop Branch Washington, DC 20390	1	Director National Bureau of Standards ATTN: Mr. C. K. S. Miller Div 276.106 Boulder, CO 80302
1	AFATL/DLB Eglin AFB, FL 32542	1	Goodyear Aerospace Corporation Arizona Division ATTN: Mr. Fred Wilcox Litchfield Park, AZ 85340
1	AFATL (DLTG, Mr. F. H. Prestwood) Eglin AFB, FL 32542	1	Honeywell Inc. Systems and Research Division ATTN: Mr. Ray Zirkle 2700 Ridgway Parkway Minneapolis, MN 55413
2	AFATL (DLY/DLDG) Eglin AFB, FL 32542	1	Hughes Aircraft Company Aerospace Group Advanced Program Development Systems Division ATTN: P. B. Reggie Canoga Park, CA 91304
1	ADTC/ADBPS-12 Eglin AFB, FL 32542	1	Hughes Aircraft Company Aerospace Group Radar Division ATTN: Dr. R. Wagner Culver City, CA 90230
1	ADTC/ADA Eglin AFB, FL 32542	2	Hughes Aircraft Company Aerospace Group Electron Dynamic Division ATTN: Mr. N. B. Kramer Mr. J. E. Sparacio 3100 West Lomita Boulevard Torrance, CA 90504
1	RADC/EMATE Griffiss AFB, NY 13440	1	LTV Aerospace Corporation Michigan Division ATTN: Dr. J. Mayersak P.O. Box 909 Warren, MI 48090
2	AFGL (LZ, Mr. C. Sletten) (LZN, Dr. E. E. Altschuler) Hanscom AFB, MA 01731		
1	AFWL/DEV Kirtland AFB, NM 87117		
1	AFAL/WRP (Mr. Leasure) Wright-Patterson AFB, OH 45433		
1	AFAL (RWN-1, Mr. Ray Bruns) Wright-Patterson AFB, OH 45433		
1	AFWL/TEM-4 (CPT J. Schell) Wright-Patterson AFB, OH 45433		

